TME 3166

DELAWARE MOUNTAIN GROUP (DMG) HYDROLOGY - SALT REMOVAL POTENTIAL

Waste Isolation Pilot Plant (WIPP) Project

Southeastern New Mexico

December 1982

U. S. Department of Energy

Waste Isolation Pilot Plant

Albuquerque, New Mexico

TME 3166

Delaware Mountain Group (DMG) Hydrology-
Salt Removal Potential
Waste Isolation Pilot Plant (WIPP) Project
Southeastern New Mexico

AUTHORS:

B. J. Wood — 12/28/82 Date
D'Appolonia Consulting Engineers, Inc.

R. E. Snow — 12/28/82 Date
D'Appolonia Consulting Engineers, Inc.

D. J. Coster — 12/28/82 Date
D'Appolonia Consulting Engineers, Inc.

S. Haji-Djafari — 12/28/82 Date
D'Appolonia Consulting Engineers, Inc.

APPROVED FOR SUBMITTAL TO WESTINGHOUSE BY:

D. K. Shukla — 12/28/82 Date
D'Appolonia Consulting Engineers, Inc.

J. K. Register — 12/28/82 Date
D'Appolonia Consulting Engineers, Inc.

COGNIZANT MANAGER:

C. C. Little — 12/28/82 Date
Westinghouse Electric Corporation

TABLE OF CONTENTS

TABLE OF CONTENTS
(Continued)

LIST OF TABLES

LIST OF FIGURES

LIST OF FIGURES
(Continued)

NOMENCLATURE

SYMBOL	DEFINITION	UNITS
a	Radius of convective dissolution zone	L
b	Effective aquifer thickness	L
C	Concentration	M/L^3
D	Molecular diffusion coefficient	L^2/T
D_{eff}	Effective molecular diffusion coefficient	L^2/T
g	Acceleration due to gravity	L/T^2
i	Hydraulic gradient	L/L
K	Hydraulic conductivity	L/T
k	Intrinsic permeability	L^2
M_d	Mass flux per unit area	M/L^2T
N_s	Nusselt number	Dimensionless
n	Porosity	Dimensionless
n_e	Effective porosity	Dimensionless
Q	Aquifer flow rate	L^3/T
R_s	Rayleigh number in a tube or fracture	Dimensionless
R_s^p	Rayleigh number for porous zone	Dimensionless
τ^*	Tortuosity	Dimensionless
Δz	Height of diffusion zone	L
Z	Height of convective dissolution zone	L
ρ	Density	M/L^3
μ	Dynamic viscosity	M/LT

TABLE OF UNIT CONVERSION
METRIC TO ENGLISH SYSTEM

PARAMETER	METRIC SYSTEM	ENGLISH SYSTEM
Distance	1 kilometer (km)	0.62 mile (mi)
Thickness	1 meter (m)	3.28 feet (ft)
Flow Rate	1 cubic meter per year (m^3/yr)	0.72 gallons per day (gpd)
Hydraulic Conductivity	1 meter per year (m/yr)	3.28 feet per year (ft/yr)
Concentration	1 kilogram per cubic meter (kg/m^3)(1)	1,000 parts per million (ppm)
Mass Transport Rate	1 kilogram per year (kg/yr)	2.20 pounds per year (lb/yr)

(1) 1 kilogram per cubic meter (kg/m^3) is equivalent to 1,000 milligrams per liter (mg/ℓ).

INTRINSIC PERMEABILITY AND HYDRAULIC CONDUCTIVITY CONVERSION[1]

UNITS	INTRINSIC PERMEABILITY, k			HYDRAULIC CONDUCTIVITY, K	
	CM^2	Darcy	M^2	CM/SEC	M/YR
CM^2	1	1.01×10^{8}	10^{-4}	9.8×10^{4}	3.09×10^{10}
Darcy	9.87×10^{-9}	1	9.87×10^{-13}	9.61×10^{-4}	3.03×10^{2}
M^2	10^{4}	1.01×10^{12}	1	9.8×10^{8}	3.09×10^{14}
CM/SEC	1.02×10^{-5}	1.04×10^{3}	1.02×10^{-9}	1	3.15×10^{5}
M/YR	3.23×10^{-11}	3.30×10^{-3}	3.23×10^{-15}	3.17×10^{-6}	1

[1] Adapted from Bear (1972). Values are for fresh water at 20°C.

1.0 INTRODUCTION AND SUMMARY

This report provides an account of studies performed to evaluate the potential for salt dissolution in the Castile Formation, removal of dissolved salt by fluids in the Bell Canyon aquifer within the Delaware Mountain Group (DMG), and the potential impact of this process on the long-term integrity of the Waste Isolation Pilot Plant (WIPP) facility.

The results of this study provide responses to the stipulated agreement of July 1, 1981 with the U.S. Department of Energy (DOE) and the state of New Mexico regarding the DMG hydrologic investigation. This study was performed and this report prepared by D'Appolonia Consulting Engineers, Inc. (D'Appolonia), under Subcontract S9-CJR-45451 with Westinghouse Electric Corporation, Advanced Energy Systems Division, under Contract DE-AC04-78-ET05346 with the DOE. The Westinghouse team is serving as the Technical Support Contractors (TSC) to the DOE for the WIPP project.

This report is divided into the following six chapters:

- Introduction and Summary (1.0)
- Site Conditions (2.0)
- Salt Dissolution Features and Mechanisms (3.0)
- Evaluation of Dissolution Mechanisms in the Delaware Basin (4.0)
- Assessment of Salt Dissolution (5.0)
- Conclusions (6.0)

and supplementary appendices:

- Review of Numerical Simulation Techniques and Basic Governing Equations of Flow and Mass Transport (Appendix A)
- Sensitivity Analysis of Salt Dissolution and Transport Parameters (Appendix B)

Chapter 1.0 provides an overview of the project and is intended to facilitate an understanding of the project scope and findings. Section 1.1 includes information on the WIPP project and geologic setting. The purpose of the study is identified in Section 1.2. The methods of evaluation used in conducting this study are described in Section 1.3. The results of the study are summarized in Section 1.4. Subsequent chapters, as identified above, provide the necessary details on DMG hydrology and the potential for salt removal.

This report has been prepared utilizing the metric system. A conversion table from the metric system to the English system has been provided following the Table of Contents.

1.1 THE WIPP PROJECT AND GEOLOGIC SETTING

As defined by current legislation (PL 96-164), the WIPP project is to provide a research and development facility to evaluate methods for the safe disposal of transuranic (TRU) radioactive wastes resulting from the defense activities and programs of the United States. The authorized WIPP project involves the disposal of defense TRU wastes in thick deposits of bedded salt located deep below the ground surface. Under the plans for the WIPP project, a mine for waste disposal would be excavated in a salt formation at a depth of about 650 meters. The site for this activity is located about 42 kilometers east of Carlsbad, New Mexico (Figure 1-1).

The WIPP site is a topographically monotonous, slightly hummocky plain covered with caliche and sand. It is near a drainage divide without well-delineated surface drainage patterns and separates two major, actively developing solution-erosion features: Nash Draw to the northwest and the San Simon Swale to the southeast (Figure 1-2). The site area drains to the Pecos River.

DRAWING NUMBER	NM78-648 A34
CHECKED BY	RW 10-13-80
APPROVED BY	540 12-22-81
DRAWN BY	3 3
50% BWN.	

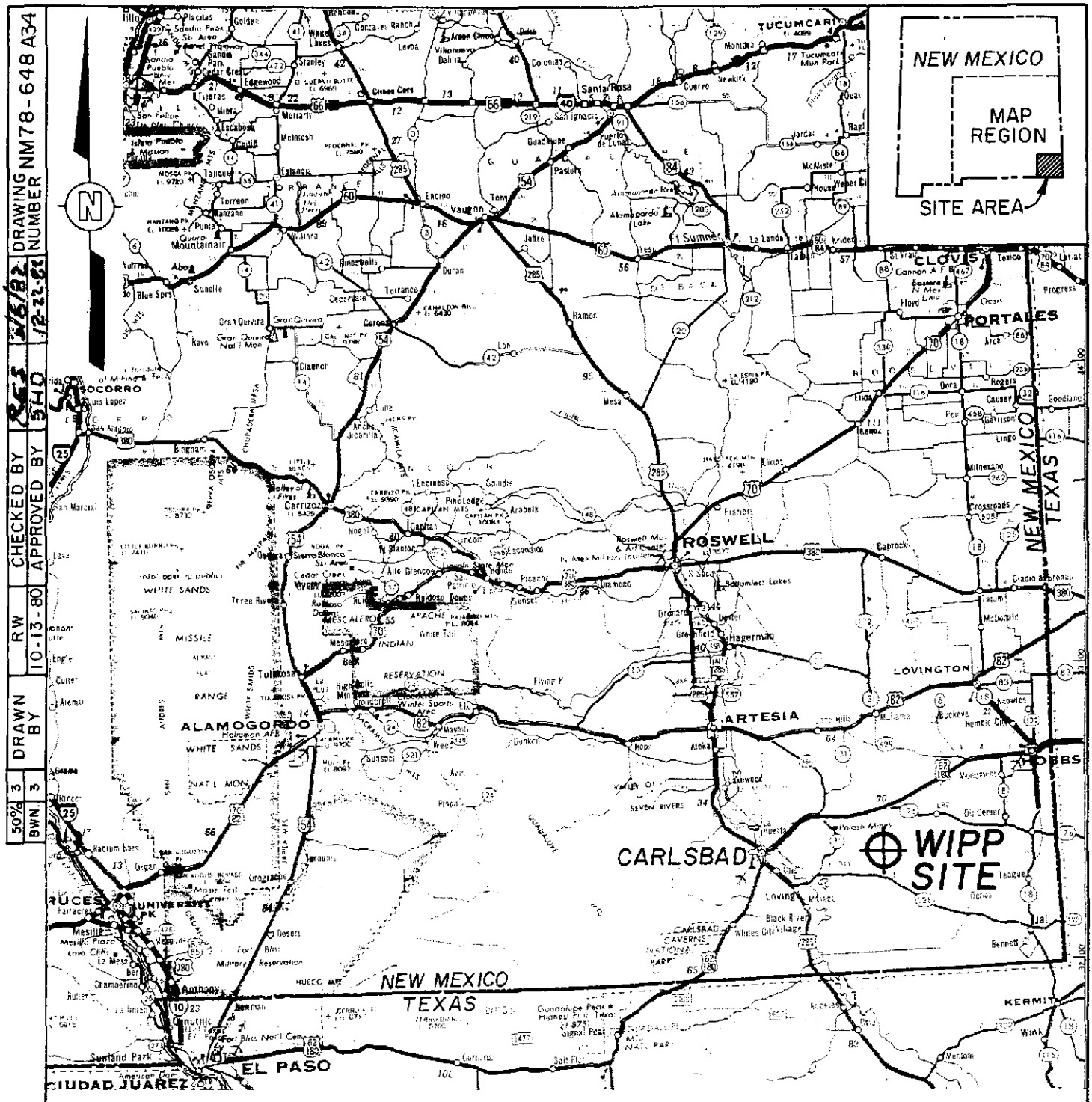

FIGURE 1-1

SITE LOCATION MAP

PREPARED FOR

WESTINGHOUSE ELECTRIC CORPORATION
ALBUQUERQUE, NEW MEXICO

D'APPOLONIA

DRAWN BY	CHECKED BY	APPROVED BY	DRAWING NUMBER
RAL 12-2-81	RES 12/8/82	CHD 12/8/82	NM78-648-842

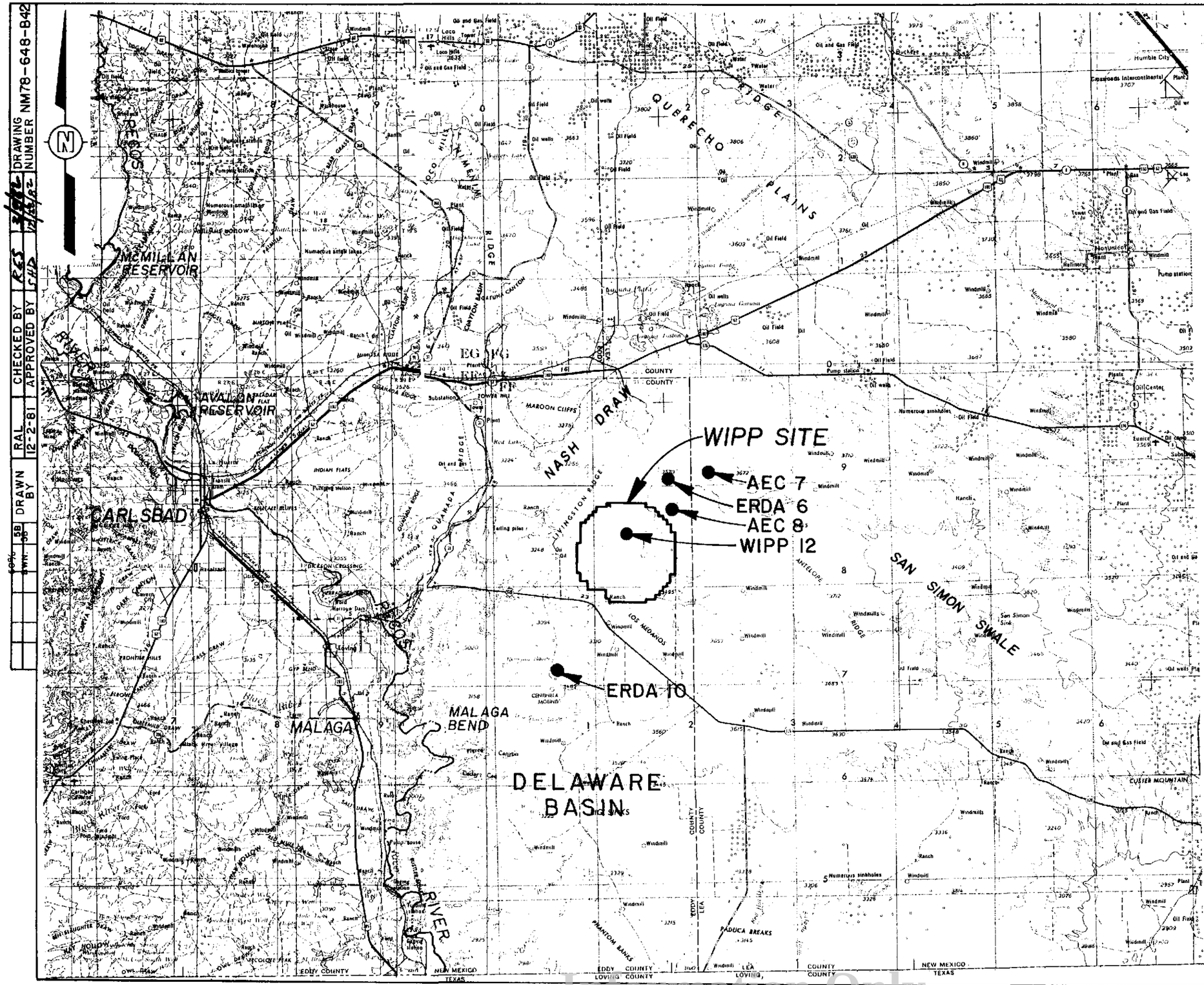

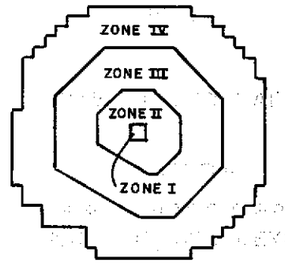

ZONE I (SURFACE FACILITIES)
ZONE II (UNDERGROUND FACILITY)
ZONE III (NO MINING OR DRILLING)
ZONE IV (DOE-CONTROLLED MINING AND DRILLING.)

0 5KM
0 1 2 3 4 MILES

WIPP SITE ZONATION

REFERENCES:

1. U.S. ARMY TOPOGRAPHIC COMMAND, MAPS OF UNITED STATES: CARLSBAD, N.M.-TX., NI13-11 (REVISED 1972); AND HOBBS, N.M.-TX., NI13-12 (REVISED 1973) SCALE 1:250,000.

2. U.S. DEPARTMENT OF ENERGY, 1980 a AND b

3. POWERS, et. al, 1978

CONTOUR INTERVAL = 100 FEET

SCALE
0 10 20 KM.
0 6 12 MILES

FIGURE 1-2

SITE VICINITY MAP

PREPARED FOR

WESTINGHOUSE ELECTRIC CORPORATION
ALBUQUERQUE, NEW MEXICO

D'APPOLONIA

The site is located in the north-central portion of the Delaware Basin, a region in which an inland sea deposited about 1,100 meters of evaporites during the Permian period (280 to 230 million years ago). The basin is bounded by a horseshoe-shaped (open to the south) massive limestone reef, the Capitan Formation. The Delaware Basin is considered to be tectonically stable. Major tectonic activity and basin subsidence ended with the Permian; since then, regional eastward tilting has been the principal geologic movement in the site area.

Sediments of the DMG underlie and interfinger with the Capitan limestone and form the floor of most of the Delaware Basin evaporite sequence. Three lithologically separable sandstone units, each about 300 meters thick, form a single aquifer system bearing brackish water. This water flows northeastward with connection and some discharge at the base of the Capitan limestone. The uppermost sandstone unit of the DMG is the Bell Canyon Formation.

The Castile Formation, which contains thick, massive, and laminated anhydrite units alternating with halite units, overlies the Bell Canyon. The Salado Formation overlying the Castile is primarily halite with lesser amounts of anhydrite, sylvite, and polyhalite. The WIPP underground facility is planned to be developed in the bedded salts of the Salado Formation at a depth of about 650 meters, near the middle of the thick evaporite sequence. Accordingly, the planned disposal horizon is hydrologically isolated from overlying nonevaporite rocks by about 400 meters of evaporites and from underlying nonevaporite rocks by over 500 meters of evaporites.

1.2 PURPOSE OF THE STUDY

As part of the overall study of safety considerations for the WIPP project, analyses of the long-term consequences to public health and safety of emplacing radioactive wastes in the WIPP facility have been performed. These analyses are reported in Chapter 8 of the WIPP Safety Analysis Report (SAR) (U.S. Department of Energy, 1980b).

It has been proposed to locate the WIPP facility in Permian age salt beds (formed more than 230 million years ago) in order to isolate the radioactive waste from the biosphere for a period of at least several thousand years. This period is sufficient to allow virtually complete decay of the short-lived high activity nuclides such as Cs-137 and Sr-90 and thus to substantially reduce the hazard posed by the waste. However, the dominant component of the evaporite deposits of Permian age within the Delaware Basin is halite (NaCl), a water-soluble mineral. Dissolution of this mineral can begin if it is contacted by unsaturated brine. While the WIPP facility is located in an area in which salt dissolution appears to be insignificant, there is evidence of dissolution in other parts of the Delaware Basin. Therefore, some concern has risen regarding the potential effects of such salt dissolution on the integrity of the WIPP facility. A model has been developed to enable prediction of salt removal rates from the Castile and Salado Formations through the agency of fluids in the DMG. The objective of this study was to predict the possible impact of future dissolution rather than to evaluate the geologic evidence for dissolution since deposition.

On the basis of the above objectives, the following tasks for this study have been developed:

- Review and compile geologic, hydrologic, and geochemical characteristics of the DMG, including information such as direction and volume of the flow, potentiometric levels, and regional hydraulic conductivities.
- Assess the various salt dissolution hypotheses that involve the Bell Canyon or Capitan Reef Formations.
- Assess the potential for dissolution in the Castile and Salado Formations by the Bell Canyon fluids.
- Establish a hydrogeologic model for evaluation of the potential for salt removal from the Castile and Salado Formations by fluids in the underlying DMG units.

- Assess the potential dissolution rates and the possible dimensions of solution cavities.

- Evaluate the sensitivity of the salt dissolution rate to basic hydrologic and geochemical parameters.

In preparation of the scope of this study and this document, the following criteria are used:

- The data base consists of the available reported DMG hydrologic and geochemical data. No specific field data were collected for any part of this study.

- This topical report includes sufficient information on the DMG hydrogeologic characteristics to provide a basis for evaluation of salt dissolution mechanisms. Detailed hydrological characteristics of the DMG are provided in the appropriate references.

1.3 METHOD OF EVALUATION

To provide a comprehensive report regarding salt dissolution by the DMG aquifer and its impact on the WIPP facility integrity, the following steps have been undertaken:

- Review of existing hydrogeological and geochemical data - The available data from the United States Geological Survey (USGS), WIPP SAR, and other sources relative to the DMG and overlying evaporite deposits have been reviewed and pertinent information compiled.

- Review of dissolution features and their potential origins - The geologic evidence consisting of observed surface and subsurface features reflecting dissolution phenomena has been reviewed. In addition, information on the concentration of salt and chloride in the DMG and the nature of overlying evaporite deposits has been summarized.

- Review of salt dissolution hypotheses - The various salt dissolution hypotheses and dissolution mechanisms were reviewed and summarized. In addition, their application for salt removal from the Castile and Salado Formations by the DMG for

site hydrogeologic and geologic conditions was investigated.

- Review of governing equations - The various equations reflecting either the physical representation of salt dissolution or transport of the fluid through porous media were reviewed. This review included diffusion and convective dispersion transport.

- Development of a model which incorporated pertinent features of the DMG - A physical model depicting pertinent information such as the locations of the reefs, Castile Formation, and the WIPP facility was prepared. The various features significant to the dissolution evaluation were noted on this model.

- Performance of analytical evaluation and numerical modeling - The salt dissolution rates were evaluated using analytical solutions as well as numerical models.

- Performance of sensitivity analysis - To evaluate the significance of various parameters on the salt dissolution rate, a sensitivity analysis was conducted by studying the range of parameters and noting their effect on the rate of dissolution. Potential future changes in the flow system were also incorporated to assess long-term dissolution. Various graphs depicting the significance of the parameters were prepared.

In addition to these analyses, two implausible worst-case scenarios were developed to assess the potential for dissolution cavity formation due to the concentration gradient in the Bell Canyon aquifer. These analyses provided an understanding of the impacts of such unlikely dissolution on facility integrity.

Using this approach, it is believed that implications of salt dissolution and its removal by Bell Canyon fluids have been addressed.

1.4 SUMMARY AND CONCLUSIONS

This study has been performed (1) to assess potential salt dissolution from the evaporite sequences by the underlying aquifer and (2) to evaluate the impact of this process on the WIPP facility integrity. The hydrogeologic and geochemical characteristics of the DMG have been reviewed and the various salt dissolution hypotheses and mechanisms have been examined. Based on analytical and numerical evaluations, the following conclusions have been reached:

- The potential dissolution mechanisms include diffusion and convection from halite layers to the Bell Canyon and Capitan Reef aquifers. Computation of the present dissolution rate based on observed chloride concentration levels in the Bell Canyon aquifer indicates that diffusion and possibly very weak convection result in removal of halite from the Castile overlying the DMG. However, convection may be significant at locations adjacent to the Capitan Reef aquifer.

- Evaluation of the DMG hydrogeologic conditions and review of the range of values for the hydrogeologic and geochemical parameters which influence salt removal indicate that general salt removal by the diffusion process would produce an advancement of the dissolution front of only 0.3 centimeter in 10,000 years. This would have an insignificant effect on the integrity of the facility.

- Based on an analysis of potential changes in the hydrologic characteristics (e.g., hydraulic gradient and associated flow rate) of the Bell Canyon aquifer, an increase in flow rate of even one order of magnitude (from an estimated rate of 0.135 cubic meter per year per meter of width to 1.35 cubic meter per year per meter) would not increase the salt removal from the Castile Formation by more than 17 percent (from a calculated rate of approximately 0.3 centimeter in 10,000 years to less than 0.4 centimeter in 10,000 years). The unlikely occurrence of a change in hydrogeologic characteristics and the associated potential dissolution are not anticipated to have any effect on the facility integrity.

- An analysis of implausible worst-case dissolution rates associated with both diffusive and convective dissolution at the Bell Canyon aquifer-Castile Formation interface suggests that the structural integrity of the WIPP facility located more than 400 meters above would not be affected. In this analysis, it was determined that the theoretical maximum cavity radius would be seven meters over a fracture and one meter above a circular porous zone in a period of 10,000 years.

2.0 SITE CONDITIONS

The WIPP site is located in the Pecos Valley section of the Great Plains Physiographic Province. This area is characterized by a hummocky topography with numerous karst features. The ground surface slopes to the southwest (Figure 1-2) and surface drainage is directed to the Pecos River which lies approximately 30 kilometers west of the proposed site. The description of site conditions based on analysis of available data follows.

2.1 GEOLOGY

The geologic setting for the WIPP site is the Delaware Basin, a broad structural depression (160 kilometers wide by 265 kilometers long) which is Paleozoic in age. During the Paleozoic, approximately 600 to 230 million years before present (MYBP), as much as 6,100 meters of sediments were deposited in the basin. The "basement" rock underlying the sedimentary sequence is composed of Precambrian igneous and metamorphic units.

The following is a description of the development of the Delaware Basin through geologic time. A generalized stratigraphic column (Figure 2-1) and a chronology of major geologic events (Figure 2-2) are presented to aid in the discussion.

2.1.1 Geologic History of the Delaware Basin

During early and mid-Paleozoic time (600 to 280 MYBP), the Precambrian basement was covered with marine sediments that were predominantly carbonates. During this time, the region was part of the Tabosa Basin, a large depression which was the precursor of the Delaware and Midland basins.

The Tabosa Basin subsided until late Pennsylvanian time (280 MYBP). Although there were intermittent periods of emergence and erosion, the sedimentary record is virtually continuous from the Ordovician through

DRAWN TEJ 1-7-82 | CHECKED BY Best | APPROVED BY Lyle | DRAWING NUMBER NM78-648-845

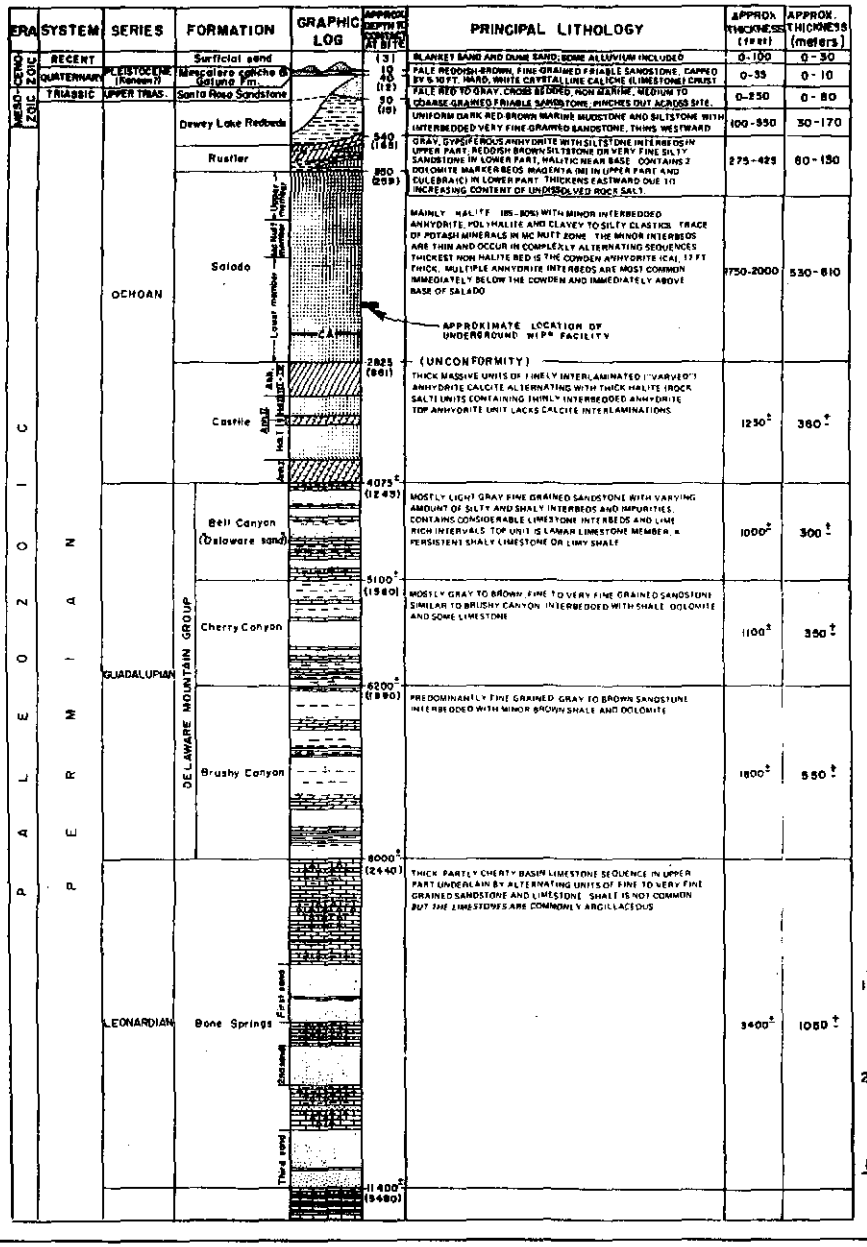

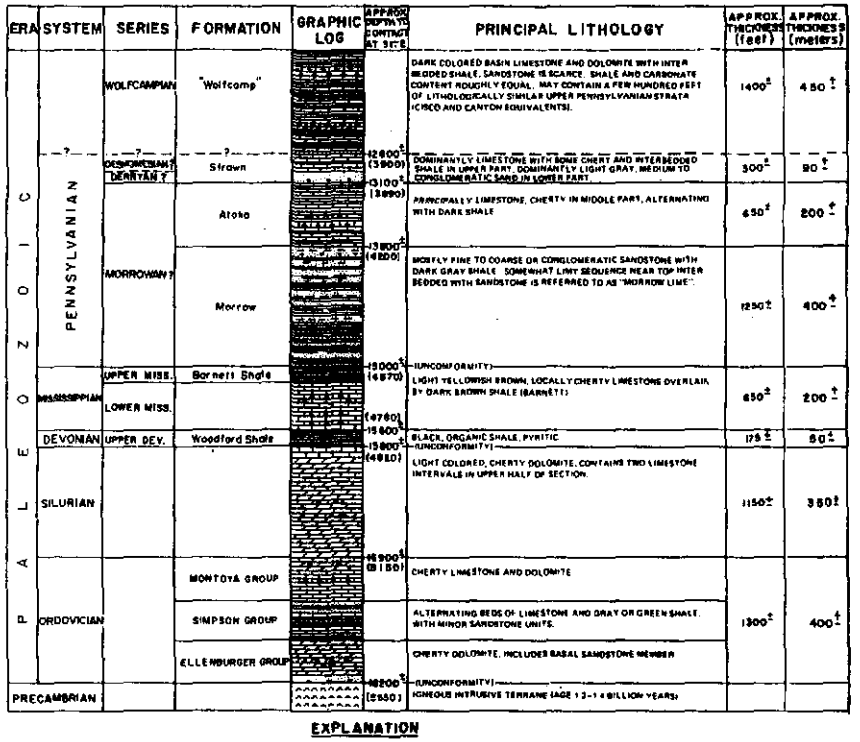

EXPLANATION

LITHOLOGIC SYMBOLS

- Sandstone
- Mudstone; siltstone; silty and sandy shale
- Shale
- *Limestone*
- Dolomite
- Cherty limestone and dolomite
- Shaly limestone
- Anhydrite (or gypsum)
- Interlaminated anhydrite-calcite
- Halite (rock salt)
- Granitic rocks

NOTES:

1. FOR APPROXIMATE DEPTH TO CONTACT AT SITE, THE FOLLOWING NOTATION IS USED:
   (3) - METERS
   10 - FEET
2. THE LOCATION OF THE UNDERGROUND WIPP FACILITY IS BASED ON THE STRATIGRAPHY PRESENTED IN THIS FIGURE. SEE FIGURES 2-4 FOR LOCATION RELATIVE TO THE BELL CANYON AQUIFER.

REFERENCE:
POWERS, et al., 1978

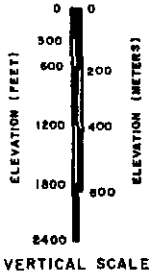

VERTICAL SCALE

FIGURE 2-1

SITE STRATIGRAPHIC COLUMN

PREPARED FOR

WESTINGHOUSE ELECTRIC CORPORATION
ALBUQUERQUE, NEW MEXICO

D'APPOLONIA

12

DRAWN BY	CHECKED BY	DRAWING NUMBER
D. Welch 12-2-81	APPROVED BY	NM78-648-B41

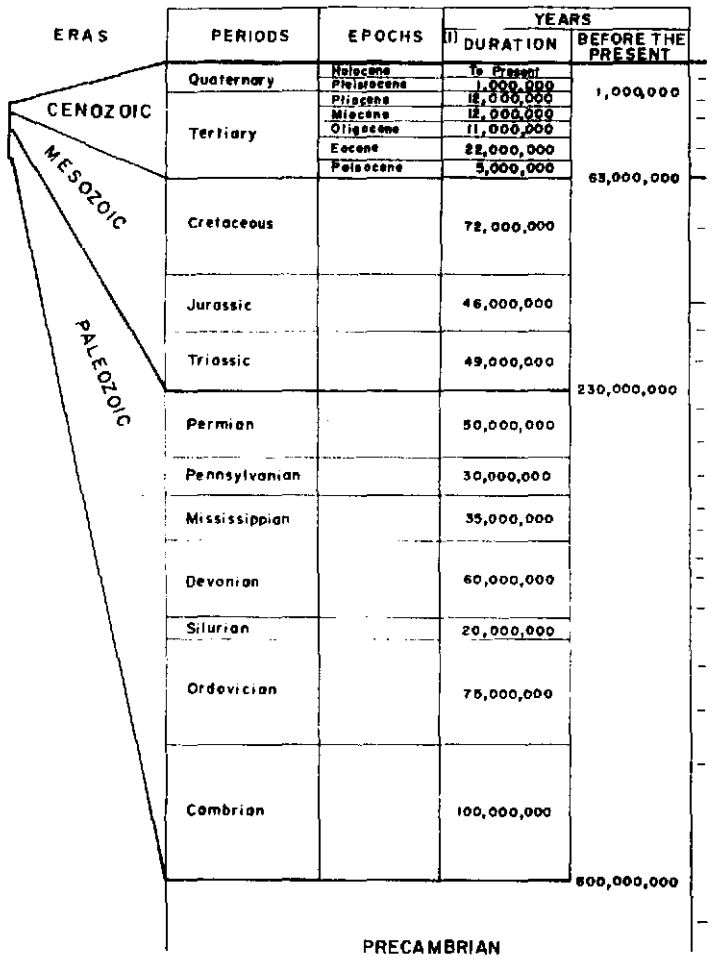

PERIODS	EPOCHS	YEARS DURATION	YEARS BEFORE THE PRESENT	MAJOR GEOLOGIC EVENTS – SOUTHEAST NEW MEXICO REGION
Quaternary	Holocene	To Present		– Eolian and erosional/dissolution activity. Development of present landscape.
	Pleistocene	1,000,000	1,000,000	– Deposition of Ogallala fan sediments. Formation of caliche caprock.
Tertiary	Pliocene	12,000,000		– Regional uplift and east-southeastward tilting; Basin-Range uplift of Sacramento and Guadalupe - Delaware Mountains.
	Miocene	12,000,000		
	Oligocene	11,000,000		– Erosion dominant. No Early to Mid-Tertiary sediments present.
	Eocene	22,000,000		
	Paleocene	5,000,000	65,000,000	– Laramide "Revolution." Uplift of Rocky Mountains. Tectonism and igneous activity to west and north.
Cretaceous		72,000,000		– Submergence. Intermittant shallow areas. Thin limestone and clastics deposited.
Jurassic		46,000,000		– Emergent conditions. Erosion. Formation of rolling topography.
				– Deposition of fluvial clastics.
Triassic		49,000,000		– Erosion. Broad flood plain pediment surface develops.
			230,000,000	
Permian		50,000,000		– Deposition of evaporite sequence followed by continental red beds.
				– Sedimentation continuous in Delaware, Midland, Val Verde Basins and on the shelf areas.
Pennsylvanian		30,000,000		– Massive deposition of clastics. Shelf, margin, basin pattern of deposition develops.
Mississippian		35,000,000		– Regional tectonic activity accelerates, folding up Central Basin Platform, Matador Arch, Ancestral Rockies.
				– Regional Erosion. Deep, broad basins to east and west of Central Basin Platform develop.
Devonian		60,000,000		– Renewed submergence.
				– Shallow sea retreats from New Mexico. Erosion.
Silurian		20,000,000		– Mild epeirogenic movements. Tobosa Basin subsiding. Pedernal Landmass and West Texas emergent, until Middle Mississippian.
Ordovician		75,000,000		– Marathon – Ouachita geosyncline, to south, begins subsiding.
				– Deepening of Tobosa Basin area; shelf deposition of clastics, derived partly from ancestral Central Basin Platform, and carbonates.
Cambrian		100,000,000		– Clastic sedimentation – Bliss sandstone.
				Erosion to a nearly level plain.
			600,000,000	
				– Mountain - building, igneous activity, metamorphism, erosional cycles.

FIGURE 2-2

MAJOR GEOLOGIC EVENTS
SOUTHEAST NEW MEXICO

PREPARED FOR

WESTINGHOUSE ELECTRIC CORPORATION
ALBUQUERQUE, NEW MEXICO

DAMPOLONIA

REFERENCES:
(1). TIME SCALE: LEET & JUDSON, 1965
(2). U.S. DEPT OF ENERGY, 1980 b.

the Pennsylvanian periods. Sediments deposited during this time consisted mainly of carbonates with lesser amounts of clay, silt, and sand.

At the end of the Pennsylvanian (280 MYBP), tectonic activity associated with the Marathon Orogeny caused the Tabosa Basin to be split into the Delaware Basin to the west and the Midland Basin to the east, separated by the Central Basin Platform (Figure 2-3).

In early Permian time, the Delaware Basin was still subsiding. During this time, various basin and shelf-type sediments were deposited including the Wolfcampian and Leonardian series which consist mainly of limestone and limy shales (Figure 2-1).

In the middle to late Permian, subsidence lessened and deposition of the Capitan, Goat Seep, and San Andres limestones began along the basin margins. The Capitan and Goat Seep limestones are reef deposits while the San Andres limestone is a shelf deposit. Contemporaneously with reef formation, clastic sediments of the DMG were deposited in the middle of the Delaware Basin. The relationship between the DMG and the Capitan Reef complex is shown in Figure 2-4.

The DMG is subdivided into three formations named (in ascending order) the Brushy Canyon, Cherry Canyon, and Bell Canyon (Figure 2-1). These formations consist basically of fine- and coarse-grained sandstone, siltstone, shale, and some limestone members. The upper portion of the Bell Canyon includes the following members in descending order from contact with the lowest anhydrite of the Castile Formation evaporites (Grauten, 1965; Gonzalez, in preparation):

> Lamar Limestone Member - A black calcareous silty shale containing several beds of shaly limestone. It is 8 to 10 meters thick.
>
> Trap Member - Interlaminated shaly siltstone and shale sequence 2 to 3 meters thick.

DRAWN BY	G.J. Graham	CHECKED BY	
	12-30-81	APPROVED BY	

DRAWING NUMBER NM78-648-844

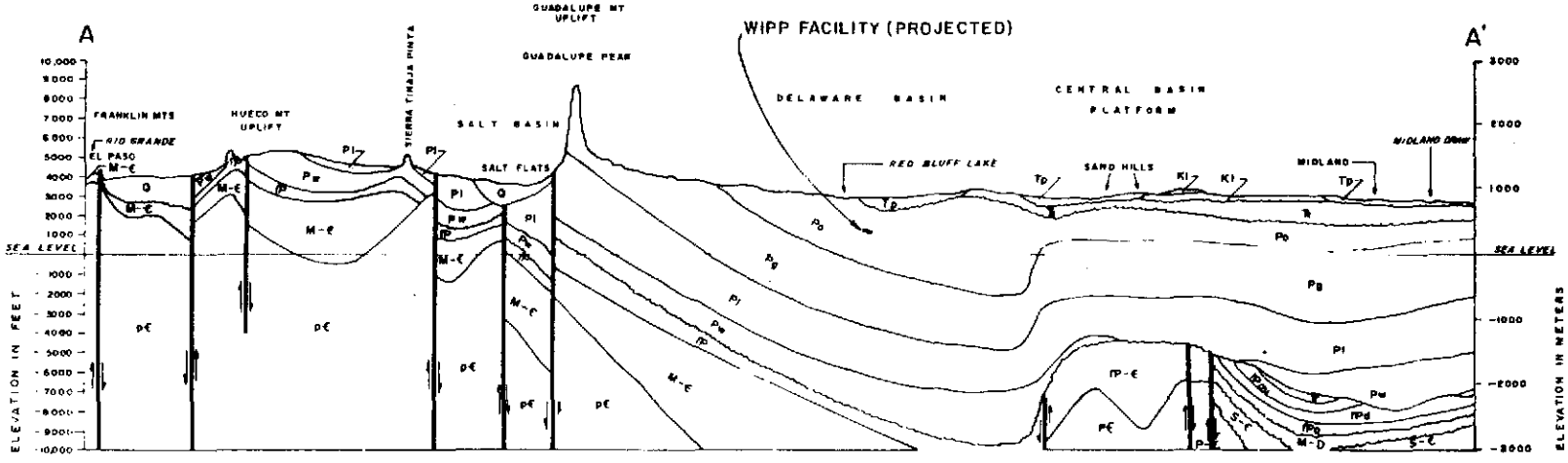

EXPLANATION

Q	Quaternary	IPm	Pennsylvanian (Missourian)
Tp	Tertiary (Pliocene – Ogallala)	IPd	Pennsylvanian (Desmoinesian)
Kl	Lower Cretaceous	IPa	Pennsylvanian (Atokan)
Ŗ	Triassic (Santa Rosa)	IP	Pennsylvanian
Po	Permian (Ochoan)	M-D	Devonian – Mississippian
Pg	Permian (Guadalupian)	IP-€	Cambrian – Pennsylvanian
Pl	Permian (Leonardian)	M-€	Cambrian – Mississippian
Pw	Permian (Wolfcampian)	S-€	Cambrian – Silurian
		p€	Precambrian
			Unconformity
			Fault

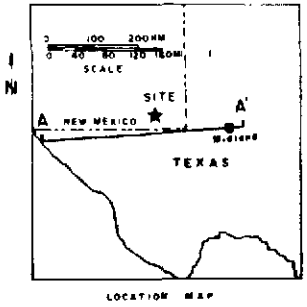

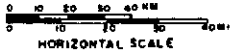

REFERENCE
U.S. DEPARTMENT OF ENERGY, 1980b.

FIGURE 2-3

REGIONAL GEOLOGIC SECTION
TEXAS-NEW MEXICO BORDER

PREPARED FOR

WESTINGHOUSE ELECTRIC CORPORATION
ALBUQUERQUE, NEW MEXICO

DAPPOLONIA

14A	100	DRAWN BY		CHECKED BY		DRAWING NUMBER	NM78-648-A44
14A	OR	D. Weick	12-21-82	APPROVED BY			

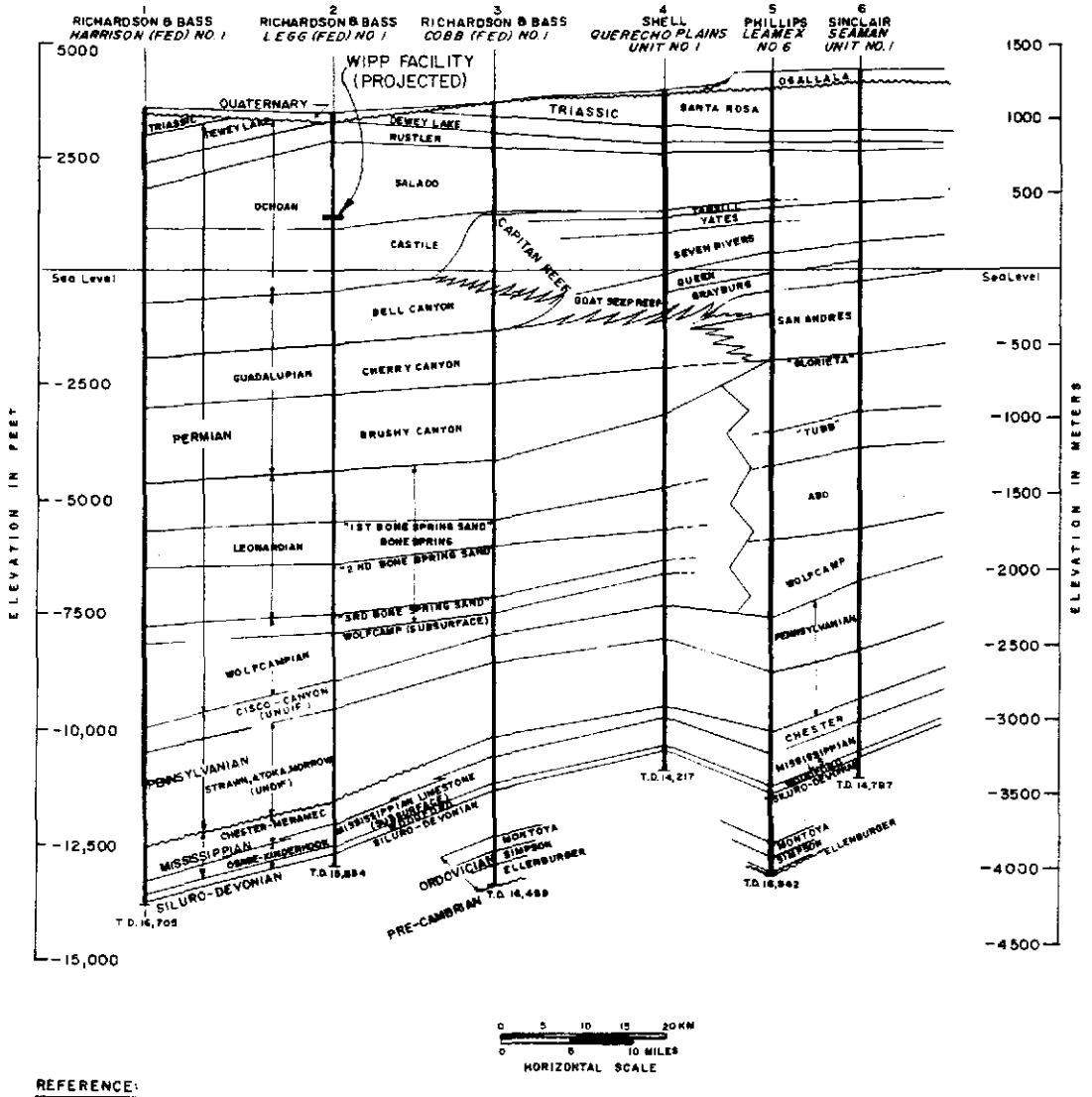

REFERENCE:

U.S. DEPARTMENT OF ENERGY, 1980 b.

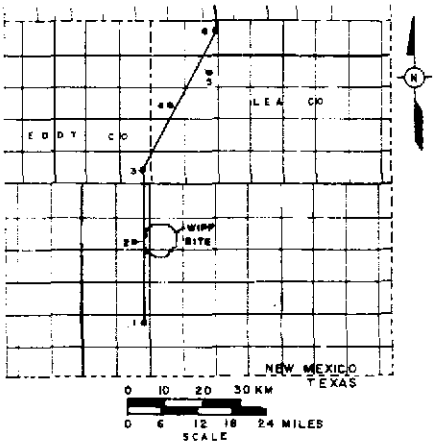

LOCATION MAP

FIGURE 2-4

REGIONAL LITHOLOGIC SECTION
SOUTHEAST NEW MEXICO

PREPARED FOR

WESTINGHOUSE ELECTRIC CORPORATION
ALBUQUERQUE, NEW MEXICO

D'APPOLONIA

Ramsey Sandstone Member - In southeastern New Mexico, the Ramsey is overlain by a dense, hard limestone 2 to 10 meters thick. The Ramsey has two main facies: (1) laminated, shaly siltstone, interlaminated with black shale and (2) clean, fine-grained sandstone with some laminations of limy, shaly siltstone, and/or black shale. It is in this member where the Bell Canyon aquifer is contained.

Ford Shale Member - Consists of a laminated shaly siltstone, overlain and underlain by black shale. This member constitutes one of the most important markers used in the Upper Bell Canyon exploration and is about 3 meters thick.

Olds Sandstone Member - Laminated and clean sandstone facies similar to the Ramsey Member, 3 to 7 meters thick.

Hays Sandstone Member - Thin sandstone and shaly zones.

These members constitute the upper portion of the Bell Canyon Formation. The Bell Canyon aquifer is confined to the upper and lower sands of the Ramsey Sandstone Member of the Bell Canyon Formation as evidenced from borehole investigations in AEC-7, AEC-8, and ERDA-10 boreholes (Powers, et al., 1978). Furthermore, these sands are over- and underlain by rock strata that are orders of magnitude less in hydraulic conductivity than the producing sands. Finally, the "aquifer" thickness varies from 2 to 14 meters and appears to be stratigraphically different throughout the basin.

During the late Permian, the circulation of seawater to the basin was restricted by the reef and the impounded seawater became highly saline, resulting in the precipitation of the Ochoan evaporite sequence. The Ochoan Series consists mainly of interbedded halite and anhydrite deposits which include (in ascending order) the Castile, Salado, and Rustler Formations (Figure 2-1). Brief descriptions of these units follow:

- Castile Formation - The Castile Formation consists of approximately 400 meters of alternating

anhydrite (labeled Anhydrites I, II, III, and IV) and halite units (Halites I, II, and III) which merge to the north, as shown in Figure 2-1. Halite III is interbedded between Anhydrites III and IV. Anhydrite I lies at the base of the formation and is approximately 100 meters thick at the WIPP site (Mercer and Orr, 1979). The anhydrite units in the formation are varved and commonly contain calcite laminations. The contact between the Castile and the overlying Salado Formation is unconformable, indicating that some erosion and/or dissolution of the Castile may have occurred prior to deposition of the Salado. In the western portion of the basin, the Castile thins due to the lack of deposition, erosion, and/or possibly dissolution.

- Salado Formation - The Salado Formation is the proposed host formation for the WIPP facility. It is approximately 570 meters thick, consisting of lower and upper halite units which are separated by the McNutt potash zone (Figure 2-1). The McNutt zone is mined approximately 6.5 kilometers west of the site for its potassium-bearing minerals. Both the lower and upper halite units contain interbeds of anhydrite, polyhalite, and clay. The Salado thins west of the proposed facility site as it nears the surface.

- Rustler Formation - This formation consists of interbedded anhydrite, polyhalite, dolomite, siltstone, and sandstone. Near the center of the WIPP site, the Rustler Formation is 168 meters below the surface and attains a thickness of 94 meters.

Beyond the reef margins, shelf sediments of the Artesia Group were deposited contemporaneously with the Castile Formation. The Artesia Group consists of 200 to 460 meters of dolomite, evaporites, and terrigenous red beds and includes the Grayburg, Queen, Seven Rivers, Yates, and Tansill Formations. Northeast of the WIPP site, the Artesia Group, which overlies and interfingers with the Capitan Reef, is about 200 meters thick.

At the close of the Permian, the region underwent broad uplift during which the Dewey Lake Red Beds, a terrigenous sedimentary unit, was deposited.

The Triassic Period (230 to 181 MYBP) was largely a period of emergence and erosion during which a floodplain-pediment topography existed at the site. This type of topography is formed when streams flow over flat-lying bedrock. At the end of the Triassic, these streams deposited a thin layer of fluvial clastics (stream sediments). These sediments are known collectively as the Dockum Group which is present only in the eastern portion of the site.

The Jurassic Period (181 to 135 MYBP) was characterized by continued emergence of the land mass from the sea. Erosion was dominant and a rolling topography was formed. The lack of Jurassic sediments in the region and the absence of Triassic rocks in the western part of the basin indicates that this was probably a period of substantial erosion (Bachman, 1974). It is also likely that some dissolution of the halite units of the Salado and Castile Formations took place during Triassic and Jurassic times (Bachman, 1974).

With the commencement of the Cretaceous Period (135 to 63 MYBP), seas returned to the area and the thin limestones and clastic sediments were deposited. The seas withdrew at the end of this period in response to the Laramide Orogeny which also gave rise to the Rocky Mountains. Subsequent erosion has removed most of the Cretaceous sediments, the occurrence of which is limited to small isolated patches throughout the Delaware Basin (U.S. Department of Energy, 1980b).

The Tertiary Period (63 to 1 MYBP) was a time of continued emergence during which erosion (probably accompanied by halite dissolution) was once again dominant. This conclusion is based on the almost complete absence of Tertiary deposits in the region.

The basin underwent a final stage of uplift accompanied by a tilting to the east-southeast possibly during Miocene time (25 to 13 MYBP). Near the end of the Tertiary (approximately 1 MYBP), the Ogallala Formation, which is composed of sediments from the nearby Rocky Mountains, was deposited. Postdating the Ogallala and overlying it in some areas is a veneer of fine-grained sandstone (Gatuna Formation). The surface of the Gatuna is overlain by a hard caliche layer named the Mescalero Caliche which probably formed in the Pleistocene approximately 600,000 years before present.

Since Pleistocene time, fluvial and eolian erosion as well as dissolution have continued, accompanied by deposition of alluvium along stream channels.

2.1.2 Geologic Structure

As mentioned, the Delaware Basin is a broad structural depression that is bounded by the Capitan Reef complex. At its maximum, the basin measures 160 kilometers in an east-west direction and 265 kilometers in a north-south direction.

Folding

Generally, Paleozoic strata in the northern portion of the Delaware Basin exhibit low, open folding associated with the development of the basin. The average dip of Paleozoic strata in and around the site is approximately two degrees to the east (Powers, et al., 1978). Locally, minor folding has been observed in the Castile Formation. This folding may be attributable to flow of halite (Jones, et al., 1973), which behaves plastically when subjected to unequal pressure from different directions. Differential unloading of overburden related to dissolution has also been postulated as a possible mechanism that could have produced flow in the Castile Formation halite units (Anderson and Powers, 1978).

Faulting and Jointing

Fracturing in the form of faulting and jointing has occurred in the region with normal faults of Paleozoic age found along the eastern and western margins of the Delaware Basin (Figure 2-3). The closest such structure to the WIPP site is the Bell Lake Fault, which lies 24 to 32 kilometers east of the site (Haigler and Cunningham, 1972). Continuous post-Wolfcampian strata indicate that major faulting had ceased before the middle Permian and hence is not believed to affect the Bell Canyon, Castile, or Salado Formations.

Although no major faults are known to exist at the WIPP site, data from boreholes drilled at the site indicate that jointing has occurred. Data concerning joint frequency and orientations are extremely sparse. Joint orientations are described as two sets of joints striking northwest and northeast (Anderson, 1978). The joints are exposed near Carlsbad Caverns, more than 40 kilometers from the WIPP site. These joints have been identified in Delaware Basin rocks and may extend into the water bearing sandstone.

2.1.3 Surficial Geology

A number of periods of emergence and erosion of the Delaware Basin during geologic time have been identified in the preceding discussion. Because of the great thicknesses of halite units in the Permian sequence, it is to be expected that a certain amount of salt dissolution accompanied normal erosion processes during these periods (Bachman, 1974). According to Anderson (1978), halite dissolution has also occurred in the most recent period since uplift and tilting of the Delaware Basin at 4 to 5 MYBP. Dissolution of halite is probably responsible for the hummocky topography and for a wide range of surface and subsurface dissolution features (Bachman, 1974; Anderson, 1978). Among these features are sinkholes, large depressions (e.g., Nash Draw and San Simon Swale) and domal features [e.g., Hill C (Dome C); Vine, 1960]. The latter is a deep-seated "breccia pipe" or "chimney" possibly indicative of dissolution generally associated with the Capitan Reef aquifer.

2.2 HYDROGEOLOGY

Groundwater throughout most of the Delaware Basin typically contains high concentrations of dissolved solids and is unsuitable for most domestic purposes. Hiss (1975a and 1975b) reported dissolved solids levels often greater than 10 kilograms per cubic meter (kg/m^3), equivalent to concentrations greater than 10,000 milligrams per liter (mg/ℓ). Where dissolved solids levels are in the 1.0 kg/m^3 (1,000 mg/ℓ) range, some groundwater is used for watering livestock. Most of the groundwater used east of the Pecos is limited to oil field flooding.

Aquifers likely to interact with the relatively impermeable Castile and Salado Formations include the Capitan Reef complex and portions of the Bell Canyon and Rustler Formations. The hydrogeology of these units is described below.

Delaware Mountain Group

The DMG consists of the Brushy Canyon, Cherry Canyon, and Bell Canyon Formations. The combined thickness of the DMG at the site is approximately 1,220 meters. Based on its proximity to overlying evaporite deposits, the Bell Canyon Formation has been considered the primary transport medium for any downward migrating dissolved halite. The hydraulic conductivity of the Bell Canyon aquifer [based on core sample measurements (Hiss, 1975a)] ranges from 1.1 to 2.9 meters per year and averages approximately 1.8 meters per year. One measurement of hydraulic conductivity of 18 meters per year has also been reported; however, it does not appear representative of the basin. Drill-stem tests in Borehole AEC-7 indicate (1) the Lamar Shale is practically impermeable and (2) hydraulic conductivity of the brine production zone (Ramsey Sandstone) penetrated by this boring is about 1.2 meters per year (Lynes, Inc., 1979). These results are in general agreement with Hiss' (1975a) data. Similarity of the laboratory and field data suggests that flow in the Bell Canyon aquifer is predominantly controlled by primary porosity and hydraulic conductivity. The average porosity of the Bell Canyon aquifer is 16 percent (Hiss, 1975a). It should also be

stated that the formation is not homogeneous with respect to hydrogeologic properties. Field tests indicate that much of the Bell Canyon Formation, which is approximately 300 meters thick, exhibits very little water-bearing potential (Mercer and Orr, 1979) and that total transmissivity is limited to several thin zones. Anderson, et al. (1978), suggests that the effective aquifer thickness is approximately 30 meters. This value is larger than the reported aquifer thickness (Section 2.1.1); however, it has been selected as a representative value and assumed uniform throughout the basin. Table 2-1 presents a summary of the hydrogeologic characteristics for the Bell Canyon aquifer.

Groundwater flow in the DMG is shown in Figure 2-5, which is reproduced from the work of Hiss (1975a). A large number of the data points which were used by Hiss to construct potentiometric surface and chloride concentration contours are omitted from the figure because of their proprietary nature. The potentiometric surface, corrected for fluid density, indicates that flow should be generally in a northeasterly direction, with an average hydraulic gradient of approximately 0.0025 meter per meter. Irregularities in hydraulic gradient may reflect basin-wide variability in transmissivity or fluid density in the DMG. The general direction of flow of the DMG suggests that the location of recharge is in the southwest basin vicinity.

The influence on the computed flow rate in the Bell Canyon aquifer for ranges of values for the hydrogeologic characteristics is shown in Figure 2-6. Based on the available data, the representative value for the flow rate is 0.135 cubic meter per year per unit width of aquifer. As shown in Figure 2-6, the probable range for the flow rate is from 0.02 to 0.40 cubic meter per year per meter, which reflects the possible values for hydraulic conductivity, effective aquifer thickness, and hydraulic gradient.

TABLE 2-1

HYDROGEOLOGIC CHARACTERISTICS OF THE BELL CANYON FORMATION[1]

PARAMETER	PARAMETER VALUE	UNITS
Average Hydraulic Conductivity of Bell Canyon Aquifer[2,3]	1.1 to 2.9	Meters per year (m/yr)
Average Effective Porosity of Bell Canyon Aquifer[2]	0.16	Dimensionless
Total thickness of Bell Canyon Formation[4]	300	Meters (m)
Permeable Thickness of Upper Bell Canyon[5,6]	less than 30	Meters (m)
Thickness of Anhydrite I in the Castile Formation[5]	70 to 100	Meters (m)
Hydraulic Gradient in the Bell Canyon Formation[2]	0.002 to 0.003	Meters per meter

(1) *Hydrologic characteristics of the Bell Canyon Formation are identified in the vicinity of the WIPP site.*

(2) Hiss, 1975a.

(3) Lynes, Inc., 1979.

(4) U.S. Department of Energy, 1980b.

(5) Anderson, 1978.

(6) Gonzalez, 1982.

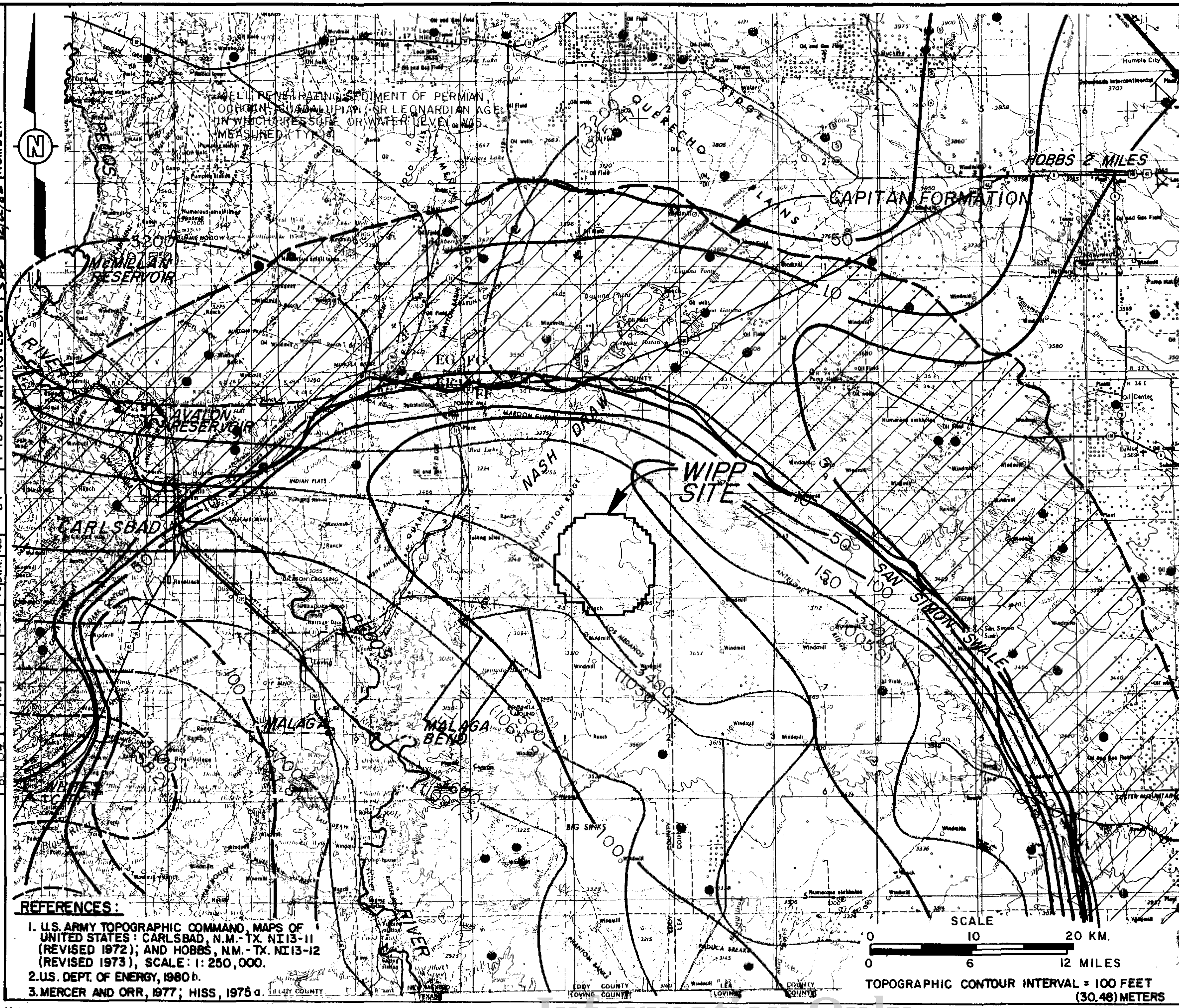

LEGEND:

POSITION OF CAPITAN FORMATION:

- APPROXIMATE POSITION OF EXTREME SHELF-WARD EDGE
- BASINAL EDGE
- HEAD MEASURED IN DELAWARE MOUNTAIN GROUP AQUIFER SYSTEM, DASHED WHERE INFERRED
- HEAD MEASURED IN THE CAPITAN AND SHELF AQUIFER SYSTEM.
- LINE OF EQUAL CHLORIDE-ION CONCENTRATION IN KILOGRAMS PER CUBIC METER IN THE DELAWARE MOUNTAIN GROUP, CAPITAN REEF AND SHELF DEPOSITS.
- 3200 (9754) HEAD CONTOUR INTERVAL IN FEET (METERS)
- GENERAL FLOW DIRECTION

NOTES:

1. CONTOURS OF HEAD ARE IN FEET (METERS) ABOVE SEA LEVEL. VALUES OF HEAD ARE EXPRESSED AS WATER WITH SPECIFIC GRAVITY OF 1.00. CONTOURS ARE DASHED WHEREVER DATA ARE SPARSE OR OF DOUBTFUL RELIABILITY.
2. THE CONTOURS EXPRESS A GENERALIZED REGIONAL HEAD CONSIDERED TO BE REPRESENTATIVE DURING THE PERIOD 1960 TO 1970. SIMILARLY, CONTOURS IN THE CAPTAIN AQUIFER ARE AN INTERPRETATION OF THE HEAD REPRESENTATIVE FOR THE LATER PART OF 1972.
3. CONSIDERABLE SUBJECTIVE JUDGMENT WAS USED IN CONTOURING THE HEAD DATA POINTS. CONSIDERATION WAS GIVEN TO THE YEAR IN WHICH THE HEAD WAS MEASURED AND THE RELIABILITY OF THE DATA.
4. THE CHLORIDE CONCENTRATION ISOPLETHS ARE BASED ON INTERPRETATIONS BY HISS (1975a). CHLORIDE CONCENTRATION ISOPLETHS ARE BASED ON LOWEST CONCENTRATION SHOWN OR INTERPRETED TO BE PRESENT. WITHIN ANY AREA DELINEATED BY TWO LINES, GROUNDWATER HAVING A CHLORIDE CONCENTRATION INDICATED BY THE LINE VALUES IS PROBABLY PRESENT IN AT LEAST ONE WATER BEARING ZONE; GROUNDWATER AT HIGHER CHLORIDE-ION CONCENTRATION THAN THAT INDICATED BY THE CONTOUR VALUES IS GENERALLY PRESENT ALSO.
5. THE 100 KG/M^3 CHLORIDE ISOPLETH SOUTHWEST OF MALAGA IS NOT SUBSTANTIATED BY MEASURED DATA (HISS, 1975a).

FIGURE 2-5

POTENTIOMETRIC SURFACE AND CHLORIDE CONCENTRATION ISOPLETHS OF THE DELAWARE BASIN

PREPARED FOR

WESTINGHOUSE ELECTRIC CORPORATION
ALBUQUERQUE, NEW MEXICO

D'APPOLONIA

DRAWING NUMBER NM78-648-B51 | DRAWN BY RGN 1-13-82 | CHECKED BY RES | APPROVED BY SHD

19 1253 HERCULENE. A&B SMITH CO., PGH., PA

DRAWN BY	D. Weick	CHECKED BY	RE	DRAWING NUMBER NM78-648-A41
	12-21-82	APPROVED BY	[illegible]	

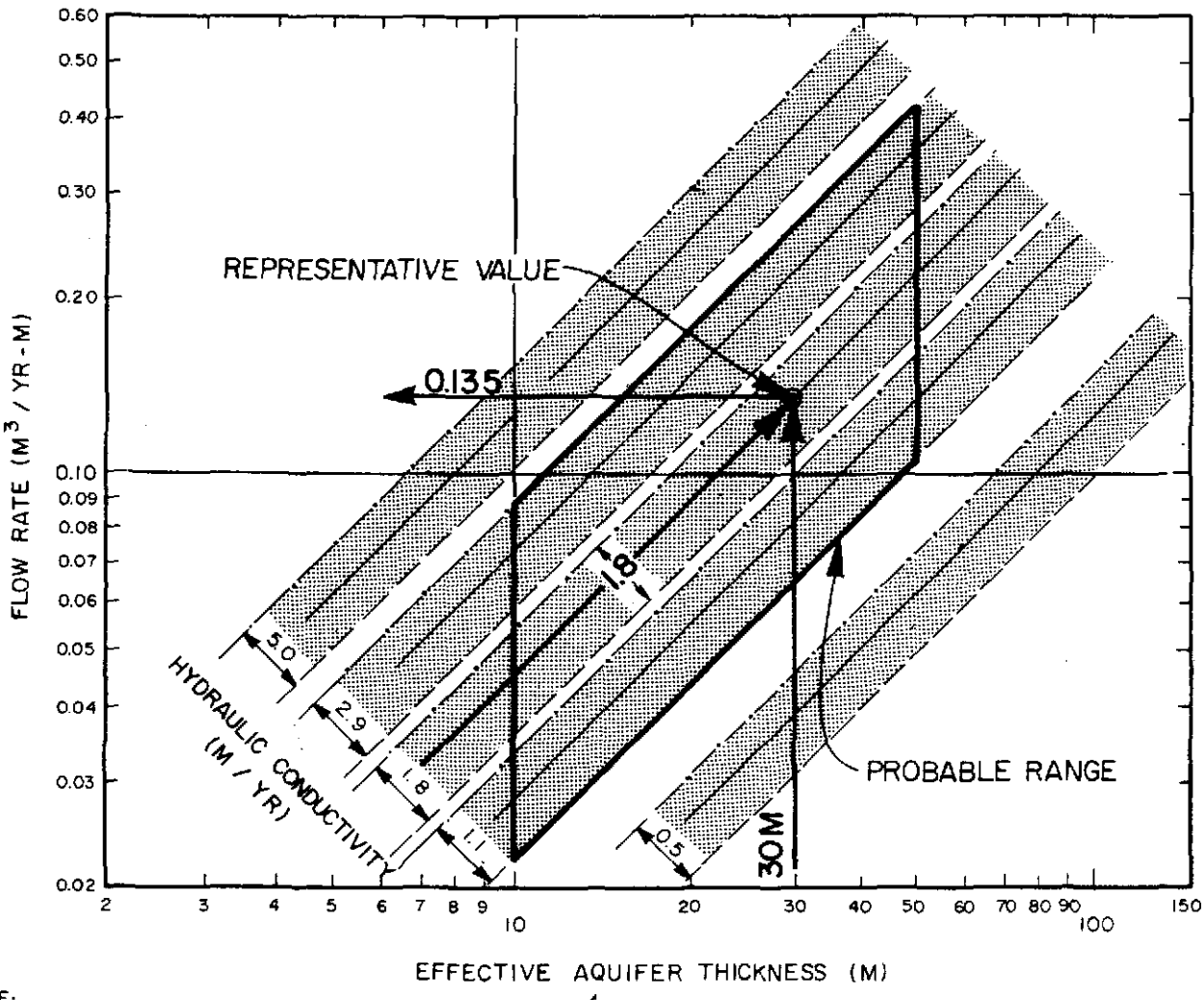

NOTE:
RANGE OF HYDRAULIC GRADIENT (M/M) IS SHOWN AS FOLLOWS:

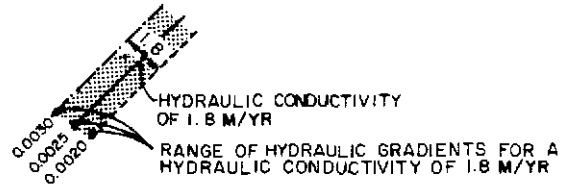

NOTES:

1. TO DETERMINE FLOW RATE SELECT AN EFFECTIVE AQUIFER THICKNESS, MOVE VERTICALLY UNTIL INTERSECTION WITH THE HYDRAULIC GRADIENT LINE FOR THE HYDRAULIC CONDUCTIVITY SELECTED THEN MOVE HORIZONTALLY TO READ THE FLOW RATE.
2. RANGE OF VALUES BASED ON DATA DISCUSSED IN SECTION 2.2.

FIGURE 2-6

FLOW RATE
IN THE BELL CANYON AQUIFER FOR A
RANGE OF HYDRAULIC PARAMETERS

PREPARED FOR

WESTINGHOUSE ELECTRIC CORPORATION
ALBUQUERQUE, NEW MEXICO

D'APPOLONIA

Samples taken from the Bell Canyon Formation reveal that chloride concentrations generally range from 1 to 190 kg/m^3, with dissolved solids levels typically above 20 kg/m^3 for much of the Bell Canyon fluid (Hiss, 1975a and 1975b). Figure 2-5 also shows the chloride concentration in the DMG. This map was generated by Hiss (1975a) using data obtained from oil field water quality analyses. Data concerning well depth and construction are not available and thus absolute correlation across the basin is difficult. Reportedly, the isopleths (contours of equal ion concentrations, chloride) were constructed to reflect general trends in the basin. In some instances, chloride concentrations reported at various localities are higher than indicated by the isopleths.

Chloride concentration generally increases from southwest to northeast in the basin as shown in Figure 2-5, with isopleths roughly parallel to the potentiometric surface in the DMG. The specific stratigraphic source of chloride is difficult to determine, although there is evidence that at least some of it is derived from the overlying Castile Formation. However, this evidence is not definitive enough to preclude the possibility that most of the dissolved solids originate from sources other than the Castile Formation, for instance, from within the DMG.

In summary, the density-corrected potentiometric surface shows that flow in the Bell Canyon aquifer is from southwest to northeast in the region of the WIPP site. Based on an average hydraulic conductivity of 1.8 meters per year, porosity of 0.16, and hydraulic gradient of 0.0025 meter per meter, the water particle velocity is approximately 0.03 meter per year. This means that the groundwater travel time in the Bell Canyon from underneath the center of the WIPP site to the nearest point on the reef is approximately 500,000 years. The progressive gradual increase in chloride content in the direction of flow throughout most of the Bell Canyon Formation and the low aquifer flow rate suggest that a relatively uniform process involving chloride dissolution is occurring in the basin.

Communication between the DMG and the Capitan, San Andres, and shallow aquifers is determined by hydrogeologic parameters. Hiss (1975a) has compiled stratigraphic cross sections, potentiometric surface maps, and hydraulic characteristics of the DMG and Guadalupian age rocks in the Delaware Basin. Hiss' work indicates that the Capitan interfingers with members of the DMG and that the potentiometric surface in the DMG is greater than the Capitan Reef aquifer and some discharge from the DMG to the Capitan is expected.

Stratigraphic cross sections in Hiss' work show that sandstone tongues of the Cherry Canyon Formation interfinger the San Andres limestone. Thus, hydraulic communication between the two units is likely. Hiss, however, reports that the average hydraulic conductivity (based on laboratory measurement) of the shelf aquifers, including the San Andres, is about 4.8 meters per year compared with the DMG average hydraulic conductivity of 1.8 meters per year. The low conductivity of both units restricts the transfer of large quantities of groundwater. The head differential between the DMG and San Andres is difficult to determine from literature sources, but it appears to be similar or less than the differential at the Capitan-DMG interface.

A relatively small amount of literature information is available on the degree of hydraulic communication between shallow aquifers and the DMG. Major dissolution or fracture zones are the most probable areas where hydraulic communication between shallow aquifers and the DMG could occur.

Capitan Aquifer

This reef complex, which also includes the Goat Seep limestone, forms a long, narrow aquifer that abuts the upper DMG formations and forms the boundary of the Delaware Basin (Figure 2-5). The Capitan aquifer is more than 610 meters thick in some areas and averages 16 kilometers in width.

Pumping tests run in the aquifer indicate that hydraulic conductivity values in the area range from 120 to 2,800 meters per year, which is several orders of magnitude higher than the Bell Canyon Formation (U.S. Department of Energy, 1980b). The average value of hydraulic conductivity for the Capitan Reef has been reported as 550 meters per year (Hiss, 1975a). The relatively high hydraulic conductivity of the Capitan aquifer has resulted in the unit being used as a major supply of water for oil field flooding operations in the Delaware Basin. The effects of large amounts of pumping in the Capitan aquifer are evident when observing groundwater contours in the area (Figure 2-5). The Capitan aquifer exhibits a much lower potentiometric surface east of the WIPP site than does the adjoining DMG. This implies a much quicker response to pumping and thus a higher hydraulic conductivity in the Capitan aquifer. Flow in the Capitan is in an east-southeasterly direction with an average gradient of 0.003 meters per meter toward pumping centers located approximately 100 kilometers southeast of the WIPP site.

West of the Pecos River, water quality in the Capitan is generally good and total dissolved solids are low. However, east of the river, the chloride concentration is usually greater than 5 kg/m^3 and total dissolved solids levels render the water unusable for purposes other than oil field flooding applications. Chloride concentrations reported by Hiss (1975a) range from less than 1 kg/m^3 in the northeastern portion of the basin to greater than 25 kg/m^3 north of the WIPP facility.

Castile Formation

In areas where the Castile Formation is deep, hydraulic conductivity values of both the halite and anhydrite units are low (Mercer and Orr, 1977), and the formation acts as a confining layer. The hydraulic conductivity of the Castile Formation has been measured using drill-stem testing, with values from 10^{-6} to 10^{-7} meters per day (10^{-9} to 10^{-10} centimeters per second) recorded (Sandia, 1980b). In areas west of the WIPP site where the Castile is near the surface, leaching of halite and the effects of weathering may result in an increase in permeability.

Occurrence of fluid in the Castile has been most apparent as "isolated pockets of brine and associated hydrogen sulfide gas" (Powers, et al., 1978; Mercer and Orr, 1977) which are occasionally encountered during drilling operations. These "reservoirs" have higher potentiometric surfaces than the Bell Canyon aquifer and do not appear to be connected with the DMG.

Observations made in the WIPP-12 and ERDA-6 boreholes indicate storage and flow of brine in fractures of up to 5 millimeters aperture, with the majority of storage appearing to be in microcracks (Popielak, et al., in preparation). The brine reservoirs have formed in response to deformation and are isolated from one another by zones of Castile anhydrite of very low permeability. In addition, the brine pockets and wide (up to 5 millimeters) fractures are typically associated with the uppermost anhydrite unit in the sequence rather than with the lowermost unit overlying the Bell Canyon aquifer (Popielak, et al., in preparation). Although the presence of fractures cannot be ruled out, it is believed that the low permeabilities discussed in the previous paragraph are representative of most of the lower anhydrite unit overlying the DMG.

Salado Formation

As in the case of the Castile Formation, the evaporites of the Salado Formation exhibit very low hydraulic conductivity. Measurements taken from the Salado Formation indicate values ranging from 10^{-5} to 10^{-7} meters per day (Sandia, 1980b), which are less than the measured average hydraulic conductivity of the Bell Canyon Formation.

In the Nash Draw area, relatively permeable residuum at the Salado-Rustler contact is saturated with brine, thus forming a saline aquifer of limited areal extent (Figure 2-7). The source of the salt is probably halite near the top of the Salado Formation and the bottom of the Rustler Formation. This aquifer probably discharges to the Pecos River near Malaga Bend (U.S. Department of Energy, 1980b).

TME 3166

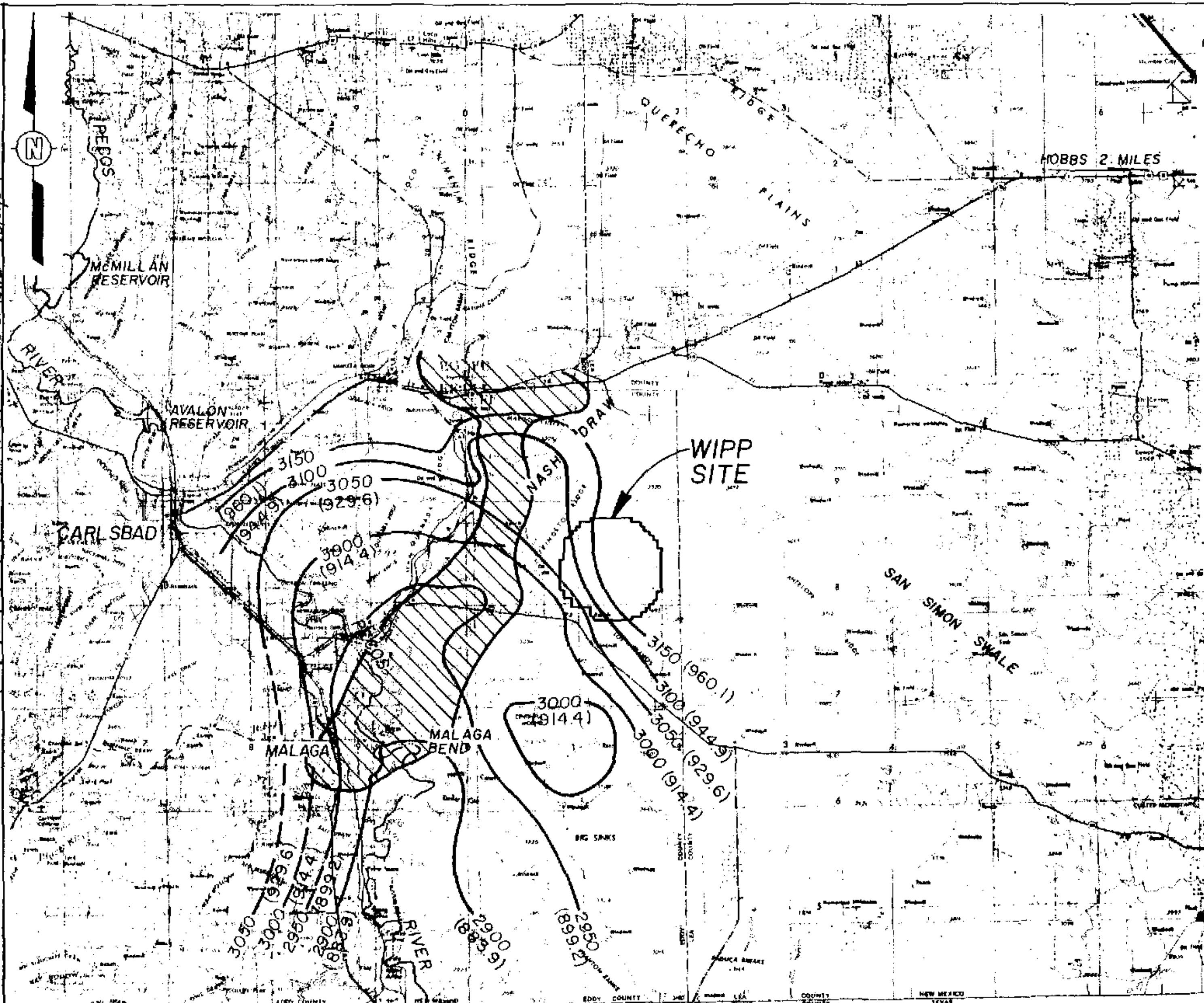

LEGEND:

FEET — 3000 (914.4) — METERS: POTENTIOMETRIC ELEVATION CONTOUR BASED ON WATER LEVELS MEASURED IN WELLS, 1952-1973. ACCORDINGLY, POTENTIOMETRIC LEVELS REFLECT NATURAL, IN SITU FLUID SPECIFIC GRAVITY. DASHED WHERE APPROXIMATELY LOCATED.

EXTENT OF BRINE AQUIFER ALONG RUSTLER-SALADO CONTACT.

REFERENCES:

1. U.S. ARMY TOPOGRAPHIC COMMAND, MAPS OF UNITED STATES: CARLSBAD, N.M.-TX., NI13-11 (REVISED 1972); AND HOBBS, N.M.-TX., NI13-12 (REVISED 1973) SCALE 1:250,000.
2. U.S. DEPARTMENT OF ENERGY, 1980b
3. MERCER AND ORR, 1977.

NOTE:

1. DATUM IS MEAN SEA LEVEL; VALUES GIVEN IN FEET (METERS).

TOPOGRAPHIC CONTOUR INTERVAL = 100 FEET (30.48) METERS

SCALE

0 10 20 KM.

0 6 12 MILES

FIGURE 2-7

OBSERVED POTENTIOMETRIC LEVELS OF THE RUSTLER FORMATION

PREPARED FOR

WESTINGHOUSE ELECTRIC CORPORATION
ALBUQUERQUE, NEW MEXICO

D'APPOLONIA

DRAWING NUMBER NM78-648-B54 | DRAWN BY G.J.G. 10-16-80 | CHECKED BY | APPROVED BY

Rustler Formation

The Rustler Formation consists of interbedded anhydrite, dolomite, siltstone, and halitic claystone. Water-bearing units include the Culebra and Magenta dolomites. Of the two units, the vuggy Culebra dolomite is more permeable and laterally persistent than Magenta, which exhibits a transmissivity between 10^{-2} and 10^{-4} square meters per day (Mercer and Gonzalez, 1981).

Permeability tests performed in the region indicate an average hydraulic conductivity in the Culebra dolomite of 4.9 meters per day (U.S. Department of Energy, 1980b). Higher conductivities exist in the Nash Draw area where the unit has undergone some collapse and fracturing (Cooper and Glanzman, 1971).

The potentiometric surface of the Rustler Formation is generally lower than the potentiometric surface in the DMG. The brine aquifer and the potentiometric surface identified in the Rustler Formation are shown in Figure 2-7. These representations are based on data compiled from wells during the period 1962 through 1973 (Mercer and Orr, 1977). Recently, some revision to the potentiometric surface has been suggested (Gonzalez, in preparation).

Water quality in the Rustler Formation is generally poor with total dissolved solids contents ranging from 10 to 118 kg/m^3 (U.S. Department of Energy, 1980b).

3.0 SALT DISSOLUTION FEATURES AND MECHANISMS

This chapter presents a brief overview of some of the evidence for dissolution of halite-rich horizons and discussion of the possible hypotheses concerning the origin of the dissolution features. An analysis of the physical and chemical mechanisms which might result in halite dissolution is also presented to assess potential rates of salt removal by these processes.

3.1 OVERVIEW OF SALT DISSOLUTION FEATURES

The currently available evidence for large- and small-scale halite dissolution in the Castile and Salado Formations of the Delaware Basin is based on outcrop, geophysical, and geochemical measurements. The evidence that some dissolution has occurred appears incontrovertible. However, of primary concern is the extent of postdepositional dissolution, its timing, and the rate and significance of its continued action. Generally, two types of dissolution have been proposed to explain the observed features: shallow dissolution and deep-seated dissolution. Shallow dissolution results from removal of soluble rock, such as limestone and halite, by downward percolating water, either from the surface or from the Rustler aquifer which overlies the Salado Formation. Deep-seated dissolution theories involve upward migration of water along fractures and through pores from the DMG and Capitan Reef aquifers into the Castile and Salado Formations with concurrent removal of halite. The potential for salt removal by the Bell Canyon aquifer and its effect on deep-seated dissolution is of prime concern in this study. This is because it is much more difficult to observe and quantify than the near-surface dissolution which is progressing at a relatively low rate and does not represent a hazard to the WIPP facility (Bachman, 1974; Bachman, 1980b).

The general evidence of deep-seated dissolution of halite deposits in the Delaware Basin consists of geochemical and geologic observations. Geochemical evidence of salt dissolution is provided by the composition of groundwater from the Bell Canyon and Capitan aquifers. Most of these

fluids are saline (Hiss, 1975a) and, while the origin of the dissolved solids is open to question, it seems likely that the groundwaters have dissolved some salt from the Salado and Castile Formations. Additionally, studies by Lambert (1977) found that saline and fresh waters from the Rustler and Capitan aquifers are meteoric (based on isotopic deuterium/hydrogen and oxygen 18/oxygen 16 ratios), indicating relatively recent origins, while saline water from the DMG and potash mine seeps from the Salado Formation appear to have longer residence time (greater age). As a result, the rate of dissolution associated with the DMG is apt to be less than that associated with the Capitan Reef.

Geologic features which have been investigated and thought by Anderson (1978) to be related to deep-seated dissolution activity are shown in Figure 3-1 and include:

- Thinning of the Halite I and II deposits in the Castile Formation in the western region of the basin.
- Big Sinks and Poker Lake depressions in the central basin area exhibit removal of portions of the Halite I and II deposits.
- San Simon Swale and Sink located adjacent to the Capitan Reef at the eastern perimeter of the basin are believed associated with dissolution of underlying halite layers.
- Smaller sinks, domes, and breccia pipes indicate localized dissolution in several areas of the basin.

Other features shown in Figure 3-1, such as Nash Draw, have generally been identified as shallow dissolution phenomena; however, the origin of numerous other small sinks, domes, and breccia pipes located in the basin is open to debate. An in-depth presentation of the dissolution features in the basin is currently being prepared (Lambert, in preparation).

DRAWING NUMBER	NW 78-648-A36
CHECKED BY	RES 12/14/82
APPROVED BY	SHD 12/14/82
RAL 1-13-82	
DRAWN BY	
4A 4A	
100% OR	
5A	

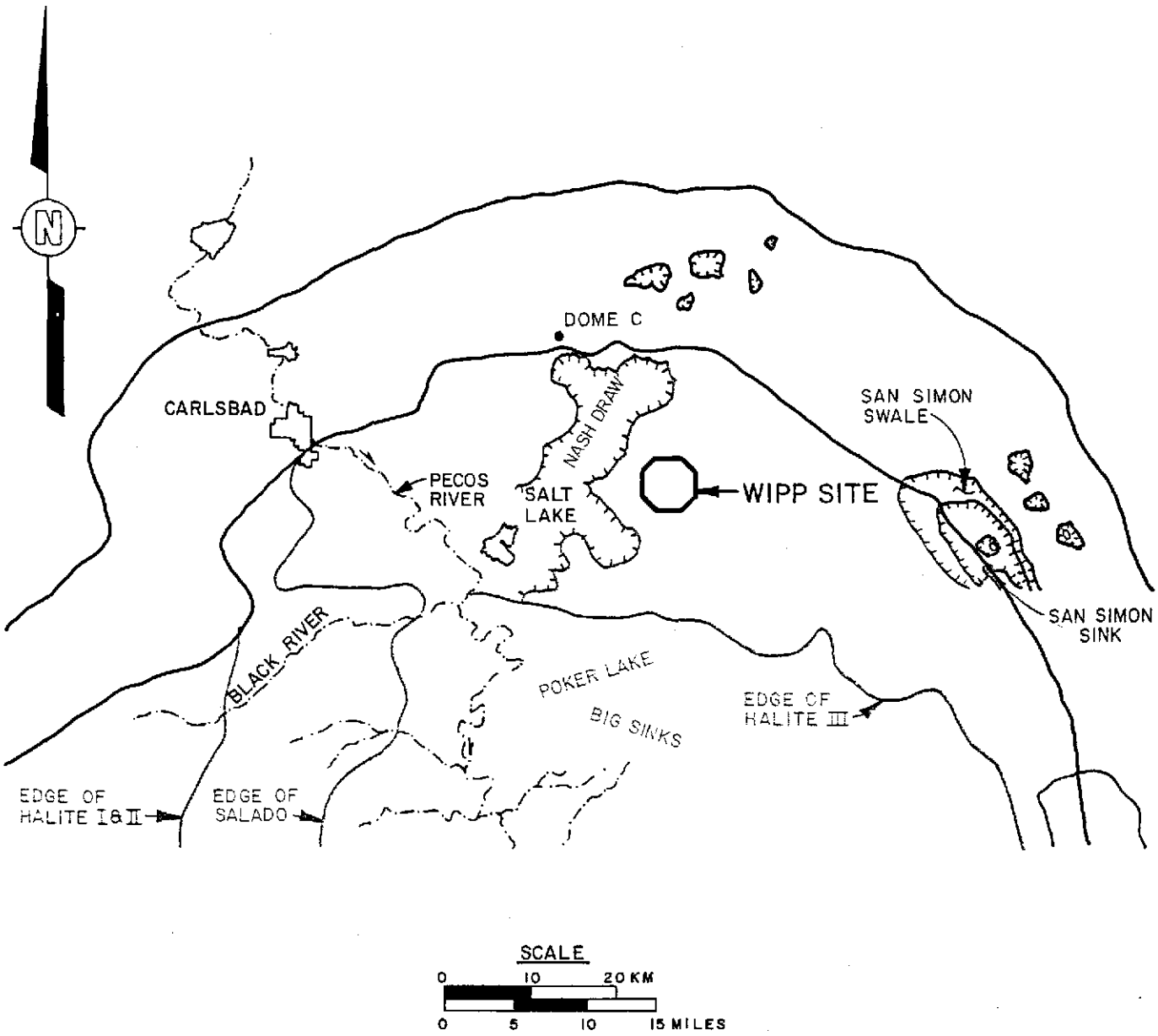

LEGEND

LARGE SINKS OR DEPRESSIONS

EDGE OF HALITE UNIT

REFERENCE

ADAPTED FROM ANDERSON, 1978.

FIGURE 3-1

DISSOLUTION FEATURES IN SITE VICINITY

PREPARED FOR

WESTINGHOUSE ELECTRIC CORPORATION
ALBUQUERQUE, NEW MEXICO

D'APPOLONIA

The western dissolution wedge identified in the Halite I and II deposits and shown in Figure 3-1 has been attributed to deep dissolution by Anderson (1978), while Bachman (1980b) cites a shallow mechanism as the cause. An apparent unconformity at the Castile-Salado interface with the absence of Halite III in the north basin area is believed a pre-Salado event (Anderson, 1978), which may be associated with shallow dissolution and erosion.

Depressions such as Poker Lake and Big Sinks suggest dissolution of Halites I and II (Anderson, 1978) due to the presence of down-dropped blocks of Halite III. Similarly, Anderson (1978) believes the San Simon Swale and Sink are associated with deep-seated dissolution phenomena, although Bachman (1980b) considers these features to be a combination of erosion, solution, and fill phenomena related to shallow dissolution.

Nash Draw, located in the northwest basin area, consists of a deep depression in which the Mescalero Caliche is absent, as shown in Figures 3-1 and 3-2. This depression is believed associated with shallow dissolution according to Bachman (1974), while Anderson (1978) ascribes related domal structures to deep-seated phenomena.

Evidence which appears incontrovertible that a certain amount of deep-seated dissolution has occurred consists of breccia pipes which extend up through the Salado Formation. However, all of the documented breccia pipes (Bachman, 1980) are located above the Capitan Reef aquifer; none are located above the DMG aquifer. Additionally, the presence of saline waters in the Bell Canyon and Capitan Reef aquifers which underlie or are adjacent halite units suggests that some form of deep-seated dissolution has occurred throughout the basin.

Other features which provide evidence of dissolution are further discussed by Anderson (1978), Bachman (1980b), and Lambert (in preparation). The features cited above are the most prominent with respect to supporting data and indicate that some deep-seated dissolution has

DRAWN BY	RW	CHECKED BY	RES	DRAWING NUMBER NM78-648-A31
	11-23-81	APPROVED BY	SHD	

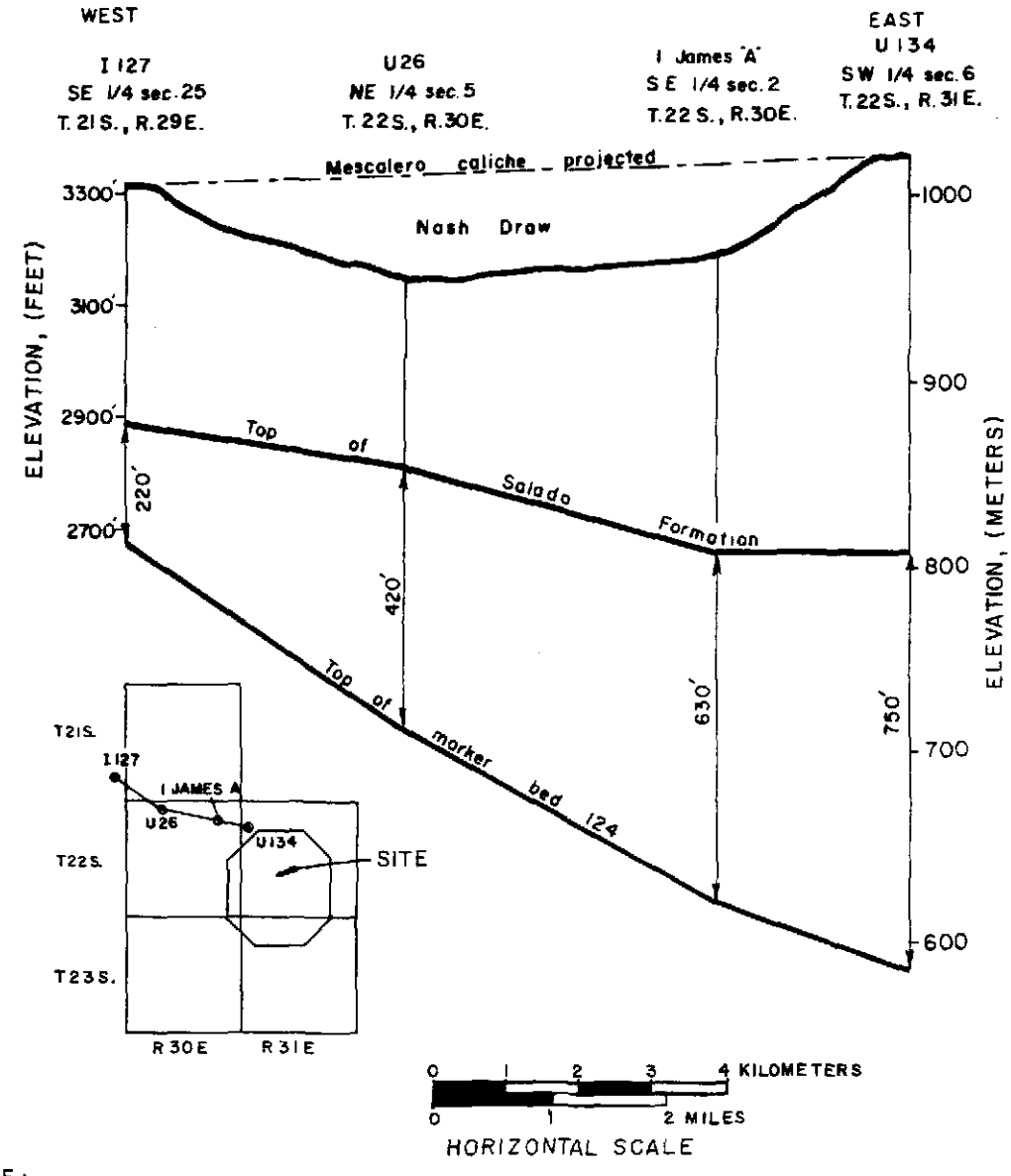

REFERENCE:

U.S. DEPARTMENT OF ENERGY, 1980b

FIGURE 3-2

CROSS SECTION SHOWING RELATIONSHIP OF SUBSIDENCE IN NASH DRAW TO DISSOLUTION OF SALT IN SALADO FORMATION

PREPARED FOR

WESTINGHOUSE ELECTRIC CORPORATION
ALBUQUERQUE, NEW MEXICO

D'APPOLONIA

occurred. As indicated above, the origin of most of the features is open to debate.

To understand if and how such dissolution could occur and where it may be important in the Delaware Basin, salt dissolution mechanisms and the transport capability of the Bell Canyon aquifer were investigated. The dissolution mechanisms by which a halite-rich horizon may be dissolved from below are discussed in Section 3.2. Additionally, the role of the aquifer system as a potential sink and transporting medium for dissolved salt has been analyzed and presented in Chapter 4.0.

3.2 MECHANISMS OF DEEP-SEATED DISSOLUTION

3.2.1 Introduction

Anderson (1978) and Anderson and Kirkland (1980) have suggested that the nature of dissolution features such as breccia pipes and sinks in the Delaware Basin is indicative of deep-seated rather than near-surface dissolution of salt. They envisage the sources of water for the dissolution process to be the Capitan limestone and Bell Canyon aquifers, which underlie the Castile and Salado Formations, rather than infiltrating surface waters. It is the purpose of this section to review the physical and chemical mechanisms by which salt may be removed from the Castile and Salado Formations by solution from below and to estimate the relative efficiency of these processes in removing salt from halite units within the Delaware Basin. In order to simplify the discussion in the remainder of this chapter, salt dissolution only in the Castile Formation will be used to illustrate the mechanisms. Salt dissolution in the Salado Formation could occur due to similar mechanisms but the dissolution rates would be smaller because of the larger distance between a dissolution front and the Bell Canyon aquifer. The larger distance yields a smaller concentration gradient and, hence, as is evident in Sections 3.2.2 and 3.2.3, a smaller rate of salt removal.

Deep-seated dissolution may occur through the agency of an underlying aquifer by way of a fracture or simply through the pores of an intervening layer between the aquifer and soluble horizon. In this case, the intervening layer would be a lower Castile anhydrite and the soluble horizon a Castile halite.

With a potentiometric surface above the lowest level of the soluble horizon, water will ascend through the fracture or porous zone until it comes into contact with the soluble rock. The ascending flow will commence dissolving until the solution is saturated. At this point, the process would essentially cease unless there is a mechanism by which the saturated solution is removed down the fracture and more unsaturated solution is allowed to ascend. The likely mechanisms for salt removal associated with fractures or porous zones are molecular diffusion and convective transport, referred to by Anderson and Kirkland (1980) as "brine density flow," through the liquid column or porous media.

Other hypotheses which include the DMG as the sink for saturated brines are downward percolation of meteoric water and Lambert's (in preparation) hypothesis of "strata-bound dissolution." In the latter, water dissolves salt while migrating approximately horizontally along soluble strata. The Bell Canyon aquifer could potentially provide a sink for saturated brines produced by this hypothesis. In the context of this report, both the convective and diffusive mechanisms may be regarded as processes occurring under conditions of the Anderson (1978) hypothesis since they require flow through Castile anhydrites in order to reach the Bell Canyon Formation. Thus, the calculated maximum rates of salt removal above a fracture or through a porous zone discussed in Chapters 3.0, 4.0, and 5.0 apply approximately to all hypotheses. Since the physical processes described by Anderson (1978) and Anderson and Kirkland (1980) are readily analyzed, their hypothesis is used in subsequent sections to illustrate the mechanisms for salt removal.

3.2.2 Diffusion Controlled Dissolution

The diffusion process is always in operation in any system in which there is a concentration gradient of solute. It is, however, an extremely inefficient mechanism for material removal and, in most natural flow systems, unobservable due to processes such as convection which can result in much greater mass transport. In general, diffusion will occur through pore spaces in a rock such as anhydrite, as well as through fluid-filled fractures.

The rate of diffusion through a fracture such as that illustrated in Figure 3-3 may be calculated from Fick's First Law of Diffusion (Crank, 1975) which, at steady state, is given by:

$$M_d = -D \frac{\Delta C}{\Delta z} \qquad (3\text{-}1)$$

where

M_d = the mass flux per unit area,

D = the diffusion coefficient,

ΔC = the concentration difference between top and bottom of the fracture, and

Δz = the height of the fracture (diffusion zone).

Diffusion coefficients for salts in water are on the order of 10^{-9} square meters per second (m^2/sec) (Weast, 1970) and a value of 1 x 10^{-9} m^2/sec has been adopted here. The solution contacting the soluble horizon (Figure 3-3) will, since salt dissolves rapidly, have a sodium chloride (NaCl) concentration close to the saturation value of 315 (kg/m^3) (Weast, 1970). It should be noted that while this value of concentration applies for 20 degrees Celsius, the effect of raising the temperature to 50 degrees Celsius is to raise solubility per unit volume by only one percent (Grabau, 1920). To obtain the concentration difference, ΔC, for diffusive mass transport through a fracture, the sodium chloride concentration in the aquifer must be established. As indicated in Figure 2-5, the concentration of chloride, and therefore NaCl, varies

11A	100	10A	100	DRAWN BY	D. Weick 12-21-82	CHECKED BY	RES 12/22/82	DRAWING NUMBER	NM78-648-A40
11A	BR	10A	OG			APPROVED BY	THD 12/22/82		

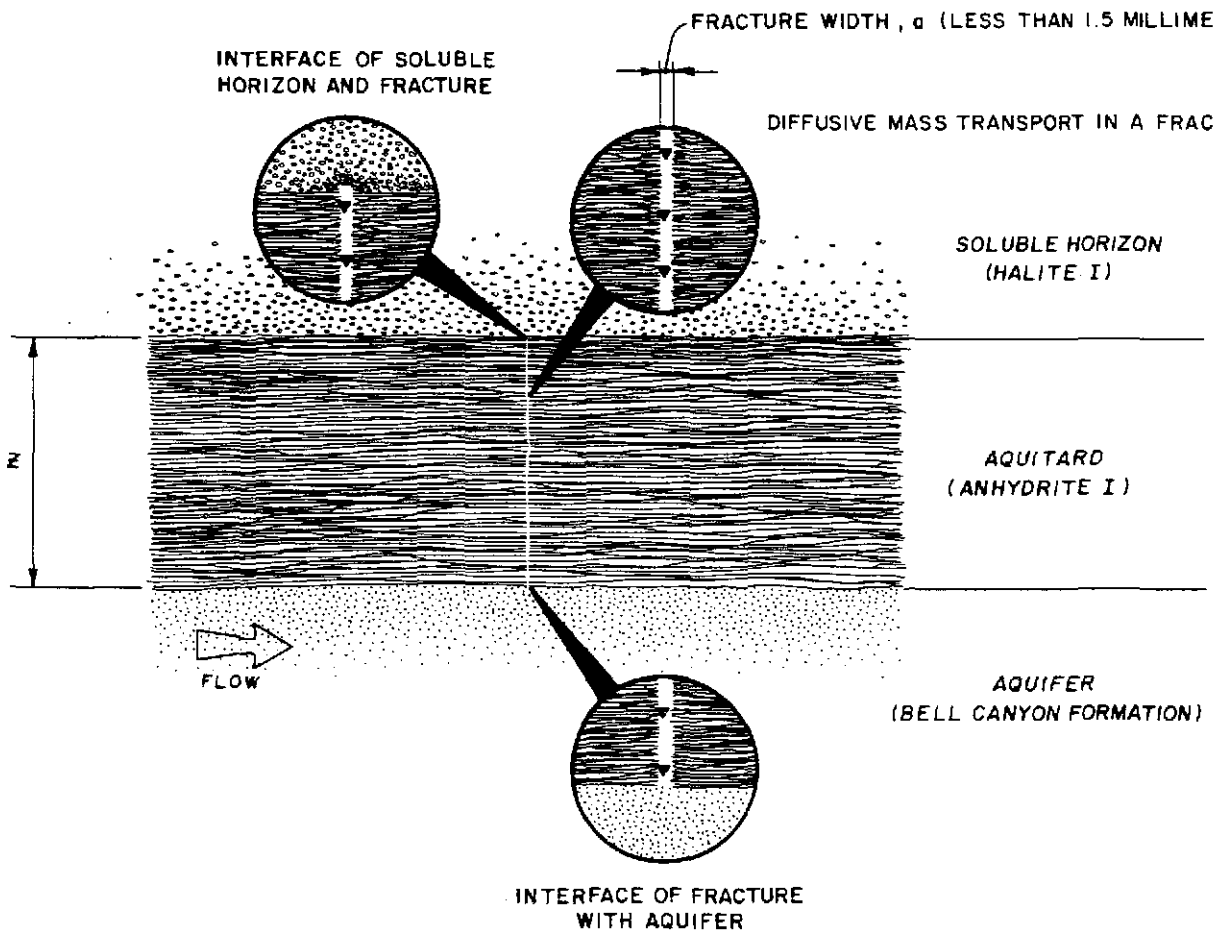

NOTE:

1. CONVECTIVE MASS TRANSPORT MAY OCCUR IN FRACTURES GREATER THAN 1.5 MILLIMETERS.

LEGEND

▼ DIFFUSION

FIGURE 3-3

SCHEMATIC OF DIFFUSION IN A SINGLE FRACTURE

PREPARED FOR

WESTINGHOUSE ELECTRIC CORPORATION
ALBUQUERQUE, NEW MEXICO

D'APPOLONIA

throughout the basin and for illustrative purposes an average value of 115 kg/m^3 NaCl (equivalent to 70 kg/m^3 of chloride; Figure 2-5) has been used. Thus, ΔC is about 200 kg/m^3 NaCl. The height of the fracture, Δz, is the distance between the aquifer and the salt horizon which is being dissolved. This is on the order of the thickness of the lowermost Castile anhydrite, 100 meters (Table 2-1). Substituting these values into Equation (3-1), a mass flow rate of 2×10^{-9} kg per square meter (kg/m^2) of fracture per second (0.06 kg/m^2 per year) is obtained.

The volume of salt removed is estimated at 3×10^{-5} cubic meters per square meter of fracture per year based on the mass flow rate and the density of salt (2,160 kg/m^3; Weast, 1970). This is equivalent to a rate of upward movement of the dissolution front of 3×10^{-5} meters per year if the front moves with the same geometry as the fracture.

In the above discussion of dissolution by diffusion through a fracture, it was assumed that a uniformly varying steady state concentration gradient had developed. For the case of instantaneous formation of a 100 meter fracture, the initial gradient at the top of the fracture is very steep, thereby resulting in a high initial propagation rate. As salt dissolution and fracture propagation continue, the variation in salt concentration becomes more gradual due to diffusion in the fracture and the propagation rate declines. To evaluate the rates at which a fracture moves under these conditions, a transient form of the one-dimensional diffusion equation (Crank, 1975) was solved. The parameter values are identical to the ones used in the steady state calculation except that the initial chloride concentration in the fracture is assumed to be constant at 70 kg/m^3 instead of uniformly varying at a 1.2 kg/m^3 per meter gradient. The analytical solution of the diffusion equation gives the chloride concentrations at different locations within the fracture as a function of time. From this information, the concentration gradient at the top of the fracture, which determines the salt dissolution and propagation rates, is determined.

The calculated propagation rates for different times beyond initial fracture formation are as follows:

TIME (years)	PROPAGATION RATE (meters per year)
1	290×10^{-5}
10	230×10^{-5}
100	89×10^{-5}
1,000	29×10^{-5}
10,000	9×10^{-5}
100,000	3×10^{-5}

This analysis indicates that on the order of 100,000 years is required for the upward fracture movement to decline to the assumed steady state rate of 3×10^{-5} meter per year. The initial rate (e.g., time = 1 year) is almost 100 times greater; but after 1,000 years, the rate is less than 10 times the assumed steady state value. Integration of the above results for the first 10,000 years after fracture formation yields a total propagation distance of approximately 2.0 meters. These transient results indicate that fracture propagation due to diffusion is a relatively slow process, even immediately after fracture formation.

Considering diffusion through the anhydrite (porous zone), Equation (3-1) must be modified to take account of variable porosity and non-linear pathways:

$$M_d = - n\overset{*}{T}D \frac{\Delta C}{\Delta z} \qquad (3\text{-}2a)$$

where

n = the porosity of the medium, and

$\overset{*}{T}$ = its tortuosity, a factor which is generally on the order of 0.5 to 0.8 (Bear, 1972).

The product of the porosity of the medium, tortuosity, and molecular diffusion coefficient is often referred to as the effective diffusion coefficient, D_{eff}, where

$$D_{eff} = n\overset{*}{T}D \qquad (3\text{-}2b)$$

The porosities of the anhydrite layer and their tortuosities are unknown. A conservative assumption (maximizing mass flux) is, however, that tortuosity is 1 and that porosity is high, on the order of 0.1. Based on these parameters, the magnitude of dissolution due to diffusion is 0.006 kg/m^2 per year or a vertical propagation rate of 3×10^{-6} meters per year over a uniform, porous area. In view of the conservative tortuosity and porosity assumptions, this is probably an upper bound on diffusive flux through Anhydrite I.

The above discussion demonstrates that diffusion-controlled dissolution is an extremely slow process. The steady state propagation of a single fracture is approximately 3×10^{-5} meter per year and the steady state movement of a dissolution front above a porous zone is on the order of 3×10^{-6} meter per year. For instantaneous formation of a fracture, the initial propagation rate is approximately 3×10^{-3} meter per year, decreasing to 2.9×10^{-4} meter per year in 1,000 years, and reaches steady state conditions (3×10^{-5} meter per year) in 100,000 years. As will be shown below, rapid propagation of a dissolution front could only take place if the effects of convection in the fracture or porous zone are significant.

3.2.3 Convection Controlled Dissolution

Anderson and Kirkland (1980) have suggested that the saturated solution produced at the top of a fracture of the type shown in Figure 3-4 is gravitationally unstable with respect to the underlying, more dilute water in the aquifer and will descend either down the same fracture or down nearby fractures. The effect of saturation on flow can be significant since, at 20 degrees Celsius, saturated brine (approximately 315 kg/m^3) has a density about 20 percent higher than pure water. Anderson and Kirkland built a small model of a fracture system in which brine density flow was observed to occur both within a single fracture and in

DRAWING NUMBER	NM78-648-A39
CHECKED BY	RES
APPROVED BY	SHS
D. Welch 12-21-82	
DRAWN BY	

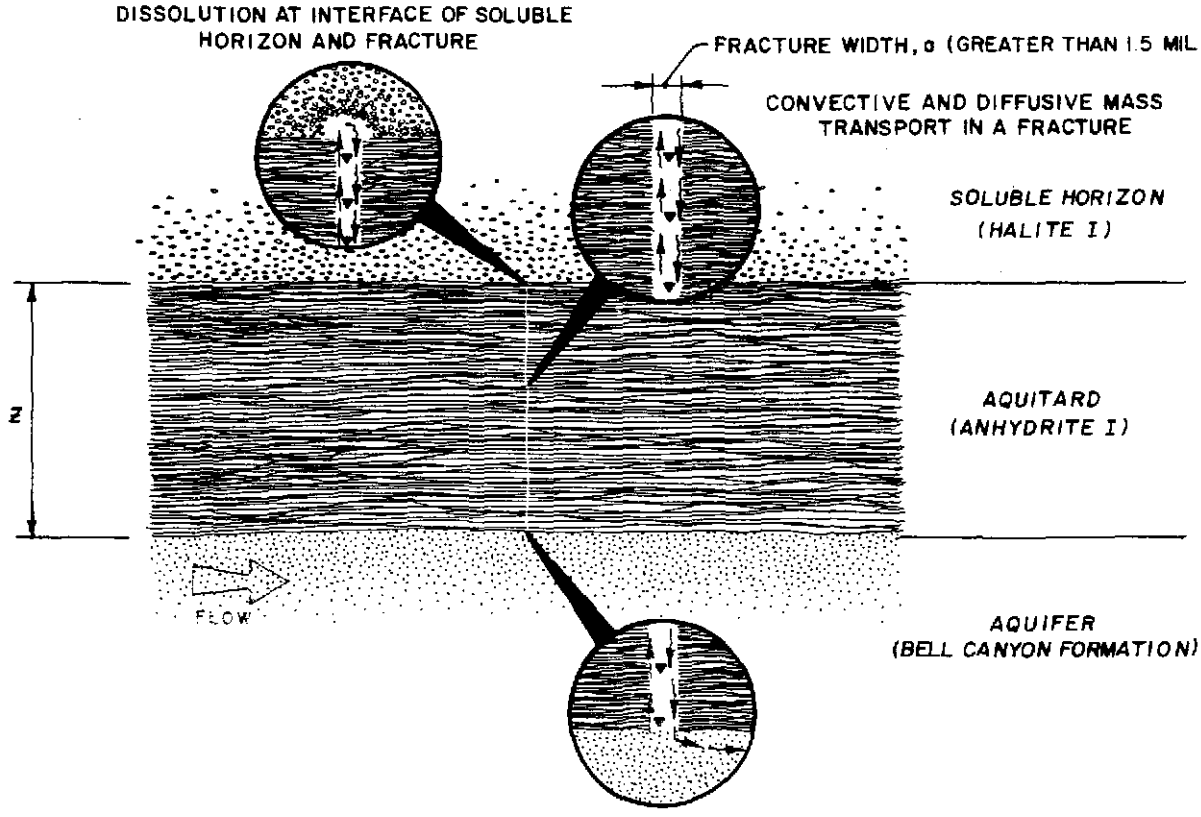

LEGEND

- CONVECTION OF FLUID AT LOWER DENSITY AND SALT CONCENTRATION
- CONVECTION OF FLUID AT HIGHER DENSITY AND SALT CONCENTRATION
- DIFFUSION

FIGURE 3-4

SCHEMATIC OF CONVECTION AND DIFFUSION IN A SINGLE FRACTURE

PREPARED FOR

WESTINGHOUSE ELECTRIC CORPORATION
ALBUQUERQUE, NEW MEXICO

D'APPOLONIA

multiple fractures in the manner depicted in Figures 3-4 and 3-5. They found that brine density flow would initiate within a single fracture when the width of the fracture was on the order of one millimeter or more. Flow began as spatula-shaped tendrils and was maintained as a narrow column of rapidly descending brine (about five centimeters per second), surrounded by stagnant or slowly upward-moving fresher water. If fractures are narrow, then two-way flow, as depicted in Figure 3-5, could develop with a concentration difference of less than 2 kg/m^3 sufficient to initiate and sustain continuous flow. Natural systems, it was argued, could be expected to contain a complex network of fractures to provide separate pathways for ascending and descending fluids. Anderson and Kirkland's model demonstrates that brine density flow is a possible mechanism for dissolving salt horizons from below. It is essentially qualitative, however, in that it does not establish relationships between viscosity, characteristic length of the system (i.e., fracture aperture or length), density gradient, and mass transport. There have, however, been a number of published reports which enable the convective dissolution mechanism to be quantified.

Threshold of Convection in Fractures and Porous Media

Taylor (1954) and Wooding (1959) made pioneering studies of convection driven by concentration gradients in open tubes and in porous media. The minimum density gradient at which convection will begin in a tube containing a solution of variable density was determined by Taylor (1954) as a function of the dimensionless Rayleigh number (R_s) defined as follows:

$$R_s = \frac{\partial \rho}{\partial z} \frac{g a^4}{\mu D} \qquad (3\text{-}3)$$

where

$\partial \rho / \partial z$ = the density gradient,

g = the acceleration due to gravity,

a = the radius of the tube,

μ = the dynamic viscosity, and

D = the solute diffusivity.

DRAWING NUMBER	NM78-648-A45
	12/21/82
CHECKED BY	RES
APPROVED BY	TWD
D. Weick	12-21-82
DRAWN BY	

17A	100	16A	100	15A	100												
17A	BR	16A	OR	15A	BL												

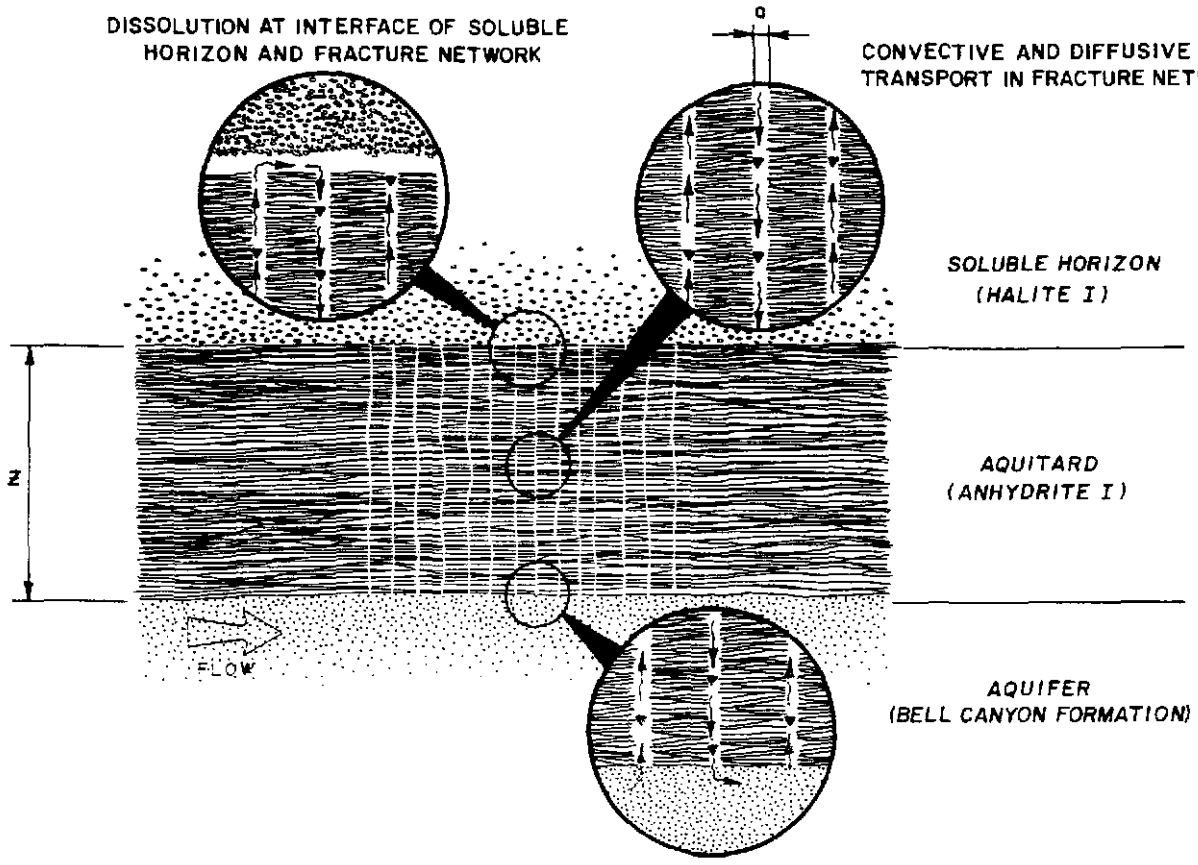

LEGEND

- CONVECTION OF FLUID AT LOWER DENSITY AND SALT CONCENTRATION
- CONVECTION OF FLUID AT HIGHER DENSITY AND SALT CONCENTRATION
- DIFFUSION

FIGURE 3-5

SCHEMATIC OF CONVECTION AND DIFFUSION IN A FRACTURE NETWORK

PREPARED FOR

WESTINGHOUSE ELECTRIC CORPORATION
ALBUQUERQUE, NEW MEXICO

D'APPOLONIA

19 1253 HERCULENE, A&B SMITH CO., PGH., PA

The critical Rayleigh number to initiate flow in a tube was found to be 67.94, a value which corresponds to a mode in which the velocities are antisymmetric about a plane through the axis of the tube. At values of R_s slightly in excess of 67.94, a column of liquid would ascend on one side of the tube and a column would descend on the other side. This is in agreement with the observations made by Anderson and Kirkland (1980).

For the case of a tube filled with a porous medium, Wooding (1959) defined the Rayleigh number R_s^P as:

$$R_s^P = \frac{\partial \rho}{\partial z} \frac{gka^2}{\mu D_{eff}} \tag{3-4}$$

The symbols have the same meaning as in Equation (3-3) except that k is the intrinsic permeability of the medium and D_{eff} refers to the effective diffusivity of solute through the porous medium [Equation (3-2b)].

The intrinsic permeability, k, is related to the hydraulic conductivity K (meters per second) by the equation (Freeze and Cherry, 1979):

$$K = \frac{k\rho g}{\mu} \tag{3-4a}$$

The critical Rayleigh number necessary to initiate flow in a tube with a porous medium was found to be 3.39 by Wooding (1959).

It is instructive to use Equation (3-3) to estimate the conditions under which a fracture would permit convective transfer of dissolved material from overlying salt horizons to an underlying aquifer containing lower salinity water. For this exercise, it will be adequate to use the relationships for cylindrical geometry although in practice such fractures or porous zones would be elongated. Consider the case of a single fracture connecting an aquifer to an overlying salt horizon. Using the same parameters as those for the diffusion calculation in Section 3.2.2 and considering a viscosity of 10^{-3} kilograms per meter per second (Weast,

1970) and a density difference (corresponding to the concentration difference ΔC of 200 kg/m^3 NaCl) of 120 kg/m^3 chloride (Weast, 1970), a primary fracture radius for convection of 1.5 millimeters is obtained. The calculation is in good agreement with the observations of Anderson and Kirkland (1980) who found that density-driven convection commenced when the fracture diameter was about one millimeter. In addition, the result is not very sensitive to the length of the tube, Z (convective dissolution zone), which was taken to be 100 meters. If, for example, the distance dividing the salt horizon from the aquifer was only one meter (the length used by Anderson and Kirkland, 1980), the critical radius would be about 0.5 millimeter.

The above calculations of critical fracture width are based on the simplifying assumption of cylindrical geometry. If the fracture is to be elongated, then the minimum width for convection is reduced, although the results are of similar order to those given above. Wooding's (1960) study may be used to estimate a minimum fracture width of approximately 0.4 millimeter for an aspect ratio (length/width of the fracture) of 20 and approximately 0.2 millimeter for an aspect ratio of 100. As aspect ratio increases, the irregularity of fracture surfaces and occasional fill materials (Popielak, et al., in preparation) will tend to interfere progressively with the convective process so that modeling as long, thin, parallel-sided fractures is inappropriate. It is likely, therefore, that the cylindrical model gives a reasonable order of magnitude calculation of the critical fracture width for solute-driven convection.

Significance of Convection in Fractures and Porous Media

Despite the presence of a five millimeter fracture in the WIPP-12 borehole in the upper anhydrite unit, there is some doubt as to the long-term stability of a small (one millimeter) fracture in a deformable medium such as the Anhydrite I unit of the Castile Formation. No fracture was observed in this unit during studies in the DOE-1 and WIPP-12 boreholes and, unlike the fractures associated with brine pockets, connection with the DMG would not produce substantial fluid pressures

capable of keeping the fracture open. However, it is of interest to consider the possible consequences of the existence of such a fracture. For a fracture which is sufficiently wide that free convection is not inhibited by its walls, it is normal to define the Rayleigh number R_s in the following manner (e.g., Golitsyn, 1979):

$$R_s = \frac{\partial \rho}{\partial z} \frac{g Z^4}{\mu D} \tag{3-5}$$

where Z, the characteristic length scale, is the thickness of the layer over which the density gradient exists rather than its width or diameter. Using 100 meters for Z and taking the density gradient to be constant between upper and lower boundaries with similar magnitudes as presented above, an R_s of 1.2×10^{21} is obtained. Under such conditions, convection would be expected to be extremely turbulent (Golitsyn, 1979) with the rate of mass transfer given by a solute Nusselt number, N_s. In the high Rayleigh number regime, the Nusselt number (ratio of convective to diffusive mass transfer) is approximately given by (Golitsyn, 1979):

$$N_s \tilde{=} 0.1 \, R_s^{1/3} \tag{3-6}$$

For the conditions discussed above, the Nusselt number is about 1×10^6. This means that the rate of convective mass transfer in the wide fracture under consideration would be about 10^6 times as great as diffusive mass transfer under the same conditions. In the previous section, it was estimated that the rate of removal by diffusion through a single fracture would be on the order of 0.06 kg/m^2 per year. Using the above relationship for the Nusselt number, a rate of salt mass transfer as high as 6×10^4 kg/m^2 per year could be obtained for convective flow.

Some recent experiments on salt transport in wide bore tubes (Knapp and Podio, 1979) tend to confirm the approximate convective mass transport relations derived and discussed here. Knapp and Podio experimentally studied brine transport in large bore tubes of 12.62 meters in length. They found that the data, although produced by a vigorous convective

process, could be modeled by using a semiempirical equation of the same form as the diffusion equation (Fick's second law):

$$\frac{\partial}{\partial z}\left(D'\frac{\partial C}{\partial z}\right) = \frac{\partial C}{\partial t} \qquad (3\text{-}7)$$

where

D' = the effective diffusion or dispersion coefficient,
C = solute concentration,
z = vertical distance along the length of the tube, and
t = time.

The effective diffusion or dispersion coefficient was found to be slightly concentration dependent with experimentally determined values on the order of 10 to 50 square centimeters per second (cm^2/sec) (10^{-3} to 5×10^{-3} m^2/sec). These values are approximately six orders of magnitude greater than the diffusion coefficient (1×10^{-9} m^2/sec), indicating that the Nusselt number for convection in these long tubes is on the order of 10^6. This number, which applies for fresh water at the bottom of the tube and saturated brine at the top is in good agreement with the calculated value of 3×10^5 using the relationship for the Nusselt number previously defined [Equations (3-5) and (3-6)]. Thus, experiments at high values of the solute Rayleigh number R_s tend to confirm the order of magnitude of mass transfer (i.e., the Nusselt number) for convection in wide fractures.

Although the long-term stability of large fractures in Anhydrite I is open to doubt, it is conceivable that zones of small fractures, 0.01 millimeter or less in width, could remain stable for extended time periods. Although they would be below the critical radius for convection (approximately 0.2 to 1.5 millimeters), convection could occur in multiple fracture zones where inflow takes place in some fractures and descent in others, similar to the method discussed by Anderson and Kirkland (1980). An analysis of such phenomena requires the use of equations developed for flow in porous media (e.g., Wooding, 1959, 1963; Elder, 1967).

To evaluate the potential rate of mass transfer through a porous zone of sufficient size to support convection, the Rayleigh number will be redefined in terms of the height, Z, of the zone in a manner similar to Equation (3-5) and inferred from work by Golitsyn (1979) and Elder (1967):

$$R_s^P = \frac{\partial \rho}{\partial z} \frac{k\, Z^2\, g}{\mu\, D_{eff}} \qquad (3\text{-}8)$$

Based on this definition and the parameters cited above, the Rayleigh number for a 100-meter-thick porous zone is about 100 for an intrinsic permeability of 10^{-16} square meters (equivalent to an hydraulic conductivity of 10^{-7} centimeters per second) and an effective diffusion coefficient of 10^{-10} m^2/sec. There have been a number of studies of convection in porous media, most of them (e.g., Wooding, 1963; Elder, 1967) for the case where the driving force for convection is a temperature gradient rather than a gradient in solute concentration. The data produced by these authors may, however, be used to model solute-driven convection because of the close analogy between the two types of processes (Golitsyn, 1979).

Elder (1967) found that the critical Rayleigh number for thermal convection in a porous medium was 40. He found that, for Rayleigh numbers up to 5,000, the Nusselt number in terms of heat transfer (ratio of convective to conductive heat transfer) was given by:

$$N_s = R_s^P/40 \pm 10\% \qquad (3\text{-}9)$$

Thus, by making the analogy between heat and mass transfer, an intrinsic permeability of 10^{-16} square meters would lead to a Nusselt number on the order of 2.5. At intrinsic permeabilities less than 4×10^{-17} square meters (equivalent to a hydraulic conductivity of 4×10^{-8} centimeters per second), the Nusselt number is 1.0 and diffusion is the only operative mass transport mechanism. The available data on hydraulic conductivity of the Castile Formation (10^{-9} to 10^{-10} centimeters per

second; Sandia, 1980b) imply that diffusion should dominate the mass transport process in the Castile Formation. The presence of smaller, more permeable zones cannot be excluded, however, and the implications of such zones may be calculated using Equations (3-8) and (3-9).

3.2.4 Salt Dissolution Rates

Two major mechanisms for deep-seated dissolution of salt from halite horizons through the agency of an underlying aquifer have been described as:

- Molecular diffusion along grain boundaries and through fractures in the intervening anhydrite layer.
- Solute-driven convection, either through a single wide fracture or through a permeable porous zone or fracture network between the halite and aquifer horizons.

The dissolution capabilities of the respective mechanisms, shape and size of the potential dissolution cavity in particular, will be considered further.

The dissolution capabilities discussed in Sections 3.2.2 and 3.2.3 are summarized in Table 3-1 which presents the hypothetical salt dissolution rates for both major mechanisms, their potential combination, and the two basic dissolution transport routes: (a) single fracture and (b) porous zone. Two cases are identified for single fracture: fracture with aperture less than 1.5 millimeters, which cannot support convection, and fracture with greater aperture. Three cases are identified for porous zones with varying intrinsic permeability between 10^{-14} to 10^{-17} square meters.

The rate of diffusive mass transport along a fracture connecting brine containing 315 kg/m^3 of sodium chloride with diluted (115 kg/m^3 NaCl) saline groundwater is on the order of 0.06 kg/m^2 of fracture per year. Considering an equivalent fracture porosity of 0.1 for the anhydrite

TABLE 3-1

HYPOTHETICAL SALT DISSOLUTION RATES
BASED ON POTENTIAL DISSOLUTION MECHANISMS(1)

DISSOLUTION MECHANISMS	SALT DISSOLUTION RATE			DISSOLUTION CAVITY HEIGHT IN 10,000 YEARS(5) (cm)
	DIFFUSION(2) (kg/m^2-yr)	CONVECTION(3) (kg/m^2-yr)	TOTAL(4) (kg/m^2-yr)	
Single Fracture Induced Dissolution				
• Fracture width insufficient to support convection (less than 1.5± millimeters)	0.06	0(6)	0.06	3
• Fracture width sufficient to support convection (greater than 1.5± millimeters)	0.06	6×10^4	6×10^4	-(7)
Porous Zone (Fracture Network) Induced Dissolution				
• Intrinsic permeability of 10^{-17} m^2	0.006	0	0.006	3
• Intrinsic permeability of 10^{-16} m^2	0.006	0.015	0.021	10
• Intrinsic permeability of 10^{-14} m^2	0.006	1.50	1.50	-(7)

(1) The potential dissolution mechanisms include salt removal by diffusion and convection.

(2) Diffusion is dependent on the concentration gradient, effective porosity, and molecular diffusion coefficient.

(3) Convection is a function of the Rayleigh number and Nusselt number.

(4) The total salt dissolution rate is the sum of diffusion and convection processes.

(5) Dissolution cavity height is based on a geometry (equal width and height) for a single fracture as shown in Figure 3-7. The height of the cavity, induced by a porous zone (fracture network), is based on cavity development directly above the porous zone as shown in Figure 3-6.

(6) A fracture of less than 1.5 millimeters will preclude convection.

(7) The salt dissolution rate for this process is much greater than the salt removal rate by the Bell Canyon aquifer. Therefore, the dissolution rate governed by this mechanism could not exist for 10,000 years and is not computed in this table.

units separating the halite formations from the underlying aquifer, the rate of salt removal across each square meter of rock would then be 0.006 kilogram per year. This is equal to a rate of removal of halite of 3×10^{-6} cubic meters per square meter per year. Thus, the general dissolution front would advance upwards at 3×10^{-6} meters per year (Figure 3-6), a rate which would have little impact on the WIPP site in 10,000 years, as indicated in Table 3-1.

A single fracture which is wide enough (greater than 1.5 millimeter) to sustain free convection would be of much greater significance to the WIPP site. With a Nusselt number calculated to be about 10^6, the rate of salt removal would be 6×10^4 kg/m^2 of fracture per year, as indicated in Table 3-1. This corresponds to a halite dissolution rate of 28 cubic meters per square meter per year.

The potential dissolution front would probably take the form of a cavity whose shape is governed by a very complex mechanism depending on many variables. Using the available information from the literature (Jessen, 1973) and adapting it for the Castile and Salado halite dissolution problem, it was determined that the cross-section of the cavity may resemble a rounded trapezoid with the base slightly shorter than the top. The width to height ratio is estimated to be about 1:1 for pure halite and, considering the influence of anhydrite impurities, the ratio may be as high as 10:1. To simplify further calculations, a conservative rectangular tunnel shape (width to height ratio of 1:1) was used. If the dissolution front were to propagate as such (Figure 3-7), then for a 1.5 millimeter wide fracture it would have advanced less than 0.2 meter in one year and less than 20 meters in 10,000 years. Despite the apparent significance of these values, a simple calculation demonstrates that this mechanism cannot be very widespread in the Delaware Basin. Using a Bell Canyon aquifer thickness of 30 meters with a porosity of 0.16, the volume of water underlying each square meter of Castile Formation is 4.8 cubic meters. This water, if completely saturated in sodium chloride, would contain a total of 1.5×10^3 kilograms of salt. The

DRAWING NUMBER	NM78-648-A43
CHECKED BY	RES
APPROVED BY	SHD
D. Weick 12-21-82	
DRAWN BY	
13A 100	
13A BR	

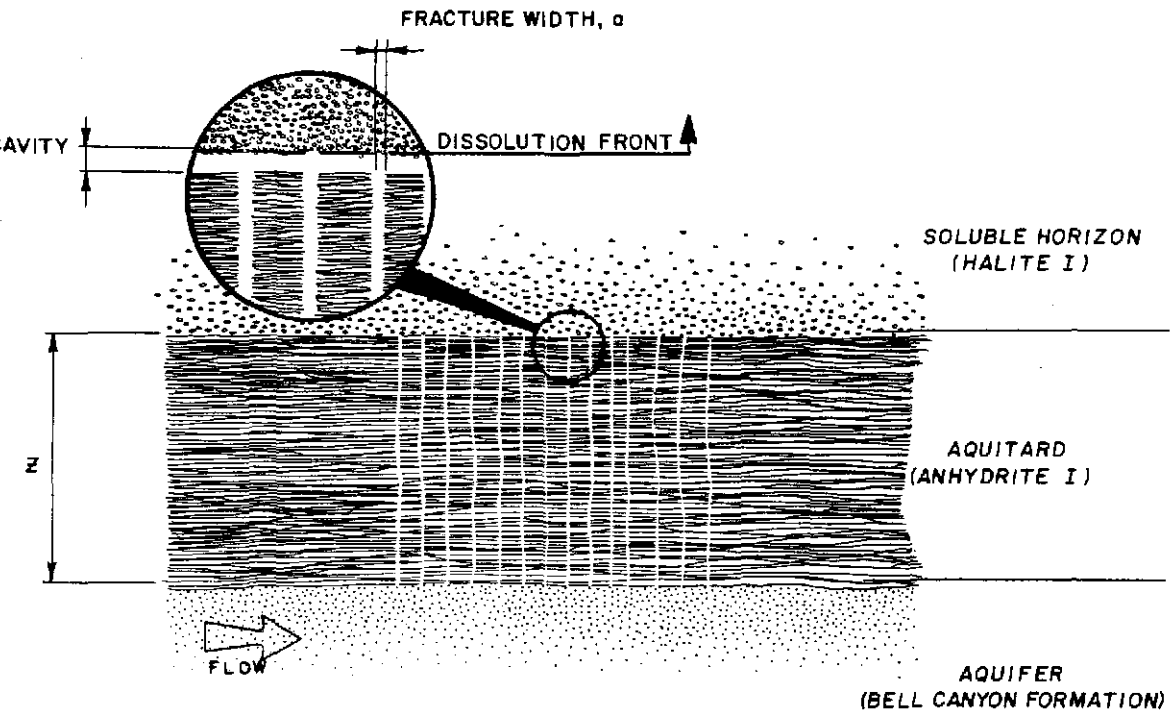

FIGURE 3-6

SCHEMATIC OF DISSOLUTION FRONT ADVANCEMENT BY DIFFUSION AND CONVECTION IN A FRACTURE NETWORK

PREPARED FOR

WESTINGHOUSE ELECTRIC CORPORATION
ALBUQUERQUE, NEW MEXICO

D'APPOLONIA

19 1253 HERCULENE. A&B SMITH CO., PGH., PA

12A	100	DRAWN BY	D. Weick	CHECKED BY	TEC
12A	BR		12-21-82	APPROVED BY	SHD

DRAWING NUMBER NM78-648-A42

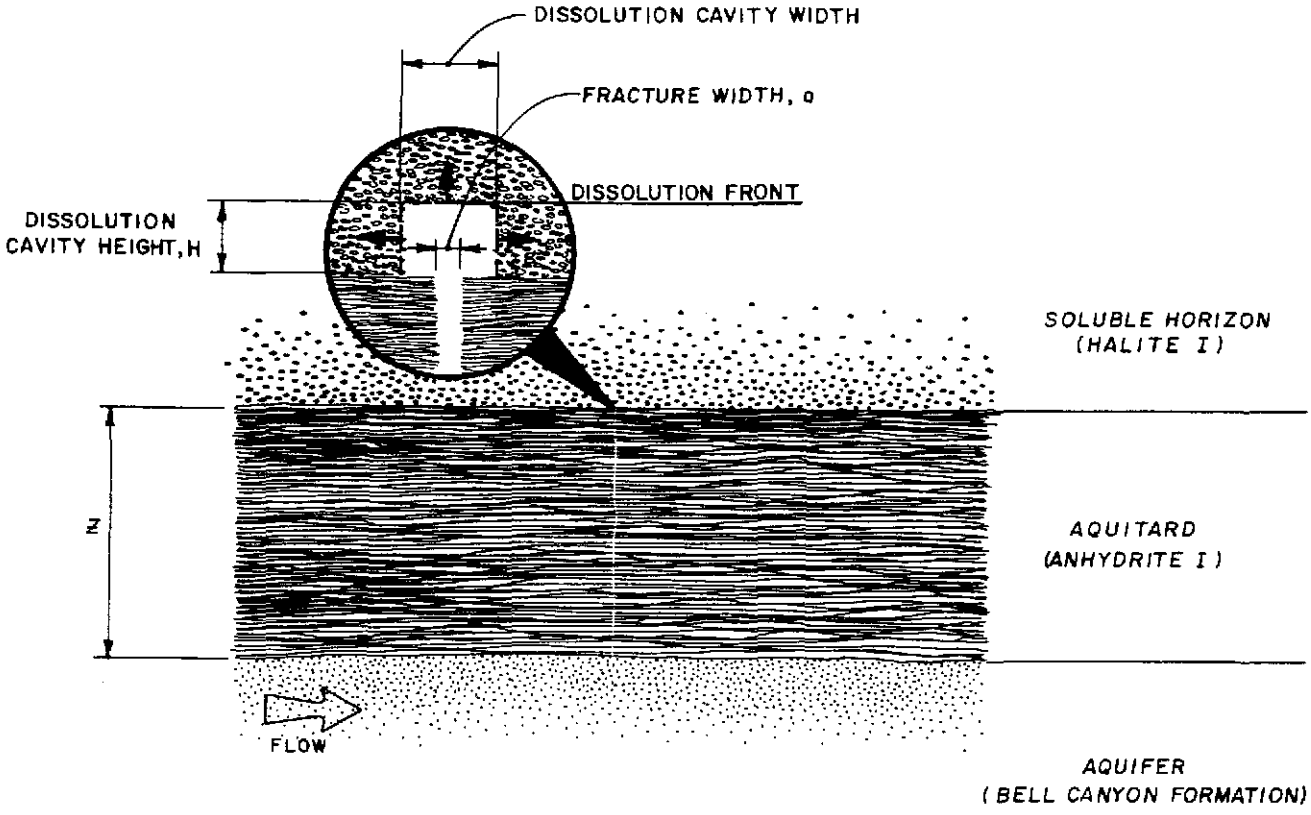

NOTE:
IN THIS SCHEMATIC OF THE TUNNEL ADVANCEMENT OF THE DISSOLUTION FRONT, THE DISSOLUTION CAVITY WIDTH IS EQUAL TO THE DISSOLUTION CAVITY HEIGHT.

FIGURE 3-7

SCHEMATIC OF TUNNEL ADVANCEMENT OF DISSOLUTION FRONT SINGLE FRACTURE CONVECTIVE MECHANISM

PREPARED FOR

WESTINGHOUSE ELECTRIC CORPORATION
ALBUQUERQUE, NEW MEXICO

D'APPOLONIA

calculated mass flux indicates that such an amount could be supplied in just a few months by a large fracture. Thus, if there were many large fractures, the aquifer groundwater would become completely saturated in a short time and dissolution would cease. Despite the existence of the Delaware Basin in its present configuration for four to six million years, however, few of the brines in the basin aquifer approach saturation in salt. Instead, a gradual salinity buildup, with distance from west (recharge) to east, is observed (Figure 2-5). This implies that the fracture transport mechanism cannot operate on a large scale, although it does not preclude the existence of a small number of localized fractures.

Similar conclusions apply to the case of convection in a porous medium with high permeability. If the intrinsic permeability were 10^{-14} square meters, then from Equations (3-8) and (3-9) the solute Nusselt number would be 2.5×10^{2}. This corresponds, for an anhydrite porosity of 0.1, to a removal of 1.5 kilograms of salt per square meter per year, as shown in Table 3-1. The time to reach complete salt saturation would be only on the order of 10,000 years. The presence of undersaturated brines and the gradual buildup in concentration across the basin (Figure 2-5) imply that the anhydrites are, in general, less permeable than 10^{-14} square meters. If the intrinsic permeability of the anhydrite were 10^{-16} square meters, the Nusselt number would be 2.5, and more than 10^{6} years would be needed to completely saturate the aquifer with sodium chloride. The time period is lengthened by the water recharge and discharge rates which would be significant in this period of time. Thus, a small Nusselt number of the order of 2.5 is not precluded by the aquifer water quality data. It would lead to a rate of advancement of the dissolution front of 1×10^{-5} meters per year or 0.1 meter in 10,000 years, as indicated in Table 3-1. As discussed above, for permeabilities less than 4×10^{-17} square meters, diffusion would be the dominant process. As a result, the available data on the Castile Formation hydraulic conductivity (10^{-9} to 10^{-10} centimeters per second; Sandia, 1980b) suggest that diffusion is the dominant process.

Vigorous convective transport, either through single fractures in anhydrite or through a highly permeable layer, could lead to rapid advancement of the salt dissolution front. The gradual change in groundwater salinity in the Bell Canyon aquifer across the Delaware Basin implies, however, that these vigorous convective mechanisms are not regionally important. A slow rate of advancement of the dissolution front associated with diffusive or weak convective flow through the anhydrite layer seems much more likely. A detailed analysis of flow in the basin aquifer (Chapter 4.0) confirms this deduction. However, a small number of fractures or high porosity zones is not precluded by these data and will be addressed in Chapter 5.0.

In summary, the mechanisms for dissolution of salt consist of diffusion and convection. Conditions required to support dissolution include a concentration gradient to drive the diffusion process and a density gradient to initiate convection. Additionally, convection is dependent on the fracture size or porous zone (fracture network) permeability. As shown in Table 3-1, convection can be substantially greater than diffusion for a fracture greater than 1.5 millimeters, or for intrinsic permeabilities greater than 10^{-16} square meters. However, for conditions in the Delaware Basin, the Bell Canyon Formation will limit the dissolution mechanism because the concentration and density gradient will be controlled by the aquifer transport rate. The following chapter addresses the Bell Canyon aquifer transport rate and the application of the dissolution mechanisms to the Delaware Basin.

4.0 EVALUATION OF DISSOLUTION MECHANISMS IN THE DELAWARE BASIN

In this chapter, the various salt dissolution mechanisms relative to the hydrogeologic and salt transport characteristics of the Delaware Basin formations are evaluated. In addition, the salt transport rates in the Bell Canyon and Capitan Reef aquifers are analyzed and compared with existing site-specific data to determine the dominant mode of salt removal from the Castile and Salado Formations. The analyses include analytical calculations and numerical modeling of mass transport in the Bell Canyon aquifer and salt dissolution in the Castile Formation. As discussed in Section 3.2.1, calculated dissolution rates in the Castile Formation provide conservative estimates of Salado salt removal.

4.1 METHODOLOGY

To evaluate the relative importance of the dissolution mechanisms, estimate possible dissolution of halite in the Castile and Salado Formations, and assess mass transport of salt in the Bell Canyon and Capitan aquifers, the following methodology has been employed:

- Establish hydrologic characteristics of the DMG.
- Examine the existing longitudinal concentration profile of chloride in the Bell Canyon aquifer and the relationships between chloride and salt concentration.
- Calculate salt transport through the Bell Canyon aquifer for various hydrologic conditions and salt dissolution mechanisms using analytical and numerical methods.
- Evaluate salt transport potential in the Capitan Reef aquifer in relation to possible dissolution mechanisms.
- Assess the sensitivity of the computed salt removal rates to the range of the hydrogeologic and geochemical parameter values.
- Compare calculated salt concentrations with corresponding available site-specific data.

4.2 HYDROGEOLOGIC DATA AND BASIC ASSUMPTIONS

The region under consideration in these analyses and the relationships of the Castile and Salado Formations to the Bell Canyon and Capitan Reef aquifers are shown in Figure 2-5 and in the cross sections of Figures 4-1 and 4-2. A detailed representation of the Bell Canyon aquifer in the vicinity of the WIPP facility is shown in Figure 4-3. It includes the Bell Canyon aquifer overlain by an anhydrite layer (Anhydrite I) 70 to 100 meters thick, followed by the Halite I which is about 115 meters thick. The Halite I is overlain by another anhydrite layer (Anhydrite II) and by the Halite II. These formations are followed by the uppermost anhydrite layers (Anhydrites III and IV) and by the Salado Formation. The WIPP facility is located in the Salado Formation, over 500 meters above the Bell Canyon aquifer. The geologic section in Figure 4-3 is 16.5 kilometers in length and was selected as the numerical study area due to the availability of chloride concentration data at both ends of the cross section.

In the remainder of this section, the basic assumptions and relevant hydrogeologic parameters in relation to the analytical and numerical computations of salt dissolution are discussed. The ranges of values are presented for the following parameters:

- Aquifer thickness
- Hydraulic conductivity
- Hydraulic gradient
- Chloride concentration

Basic Assumptions

A basic assumption in the following salt dissolution discussions is that steady-state flow and mass transport conditions may be considered to exist in the Bell Canyon and Capitan Reef aquifers and the Castile Formation. The basis of this assumption is discussed in the following paragraphs.

In the vicinity of the WIPP site, available evidence indicates that steady-state flow and transport conditions have been reached. Modeling of the flow system, as presented in subsequent sections, has shown that

358	00	DRAWN BY	TEJ	CHECKED BY	RCJ	DRAWING NUMBER	NM 78-648-B32
358	0R		11-17-81	APPROVED BY	SMD		

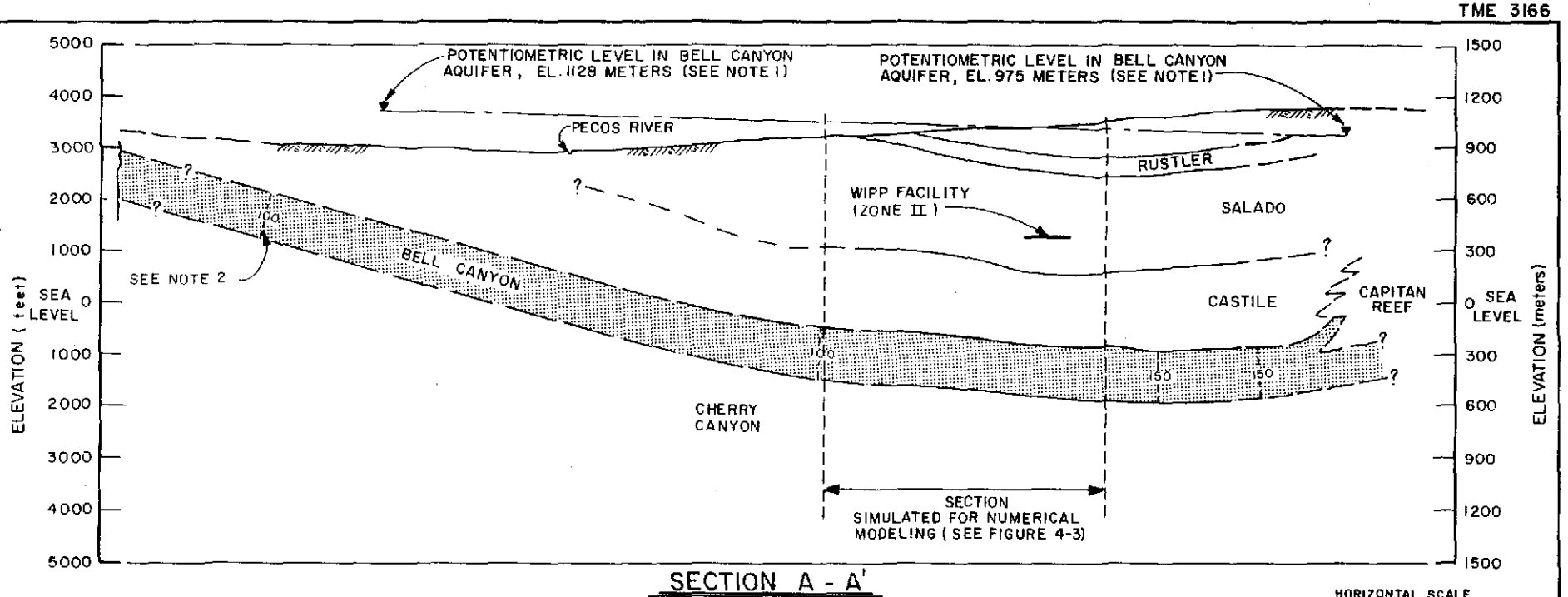

SECTION A - A'

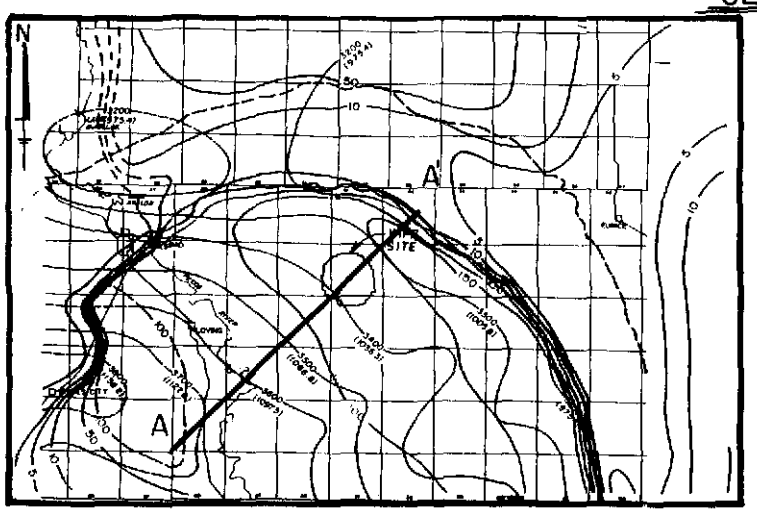

KEY PLAN

HORIZONTAL SCALE
0 6000 12,000 METERS
0 10,000 20,000 30,000 FEET

VERTICAL SCALE
0 600 1200 METERS
0 1000 2000 3000 FEET

LEGEND:

100 — LINE OF EQUAL CHLORIDE CONCENTRATION IN KILOGRAMS PER CUBIC METER (Kg/m³).

3400 (1036 m) — POTENTIOMETRIC LEVEL IN BELL CANYON FORMATION (SEE NOTE 1) IN FEET (METERS).

NOTES:

1. THE POTENTIOMETRIC LEVELS SHOWN ARE EXPRESSED AS WATER WITH A SPECIFIC GRAVITY OF 1.0.
2. CHLORIDE CONCENTRATION ISOPLETHS SOUTHEAST OF WHITES CITY, AS SHOWN IN THE KEY PLAN AND REPORTED BY HISS (1975a), ARE NOT SUBSTANTIATED BY MEASURMENTS. MEASURMENTS REPORTED BY HISS (1975a), IN ADJACENT AREAS ARE LESS THAN 100 kg/m³.

REFERENCES

U.S. DEPARTMENT OF ENERGY, 1980b
HISS, 1975a

FIGURE 4-1
GENERALIZED GEOLOGIC SECTION OF DELAWARE BASIN IN SITE VICINITY

PREPARED FOR

WESTINGHOUSE ELECTRIC CORPORATION
ALBUQUERQUE, NEW MEXICO

D'APPOLONIA

19 1253 HERCULENE, A&B SMITH CO., PGH., PA

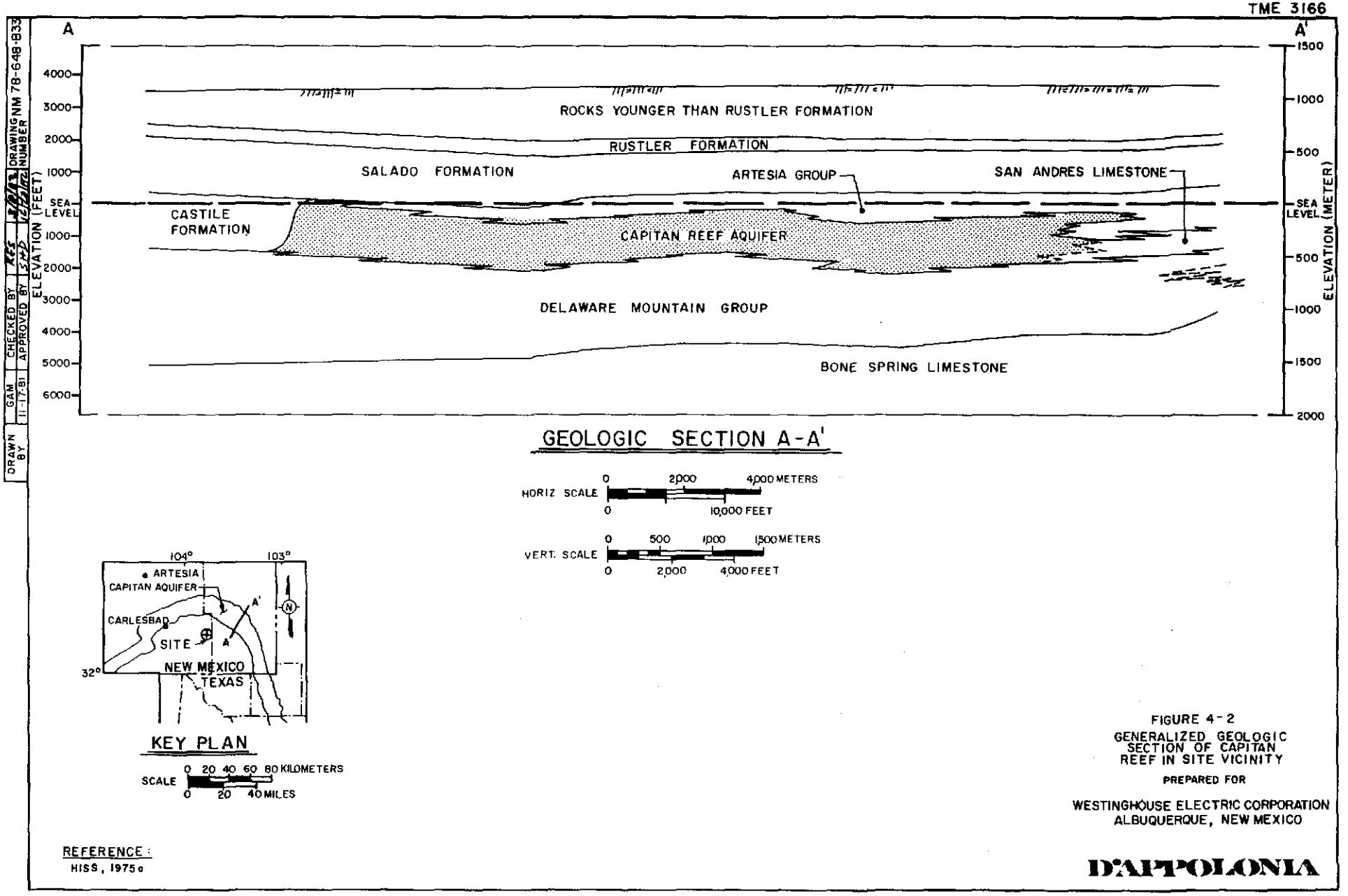

DRAWN BY GAM 11-17-81 | CHECKED BY KCS | APPROVED BY SMD | DRAWING NUMBER NM 78-648-833

GEOLOGIC SECTION A-A'

HORIZ SCALE 0 2000 4000 METERS
0 10,000 FEET

VERT. SCALE 0 500 1000 1500 METERS
0 2,000 4,000 FEET

KEY PLAN

SCALE 0 20 40 60 80 KILOMETERS
0 20 40 MILES

REFERENCE:
HISS, 1975a

FIGURE 4-2
GENERALIZED GEOLOGIC SECTION OF CAPITAN REEF IN SITE VICINITY

PREPARED FOR

WESTINGHOUSE ELECTRIC CORPORATION
ALBUQUERQUE, NEW MEXICO

D'APPOLONIA

DRAWING NUMBER NM78-648-E2

DRAWN BY	MEL	3-6-82
CHECKED BY	RES	3/6/82
APPROVED BY	SMD	12/22/81

CONSTANT HEAD BOUNDARY CONDITION EL 1059 METERS

CONSTANT HEAD BOUNDARY CONDITION EL 1019 METERS

RUSTLER

SALADO FORMATION

WIPP FACILITY (ZONE II)

HALITE

ANHYDRITE

HALITE

236 COLUMNS OF ELEMENTS @ 70 METERS = 16,520 METERS

ANHYDRITE III AND IV

CASTILE FORMATION

HALITE II

INTERLAMINATED ANHYDRITE II

DIFFUSION ZONE

DISSOLVED SALT DIFFUSES THROUGH THIS ZONE DOWN INTO THE BELL CANYON AQUIFER

CONSTANT CONCENTRATION BOUNDARY CONDITION ALONG TOP OF GRID

NO FLOW BOUNDARY

HALITE I

ΔY_2 (SEE TABLE THIS DWG)

ΔY_1 (SEE TABLE THIS DWG)

INTERLAMINATED ANHYDRITE I

NO FLOW BOUNDARY

BELL CANYON FORMATION

FLOW

SECTION B-B'

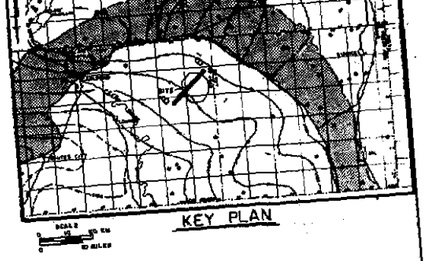

KEY PLAN

VERTICAL GRID SPACING[1] (ΔY_1, AND ΔY_2)

BELL CANYON AQUIFER		DIFFUSION ZONE IN CASTILE FORMATION	
AQUIFER THICKNESS (METERS)	GRID SPACING, ΔY_1 (METERS)	DIFFUSION ZONE THICKNESS (METERS)	GRID SPACING, ΔY_2 (METERS)
30	10	70	35
100	33.3	100	50
300	100	300	150
		600	300

(1) VERTICAL GRID SPACING WAS VARIED FOR NUMERICAL MODEL SENSITIVITY ANALYSIS OUTLINED IN APPENDIX E.

NOTES:

1. THICKNESSES OF HALITE AND ANHYDRITE LAYERS IN THE CASTILE AND SALADO FORMATIONS WERE DETERMINED FROM FIGURE 2-1.
2. CONSTANT HEAD BOUNDARY CONDITIONS WERE SELECTED TO PRODUCE A HYDRAULIC GRADIENT OF 0.0025 WHICH IS THE AVERAGE GRADIENT THROUGH THE BELL CANYON AQUIFER. (SEE FIGURE 4-1)

HORIZONTAL SCALE

0 1000 2000 METERS

0 2000 4000 6000 FEET

VERTICAL SCALE

0 100 200 METERS

0 200 400 600 FEET

FIGURE 4-3

MODEL REPRESENTATION OF THE DELAWARE BASIN

PREPARED FOR

WESTINGHOUSE ELECTRIC CORPORATION
ALBUQUERQUE, NEW MEXICO

D'APPOLONIA

establishment of steady-state conditions required a time period equivalent to the flow travel time through the aquifer. Figure 4-1 presents a section of the Bell Canyon aquifer parallel to the direction of flow, beginning at the recharge area at the southwest and ending at the Capitan Reef aquifer to the east. Based on this section, the total time required for recharging water to reach the Capitan Reef is approximately 2.5 million years. Since the basin flow system has probably remained essentially unchanged during the past four to six million years, steady-state flow conditions should have been attained.

Development of steady-state conditions relative to mass transport is dependent on the dissolution mechanism as well as on the Bell Canyon flow rate. Since brine density flow is heavily dependent on the aquifer flow rate, the mass transport due to this mechanism should require about the same time period to establish steady-state conditions. Due to the slow rate of mass transfer of dissolved salts by diffusion into underlying anhydrite, the rate of dissolution by this method is not significantly dependent on the aquifer flow rate. A pure diffusion mechanism could have commenced following deposition of halite in the Castile Formation. Based on parameters representative for the medium, a period on the order of 30 million years would be required for steady-state diffusion to develop through the anhydrite. Considering the period since deposition, approximately 250 million years, it is reasonable to assume that salt concentrations in the Bell Canyon aquifer reflect essentially steady-state levels. The effect of the aquifer salinity on the mass transport and diffusion rate, and possible changes in steady-state transport conditions, will be addressed in the sensitivity analyses of Section 4.4.4.

The permeability of the Capitan Reef aquifer is much greater (several orders of magnitude) than that of the Bell Canyon aquifer. However, recent extraction of large amounts of water from the Capitan Reef aquifer (Hiss, 1975a) has changed the hydraulic gradient in this aquifer. The lowering of the potentiometric surface in the Capitan Reef has not influenced the present flow rate through the Bell Canyon aquifer and is

not anticipated to have any major effect because of the very low hydraulic conductivity of the latter. However, this condition will be assessed in the analyses of future salt dissolution and mass transport in the Delaware Basin by investigating a range of hydraulic gradients during the sensitivity analyses.

Aquifer Thickness

As discussed in Section 2.2, the thickness of the Bell Canyon Formation is estimated as approximately 300 meters; however, much of the data suggest that less than 30 meters of the formation can transmit groundwater. For the purposes of the dissolution analyses, effective aquifer thicknesses ranging from 10 to 60 meters have been used.

Hydraulic Conductivity

Based on laboratory measurements of the core samples (Hiss, 1975a) and analysis of drill stem tests in Borehole AEC-7 as discussed in Section 2.2, the representative hydraulic conductivity of the Bell Canyon aquifer ranges from 1.1 to 2.9 meters per year with a weighted average value of 1.8 meters per year. An average hydraulic conductivity of 550 meters per year has been reported for the Capitan Reef aquifer (Hiss, 1975a).

Hydraulic Gradient

Flow in the Bell Canyon aquifer appears to be relatively constant as indicated by the potentiometric surface presented in Figures 2-5 and 4-1. From Figure 2-5, the hydraulic gradient in the vicinity of the WIPP site was estimated to be 0.0025 meter per meter with an approximate range of 0.002 to 0.003 meter per meter.

Groundwater flow in the Capitan Reef aquifer has been substantially affected by development of the petroleum industry in the past 45 years. The current potentiometric surface indicates flow is generally parallel to the reef margin and flows toward the east and south. An average gradient of 0.001 to 0.004 meter per meter has been reported for this

aquifer (Hiss, 1975a). The reduction or termination of the pumping in the Capitan Reef will result in raising the potentiometric surface in this aquifer. This in turn will reduce the hydraulic gradient within the Capitan Reef and between this aquifer and the Bell Canyon aquifer.

Chloride Concentrations

Figure 2-5 presents the chloride concentration contours in the Bell Canyon aquifer underlying the Castile Formation. As shown in Figures 2-5 and 4-1, the concentration of chloride increases in the direction of flow to the northeast. The concentration contours observed in the basin, as discussed in Section 2.2, increase from approximately 50 kg/m^3 at the southwestern margin to more than 150 kg/m^3 in the northeast, adjacent the Capitan Reef aquifer. Although a 100 kg/m^3 contour is shown at the upgradient end of the Bell Canyon aquifer in Figure 2-5, none of the measurements presented by Hiss (1975a) confirm such a high chloride concentration in this vicinity. The illustrated decrease in concentration at the downgradient end of the aquifer is also subject to interpretation due to the lack of data.

The Capitan Reef borders the Salado and Castile Formations north and east of the Delaware Basin. The contact between the Capitan Reef and Castile and Salado Formations near the northeast margin of the basin is shown in Figure 4-2. Based on data compiled by Hiss (1975a), chloride concentrations in the Capitan aquifer range from less than 1 kg/m^3 to as high as 42 kg/m^3, with most values within the range of 5 to 20 kg/m^3 in this vicinity. Concentrations appear to be greatest at the north margin of the Delaware Basin and reduce in the direction of flow (towards the southeast).

4.3 ANALYTICAL EVALUATION OF SALT DISSOLUTION AND TRANSPORT RATES

In this section, the analytical methods for evaluating the potential dissolution of salt and its transport by the Bell Canyon aquifer are presented. In addition, the dissolution process associated with the Capitan Reef aquifer is discussed.

4.3.1 Dissolved Salt Transport in the Bell Canyon Aquifer

The salt transport rate in the Bell Canyon aquifer depends on the aquifer flow rate and the salt concentration gradient in the direction of flow. Various mechanisms might result in halite dissolution and transport to the Bell Canyon. However, the efficiencies of these mechanisms are controlled by the capability of the aquifer to convey the dissolved salt away from the source such that a concentration gradient at the Castile-Bell Canyon interface is maintained. Dissolution will cease if (1) the physical conditions necessary for the dissolution mechanism are not plausible or (2) the concentration gradient between the source (Halite I) and transporting zones (Bell Canyon aquifer) cannot be sustained. In the following paragraphs, the range of dissolution rates based on hydrologic and geochemical properties of the DMG is examined.

Flow-Controlled Transport Rate

The range of characteristic hydrologic values of the Bell Canyon aquifer is discussed in Section 4.2 and summarized in Table 2-1. The average values are as follows:

- Effective aquifer thickness — 30 meters
- Hydraulic conductivity — 1.8 meters/year
- Hydraulic gradient — 0.0025 meter/meter

Based on these properties, the flow per unit width in the Bell Canyon aquifer is approximately 0.135 cubic meter per year per meter (m^3/yr-m). The flow rate for various ranges of hydrologic characteristics was calculated and is presented in Figure 2-6. According to this figure, the plausible flow rate in the Bell Canyon might range from as little as 0.02 m^3/yr-m to a maximum of 0.4 m^3/yr-m.

Taking into account the inference that flow and chloride transport in the Bell Canyon aquifer approach steady-state, a mass balance calculation enables an average rate of salt dissolution in the basin to be estimated. At steady-state, the rate of increase of chloride content of the Bell Canyon water with distance along the flow path is exactly balanced by dissolution of halite or other chloride minerals. As an

approximation, it has been assumed that the chloride buildup in groundwater is entirely due to dissolution of halite (NaCl) from the overlying Castile Formation. This provides an upper bound on the halite dissolution rate because the Bell Canyon brines are not entirely sodium chloride, having a substantial calcium chloride content in addition (Lambert, 1977). Based on a flow rate of 0.135 m^3/yr-m and the observed chloride concentration profiles, the average thickness of salt removal in the basin was calculated to range between 0.07 and 0.62 centimeter in 10,000 years. This corresponds to a chloride concentration difference (ΔC) between upgradient and downgradient ends of the aquifer varying from 10 to 100 kg/m^3 across the basin, resulting in a salt removal rate ranging from 2.2 to 22.2 kg/yr-m, respectively. In reality, most of the dissolution will take place upgradient (southwest) where the salt concentration gradient between the potential source (Halite I) and the Bell Canyon aquifer is greater. The calculated variation of salt dissolution along a 16,500 meter section beneath the WIPP facility is presented in Section 4.4.2 which describes numerical model results.

The potential diffusive and convective mass transport of salt from the Castile to the Bell Canyon aquifer was discussed in Section 3.2. It was shown that diffusion through the lower anhydrite layer from halite zones in the Castile can result in a net vertical mass inflow of NaCl of approximately 0.006 kilogram per year per square meter (kg/yr-m^2) to the Bell Canyon which represents a dissolution rate of 3 centimeters per 10,000 years (Table 3-1).

The important assumptions embodied in this calculation were anhydrite porosity of 0.1 and concentration difference across the porous zone of 200 kg/m^3 sodium chloride. In the area beneath the WIPP facility, the rate of increase of chloride concentration (50 kg/m^3 in 16,500 meters; Figure 4-3) corresponds to an NaCl dissolution rate of only 0.3 centimeter in 10,000 years. The difference between the results of Chapter 3.0 and the present calculation implies that Anhydrite I has a lower effective porosity than 0.1. It may be concluded, however, that the

diffusive process is more than adequate to supply the salt being carried by the Bell Canyon aquifer.

The convective mechanism of salt dissolution provides the potential for substantially more mass flux into the Bell Canyon aquifer. A fractured porous zone could support convection from the first halite layer of the Castile Formation down to the Bell Canyon aquifer, a distance of approximately 100 meters. The potential NaCl convective dissolution rate was found to be 1.5 $kg/yr-m^2$ for an anhydrite intrinsic permeability of 10^{-14} square meters and 0.015 $kg/yr-m^2$ for an intrinsic permeability of 10^{-16} square meters. Even with the lower permeability (10^{-16} square meters), convective dissolution would require a chloride concentration increase of 1,120 kg/m^3 beneath the WIPP site (Figure 4-3), which is substantially greater than the existing increase in concentration of 50 kg/m^3 and is well above the level for chloride saturation (190 kg/m^3). It is possible to conclude that a porous zone of convection can only exist at isolated locations. This is consistent with the measured anhydrite permeability of 10^{-9} to 10^{-10} centimeters per second (10^{-18} to 10^{-19} square meters) (Section 2.2). Assuming permeable anhydrite (10^{-16} square meters) and considering all observed mass flux is due to convection in a porous or fractured zone, the length of the dissolution area could be only about 800 meters. Dissolution will cease beyond this point if brine becomes fully saturated, a situation which is not apparent in the Bell Canyon aquifer.

Since diffusion will occur regardless of the presence of continuous fractures, it appears that the diffusion mechanism is primarily responsible for the present transport of salt in the Bell Canyon aquifer because the existing mass transport is of the same order as that calculated using the one-dimensional diffusion equation. Dissolution by convection must be restricted to a very small area since convective mass removal over a large area would far exceed the capacity of the Bell Canyon aquifer to remove the dissolved material.

4.3.2 Dissolution Associated with the Capitan Reef Aquifer

Flow and chloride concentration data for the Capitan Reef aquifer were discussed in Section 4.2. The total mass transport of chloride in the reef aquifer is in the range of 0.3×10^8 to 4.4×10^8 kilogram per year (kg/yr) based on an aquifer thickness of 500 meters and width of approximately 20 kilometers (Figure 4-2). As a comparison, assuming the Bell Canyon discharges into the reef along a 60-kilometer stretch adjacent the northeast basin margin, based on the potentiometric surface shown in Figure 2-5, the chloride mass inflow from the Bell Canyon could be as high as 1.3×10^6 kg/yr. Over this length of reef margin, diffusion from the Castile Formation alone would result in a mass through the anhydrite flux on the order of 10^6 kg/yr. Considering diffusion from the overlying Salado Formation, through the Artesia Group, to the Capitan Reef, the mass flux is also on the order of 10^6 kg/yr. In summary, only about 3×10^6 kg/yr of chloride is accounted for by diffusion and inflow from the Bell Canyon, which is far less than the total estimated rate of 20 to 440×10^6 kg/yr. Therefore, it appears that another mechanism is contributing to dissolution and mass flux into the Capitan Reef aquifer.

As indicated in Figure 3-1, significant deep dissolution has been postulated by Anderson and Kirkland (1980) at the reef margin in the northern and eastern portions of the Delaware Basin. If one considers the potential extent of contact of these features with the Capitan Reef, the range of material properties of the Castile and Capitan units, and the possible concentration gradient developed at the interface, there is evidence to suggest that active convective dissolution of the overlying Salado Formation together with the diffusion from halite layers can result in the observed mass transport rate in the Capitan Reef aquifer. While the range of values for the mass transport parameters associated with convection is too large to state conclusively that convective dissolution is responsible for the concentrations observed in the Capitan Reef, it is clear that diffusion alone is not sufficient. Furthermore, the presence of deep dissolution features at the reef margin suggests

that, at preferred locations, dissolution may be associated with convective as well as diffusive mechanisms. It appears, therefore, that diffusion alone is adequate to explain mass transport in the Bell Canyon aquifer, but that both convective and diffusive mechanisms must apply above the reef.

4.4 NUMERICAL MODELING OF SALT REMOVAL POTENTIAL

The purpose of the numerical modeling is to simulate salt dissolution in the Castile Formation and potential removal by the Bell Canyon aquifer. The main difference between the numerical and analytical approaches is that the former enables estimates of the effects of hydrodynamic dispersion and of transient conditions to be evaluated while the latter does not. This also permits a detailed sensitivity analysis to be made and incorporates the two-dimensional aspects of the problem.

The methodology for and the results of the simulation are presented in the following sections. The modeling methodology and basic assumptions are provided in Section 4.4.1 and the results of the simulation and its comparison with observed data are presented in Section 4.4.2. The sensitivity of dissolution rates to the relevant hydrologic and geochemical input parameters is discussed in Section 4.4.3. Theories related to salt transport simulation techniques are reviewed and the relevant governing equations describing these processes are given in Appendix A.

4.4.1 Modeling Methodology and Implementation

The amount of salt that can be removed from the Castile Formation along a certain horizontal distance is controlled by the dissolution mechanism, the hydraulic conductivity of the Bell Canyon aquifer, and the saturation concentration level. These are in turn related to the concentration gradient along the direction of flow. For example, the steady-state salt removal rate (mass per unit time) from halite layers, regardless of whether diffusive or convective transport dominates, cannot be greater than the product of the aquifer flow rate, Q, and the concentration difference, ΔC, between the upgradient and downgradient

ends of the section under consideration (i.e., salt removal rate = Q x ΔC). As a result, quantitative theories for material removal from beneath the WIPP site must be consistent with the mass transport capacity of the Bell Canyon aquifer.

The preliminary calculations in Sections 4.3 and 3.2 indicate that salt removal by molecular diffusion in the basin dominates over any of the convective mechanisms considered. Removal rates from the Castile Formation based on convective transport mechanisms are estimated to be significantly greater than the salt transport capacity of the Bell Canyon aquifer. The numerical modeling described herein was performed in order to include the two-dimensional aspects of the transport problem using a more detailed representation of the DMG hydrogeology than was used for the simple analytical calculations. The results of this simulation are then compared with analytical solutions and reported field data.

The numerical model representation of the flow and salt transport regime is shown in Figure 4-3. The modeled section is a portion of the Bell Canyon and Castile Formations shown in Figure 4-1. Figure 4-3 illustrates the alternate layers of halite and anhydrite which are present in these formations. A D'Appolonia computer program code named GEOFLOW was used to simulate the potential salt removal rate. The program GEOFLOW consists of two subprograms. The first program, a hydrodynamic model, computes potentiometric heads and, consequently, velocity vectors in the domain of interest. The second program, a mass transport model, utilizes velocity vectors and mass transport parameters to compute mass concentration in the same domain. The Bell Canyon aquifer and a portion of the Castile Formation were divided into parallelograms to form a grid consisting of nodes and elements which approximate the geometry of the actual system. The grid system has 1,422 nodes and 1,180 elements. Parameters such as velocity, potentiometric head, and concentration were computed at each node by solving the flow and mass transport equations presented in Appendix A. Because of the very low groundwater velocity of the Bell Canyon and the long simulation period, the effect of fluid

density variation on calculation of the chloride concentration was neglected.

The vertical dimensions of the finite element grid (Figure 4-3) were kept variable so that the effects of the aquifer and the diffusion zone thicknesses could be investigated. The term Δy_1 represents the vertical grid spacing in the Bell Canyon aquifer and Δy_2 is the vertical spacing in the diffusion zone above the top of the aquifer. To be consistent with the parameter values used in Section 3.2 and considering the effective thickness of the Bell Canyon aquifer (Section 2.2), the grid used for the simulation represents an aquifer thickness of 30 meters. The upper section of the grid includes the lower portion of the Castile Formation which consists of a 70-meter-thick zone of anhydrite and 30 meters of the Halite I above it. Modifications of this grid (i.e., different values for Δy_1 and Δy_2) were used for portions of the sensitivity analysis.

The model assumes that dissolved chloride is diffused through the Castile anhydrite into the Bell Canyon aquifer and is transported away from the site. The concentration boundary condition at the top of the grid was set equal to the saturated concentration of chloride in water (approximately 190 kg/m^3). The fluid entering the aquifer at the upgradient portion was assumed to have a chloride level of 100 kg/m^3 based on reported data obtained from Figures 2-5 and 4-1. Constant potentiometric head boundary conditions were maintained at the ends of the grid system and no-flow boundaries were specified along the top of the Castile and bottom of the Bell Canyon. Table 4-1 contains the parameter values used for the simulation of salt removal from the Castile Formation. Since variability exists in some of these parameters, a sensitivity analysis (Section 4.4.3) was performed to determine the effects of varying each parameter over a range of values. In this manner, the extremes of potential salt dissolution rates were obtained.

TABLE 4-1

MODEL INPUT PARAMETERS FOR NUMERICAL COMPUTATIONS[1]

INPUT PARAMETER	VALUE	UNITS
Hydraulic Conductivity of Bell Canyon Aquifer, K	1.8	Meters per year (m/yr)
Effective Porosity of Bell Canyon Aquifer, n_e	0.16	Dimensionless
Molecular Diffusion Coefficient, D_m	8.7×10^{-3}	Square meters per year (m^2/yr)
Longitudinal Dispersivity of Bell Canyon Aquifer, D_L	3.048	Meters (m)
Transverse Dispersivity of Bell Canyon Aquifer, D_T	3.048	Meters (m)
Retardation Factor for Chloride, R_d	1.0	Dimensionless
Effective thickness of Bell Canyon Aquifer, b	30	Meters (m)
Thickness of Diffusion Zone in Castile Formations[2]	100	Meters (m)
Hydraulic Gradient, i	0.0025	Meters per meter (m/m)
Upgradient Chloride Concentration Boundary Condition in Bell Canyon Aquifer, C_u	100	Kilograms per cubic meter (kg/m^3)
Halite Density	2,160	Kilograms per cubic meter (kg/m^3)

(1) Refer to Appendix A for parameter definitions.

(2) Refer to Figure 4-3 for location of diffusion zone.

4.4.2 Results

The simulation yields velocity distribution through the Bell Canyon aquifer, the chloride concentration distribution, and the resulting halite dissolution rate from the Castile Formation per unit width of aquifer normal to the flow direction. The computed steady-state distribution of chloride in the lower anhydrite layer of the Castile Formation and the top 30 meters of the Bell Canyon Formation is presented in Figure 4-4. This figure illustrates the transport of chloride into the aquifer with a resulting increase in concentration from 100 kg/m^3 at the upgradient end to an average value of approximately 155 kg/m^3 at the downgradient section. A negligible vertical variation of chloride concentrations is observed throughout the simulated section. For this two-dimensional modeling, a value of the molecular diffusion coefficient equal to 0.0087 square meter per year (m^2/yr) (2.8×10^{-6} cm^2/sec) was selected so as to reproduce the general increase in chloride concentration beneath the WIPP facility indicated by available field data (Figures 4-1 and 4-3). Since chloride diffuses through the Castile anhydrite, the magnitude of the diffusion coefficient is the key indicator of whether diffusion is a valid mechanism to explain the existing dissolution rates near the WIPP site. Accepted values for the chloride diffusion coefficient in groundwater range from 0.003 to 0.03 m^2/yr (Freeze and Cherry, 1979), which indicates that the value of 0.0087 m^2/yr determined in the modeling is valid for a diffusion process. It is, however, to some extent empirical since the effective porosity and tortuosity of the medium are included in the model.

For the results shown in Figure 4-4, the steady-state velocity distribution in the aquifer is uniform at a flow rate of 0.135 $m^3/yr-m$ and the mass transport rate of chloride at the downgradient end is 20.9 kg/yr-m, representing a mass increase of 7.4 kg/yr-m chloride from the upgradient end. This increase in mass rate from upgradient to downgradient sections corresponds to an average vertical removal of 0.34 centimeter of salt per 10,000 years or 0.09 meter per 250,000 years from the Castile Formation along the 16,500-meter section shown in Figure 4-3.

DRAWN BY	R W	DRAWING NUMBER	NM78-648-E4
CHECKED BY	RES	3/8/84	
APPROVED BY	SHP	12/12/82	

MASS FLUX OF SALT TO THE BELL CANYON AQUIFER

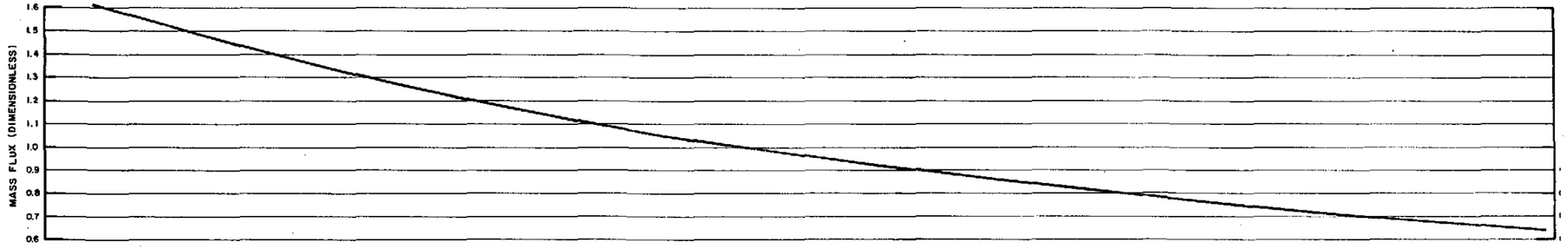

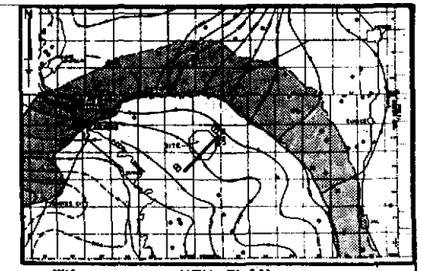

KEY PLAN

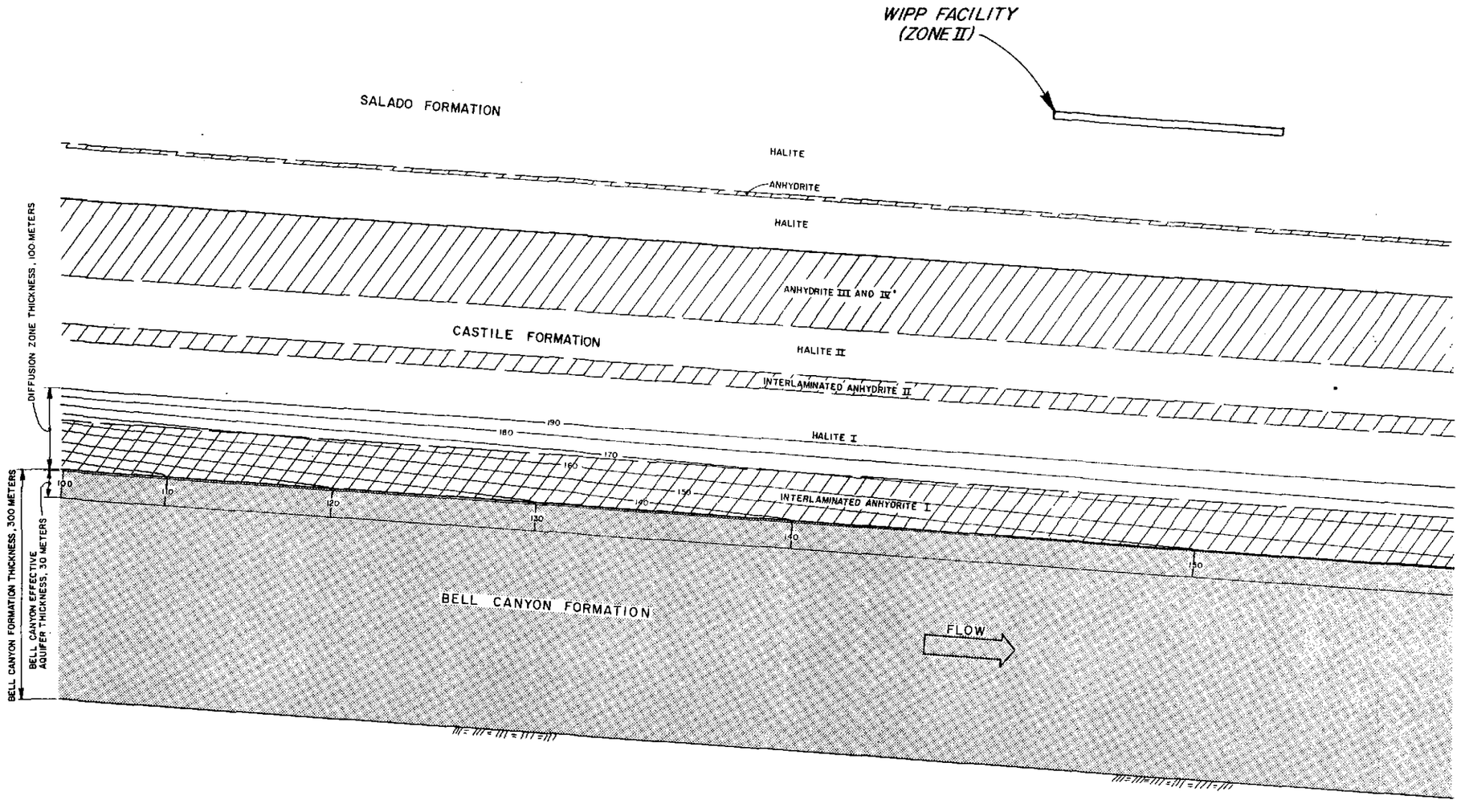

NOTES:

1. FOR MODEL REPRESENTATION OF THE FLOW SYSTEM, SEE FIGURE 4-3.
2. THE EFFECTIVE BELL CANYON AQUIFER THICKNESS FOR GROUNDWATER FLOW IS 30 METERS.
3. THE LOCATION OF THE CONSTANT CONCENTRATION SOURCE IS 100 METERS ABOVE THE BELL CANYON, OR ABOUT 30 METERS ABOVE THE BOTTOM OF THE HALITE I FORMATION. FOR SENSITIVITY OF THE MODELING RESULTS TO THE LOCATION OF THE SOURCE, AS WELL AS OTHER SYSTEM PARAMETERS, SEE FIGURE B-2.
4. THE MASS FLUX OF SALT FROM THE BELL CANYON IS BASED ON THE CALCULATED CHLORIDE CONCENTRATIONS WITH A CONSTANT UPSTREAM INFLOW CONCENTRATION OF 100 KG/M^3. THE MASS FLUX ILLUSTRATES THE DISSOLUTION PROCESS BASED ON DIFFUSION FROM THE HALITE ALONG THE LENGTH OF THE BELL CANYON AQUIFER.
5. MASS FLUX RATES WERE NONDIMENSIONALIZED WITH THE AVERAGE RATE OVER THE ENTIRE 16,500-METER SECTION WHICH HAS A VALUE OF 8.1×10^{-8} KG/YR-M^2.
6. THICKNESSES OF HALITE AND ANHYDRITE LAYERS IN THE CASTILE AND SALADO FORMATIONS WERE DETERMINED FROM FIGURE 2-1.

KEY

INDICATES CHLORIDE CONCENTRATION CONTOUR LINE (KILOGRAMS PER CUBIC METER)

HORIZONTAL SCALE
0 1000 2000 METERS
0 2000 4000 6000 FEET

VERTICAL SCALE
0 100 200 METERS
0 200 400 600 FEET

FIGURE 4-4

COMPUTED CHLORIDE CONCENTRATIONS IN THE BELL CANYON AQUIFER

PREPARED FOR

WESTINGHOUSE ELECTRIC CORPORATION
ALBUQUERQUE, NEW MEXICO

D'APPOLONIA

The actual rate, which varies as a function of horizontal location, is dependent upon the vertical concentration gradient between the halite layer and the concentrations in the aquifer. In particular, the salt flux into the Bell Canyon is a function of the vertical concentration gradient at the interface between the Castile Formation and the aquifer. A plot of the variation of NaCl mass transfer into the Bell Canyon (i.e., salt dissolution from the Castile) is also given in Figure 4-4. The higher dissolution is along upgradient portions of the section where the difference between concentrations in the Castile and Bell Canyon Formations is greatest, and it decreases as concentration within the Bell Canyon aquifer increases. As chloride accumulates in the direction of flow, the dissolution rate gradually subsides.

The results presented in this section were obtained by performing numerical computations using the input parameter values listed in Table 4-1. The results of this numerical simulation, together with the analytical calculations, indicate that a diffusive transport mechanism is a valid explanation for the observed chloride concentrations in the Bell Canyon aquifer. The input values were selected based on the best available and representative hydrogeologic and geochemical data for the WIPP site and its vicinity and, where no site-specific field data existed, conservative literature values were selected. To reduce any uncertainty on evaluation of salt removal rate associated with existing data and to assess the response of the model to various parameters, a sensitivity analysis was performed. In this analysis, the variations in average salt dissolution rate with respect to ranges of input parameters were determined. The results of the sensitivity computations are presented in Appendix B and summarized in the following section.

4.4.3 Sensitivity Analysis

A sensitivity analysis was performed to determine the range of potential salt dissolution rates beneath the WIPP site as determined by the variability of the parameters that control the dissolution. Two major categories were considered in salt dissolution evaluation:

- Diffusion-controlled salt dissolution and
- Salt removal controlled by the Bell Canyon aquifer.

The sensitivity of diffusion-controlled dissolution was determined using the numerical model discussed in Section 4.4.3. Salt removal controlled by the Bell Canyon aquifer was addressed by considering only the mass transport capacity of the underlying aquifer and longitudinal concentration gradient, but not the mechanism for salt removal.

Based on the results of the analyses presented in Appendix B, the following conclusions are made:

- The effects of neglecting density variations, as related to the diffusion-controlled dissolution results given in Section 4.4.2, are insignificant. However, the numerical simulation of salt removal by density-flow (convective) mechanisms would require that density variations be included as part of the model.
- For diffusion-controlled salt dissolution (i.e., results in Section 4.4.3), the increase in dissolution due to a change in any one parameter (Table 4-1) should not exceed 130 percent. Therefore, the average vertical removal of salt from the Castile Formation is not expected to be greater than approximately 0.2 meter per 250,000 years (less than 1 centimeter per 10,000 years) if salt removal remains controlled by diffusion.
- If convective mechanisms of salt removal (density flow) occur, the dissolution rate could be much greater than the rate for diffusion-controlled removal. The upper bound on convective dissolution rates would be determined by the salt transport capacity of the Bell Canyon aquifer. Under these conditions, the average vertical removal of salt from the Castile and Salado Formations should not exceed 8 centimeters per 10,000 years. This rate does not consider the possibility of more intense localized dissolution features.

4.5 COMPARISON OF THE RESULTS

In the initial sections of this chapter, analytical calculations for average mass flow rates in the Bell Canyon and Capitan Reef aquifers and average dissolution rates in the Castile and Salado Formations were presented. Results from numerical simulations of the flow and transport characteristics of these media were also outlined in order to give a more detailed description of salt dissolution and transport in stratigraphic units underlying the WIPP facility. Both analytical and numerical calculations indicate that salt dissolution by continuous diffusion along the 16,500-meter section beneath the WIPP facility could produce the observed chloride concentrations in the Bell Canyon aquifer. Although localized convective dissolution may be present, it is unlikely that convection occurs over a widespread area because the associated large mass dissolution rate would far exceed the capacity of the aquifer to remove the dissolved salt.

In terms of vertical propagation of a uniform cavity underlying the WIPP facility, the current dissolution rate was estimated to be in the range of 0.2 to 0.5 centimeter per 10,000 years (5 to 13 centimeters per 250,000 years) on the average over the 16,500-meter length of the section shown in Figure 4-3. However, as indicated, dissolution will be higher in the western direction where the chloride concentration is lower than the north-northeastern direction when chloride concentration in the Bell Canyon has almost reached full saturation. Future variations from these estimates due to various changes of hydrogeologic and geochemical parameters were evaluated and the results are presented in Appendix B.

Based on observed mass transport rates in the Capitan Reef and existing deep-seated dissolution features (breccia pipes), convective mechanisms such as brine density flow may be occurring at the reef margin. The deep-seated dissolution features are observed more than 20 kilometers away from the WIPP facility. They may be associated with vertical convective dissolution. Since this mechanism appears to be associated with

the specific hydrologic conditions at the reef margin, the present or potential future salt removal in the Captian Reef aquifer will not have an effect on salt removal beneath the WIPP facility.

To this point, dissolution rates have been discussed only relative to an essentially uniform dissolution along the total length of sections from which salt removal might occur. A more conservative and also implausible estimate relative to the future integrity of the WIPP facility involves concentrating the Bell Canyon Formation's potential salt transport capacity over a much smaller area beneath the site. For example, it might include investigating the dissolution from a hypothetical cylindrically shaped porous zone of relatively high permeability material in the Castile and Salado Formations which lies beneath the site. A second implausible potential mechanism is dissolution through a continuous fracture of large vertical extent. Both of these processes can be driven by density flow transport which removes material from halite layers by convection and diffusion. These computations, imposed in addition to the existing diffusion-type dissolution presently occurring, will provide an implausible "worst case" analysis of the potential dissolution effects on the WIPP facility. These analyses are discussed in Chapter 5.0.

5.0 ASSESSMENT OF SALT DISSOLUTION

The analytical calculations and numerical simulations presented in the previous chapters provide important information toward understanding the salt dissolution mechanisms occurring in the vicinity of the WIPP site. An assessment of the impact of salt dissolution on the site integrity must include consideration of the potential solution cavity that may form in the Castile or Salado Formations due to the anticipated dissolution rates. In addition, "worst case" dissolution processes which consider salt removal from a concentrated area beneath the WIPP facility as a function of the maximum Bell Canyon mass transport capacity should be considered. These worst case dissolution processes consist of convective transport of salt from halite layers through either a fracture or porous zone, as identified in Section 3.2. In the following sections, estimates of the range of likely rates of salt removal will be presented. These estimates will be followed by a discussion of the size of solution cavities which might be opened beneath the WIPP site from a worst case event and an assessment of the potential structural impacts relative to the WIPP facility.

5.1 EXTENT AND RATE OF GENERAL DISSOLUTION IN THE CASTILE FORMATION

The results of analytical calculations and numerical modeling relative to the potential average salt dissolution rate along a 16,500-meter length of section beneath the WIPP site were presented in Sections 4.3 and 4.4. In this section, the results from the previous chapters are evaluated to determine the potential range of average dissolution rates, and therefore cavity sizes, that could occur beneath the WIPP facility along an extended length assuming continuation of steady-state conditions. Dissolution associated with a more vigorous mechanism is considered in the worst case analysis presented in the following section.

The extent of possible variation in the average dissolution rate has been investigated in two separate ways. The first approach assumes that the rate of dissolution is solely controlled by the rate at which the

aquifer transports salt away from the dissolving areas. This method is independent of the actual dissolution mechanism and requires the assumption that the system remains at a steady state. The second approach assumes that a specific mechanism (diffusion in this case) operates and that the dissolution rate is affected both by the aquifer properties and by the dissolution mechanism.

The first approach is associated with the flow rate, Q, in the Bell Canyon aquifer and the reported changes of chloride concentration shown in Figure 4-1. From this figure, the average concentration variation, C, along a certain section can be determined. Therefore, from Equation (B-2) in Appendix B, the salt removal rate is directly proportional to the flow rate provided the dissolution mechanism would not restrict the vertical mass flux of salt to the Bell Canyon aquifer. Since the flow rate is dependent on the hydraulic conductivity, hydraulic gradient, and aquifer thickness, a fractional change in any one of these values produces a similar change in the salt dissolution rate. By varying the values for the parameters in Equation (B-2), the possible range of dissolution rates may be calculated. This type of approach is useful because it facilitates an understanding of the effect of possible parameter ranges on the calculated mass transport and also allows conservative estimation of the impacts of potential future changes in the flow system (e.g., hydraulic gradient) on the dissolution rate. The sensitivity analysis is presented in detail in Appendix B and summarized here. The analysis is conservative because the dissolution mechanism is assumed not to restrict the rate at which salt can be dissolved and transported. For a Bell Canyon aquifer flow rate of 0.135 $m^3/yr-m$ and a chloride concentration increase of 55 kg/m^3 (numerical model results), the average dissolution cavity height in 10,000 years would be 0.34 centimeter. Figure 5-1 presents the average dissolution zone height variation with time for a continuous solution zone formed in the Halite I overlying the Bell Canyon aquifer. If the aquifer thickness is assumed to be 60 meters rather than 30 meters, the average salt removal corresponding to a 55-kg/m^3 chloride increase would be 0.68 centimeter per 10,000 years and 17 centimeters in 250,000 years.

DRAWN BY	RW 11-19-81	CHECKED BY	
		APPROVED BY	

DRAWING NUMBER NM78-648-A25

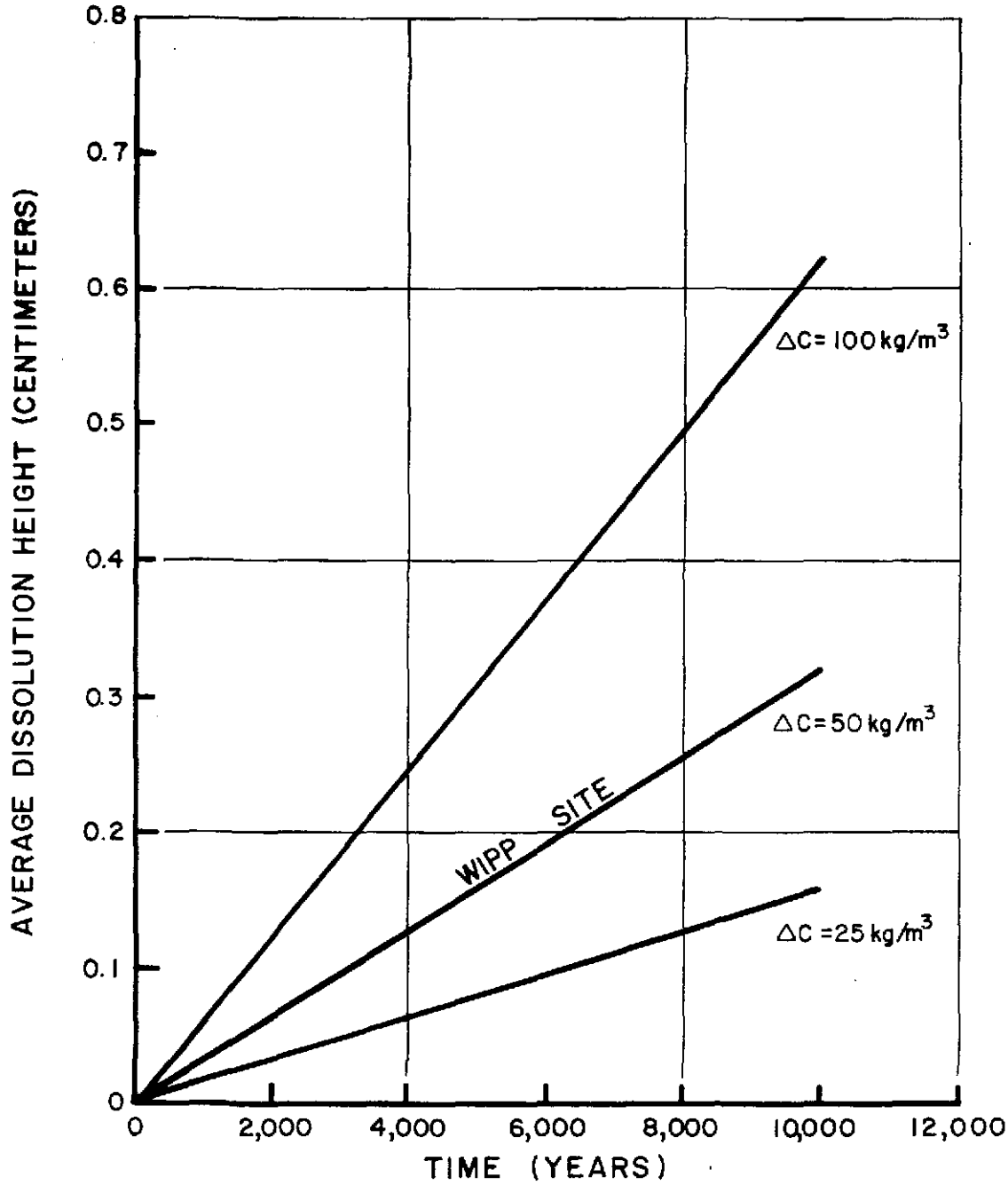

NOTES

1. FOR THIS PLOT THE FLOW, Q, IN THE BELL CANYON AQUIFER IS 0.135 CUBIC METERS PER YEAR.
2. THE AVERAGE DISSOLUTION HEIGHT IS BASED ON Q AND THE LONGITUDINAL CONCENTRATION DIFFERENCE (ΔC) OF CHLORIDE IN THE BELL CANYON AQUIFER OVER A LENGTH OF 16,500 METERS.

FIGURE 5-1

AVERAGE DISSOLUTION HEIGHT VARIATION WITH TIME

PREPARED FOR

WESTINGHOUSE ELECTRIC CORPORATION
ALBUQUERQUE, NEW MEXICO

D'APPOLONIA

As discussed previously, the potentiometric surface in the Capitan Reef aquifer has been affected by the pumping of water for oil field flooding operations and will ultimately influence the hydraulic gradient in the Bell Canyon aquifer near the reef. Similar to the assessment of the impact of effective aquifer thickness, an increase in flow rate due to a change in hydraulic gradient might change the mass transport of salt in the Bell Canyon aquifer. Based on the current potentiometric surface in the Capitan Reef aquifer as shown in Figure 2-5, the hydraulic gradient could increase in the Bell Canyon aquifer near the WIPP facility to 0.004 meter per meter. However, due to the low permeability of the Bell Canyon aquifer and hence its slow response time, the actual development of this gradient throughout the aquifer would require a period equivalent to the time of travel through the section, about 2.5 million years. Even if it is assumed that the gradient increases to 0.004 meter per meter, the calculated dissolution cavity would still be about one centimeter in 10,000 years.

These results reflect maximum obtainable dissolution rates based on the Bell Canyon aquifer characteristics. They do not consider the actual dissolution process (i.e., diffusion or convection) which may limit the inflow of dissolved halite.

The second approach to data interpretation considers the actual dissolution process and involves the sensitivity of the parameters associated with the modeling of the Castile Formation in addition to the Bell Canyon aquifer. Section 4.4.3 presented the results of numerical modeling of diffusion of chloride from halite layers in the Castile to the Bell Canyon aquifer. Analysis of the interrelationships between parameters and their effects on salt dissolution as discussed in Section 4.4.4 identified the important factors in the salt dissolution process occurring at the site and established the sensitivity of the dissolution rate to variation in parameter values. As indicated in Appendix B, the dissolution rate based on diffusion in the Castile is not linearly related to the Bell Canyon aquifer flow rate in that, at increased flow rates,

the dissolution rate does not increase as rapidly. This is illustrated in Figure 5-2 which compares the dissolution rate based solely on aquifer flow rate, as discussed in the preceding paragraph, and the dissolution rate as a function of aquifer flow rate in which the diffusion process limits the availability of the salt to be transported by the Bell Canyon aquifer.

The sensitivity of salt dissolution to future changes in flow and diffusion parameters was discussed in Section 4.4.4. The conclusion that can be drawn from these results is that the potential dissolution rate due to a change in a single parameter within its possible range of values is not expected to increase dissolution by more than a factor of two above the estimate given in Section 4.4.3 (0.34 centimeter in 10,000 years). As a result of these computations, it is apparent that the area of greatest potential uncertainty involves interpretation of the existing total flow rate and concentration distribution in the Bell Canyon Formation. Based on the discussions in Section 4.4.4 and Appendix B, the present maximum dissolution rate could conservatively be estimated to be one centimeter in 10,000 years over the 16,500-meter study section beneath the site (Figure 5-2). The structural consequences of the formation of such a cavity are assessed in Section 5.3.

Based on the observed concentrations of chloride (Figure 2-5) and the discussion of Section 4.3, convective dissolution in the Castile overlying the Bell Canyon aquifer is probably not the dominant mechanism. However, as discussed in Section 4.3, dissolution at the Capitan Reef margin in the Castile and Salado may be associated with the convective mechanism and is consistent with observed deep dissolution features which suggest a more vigorous dissolution process than diffusion. An assessment of the potential halite removal rates due to convective dissolution, should conditions in the Bell Canyon aquifer change to promote this process, is addressed in the following sections concerning worst case scenarios.

DRAWN BY	JJL 3-1-82	CHECKED BY	RET 3/1/82	DRAWING NUMBER NM 78-648-A32
		APPROVED BY	SHD 12/15/82	

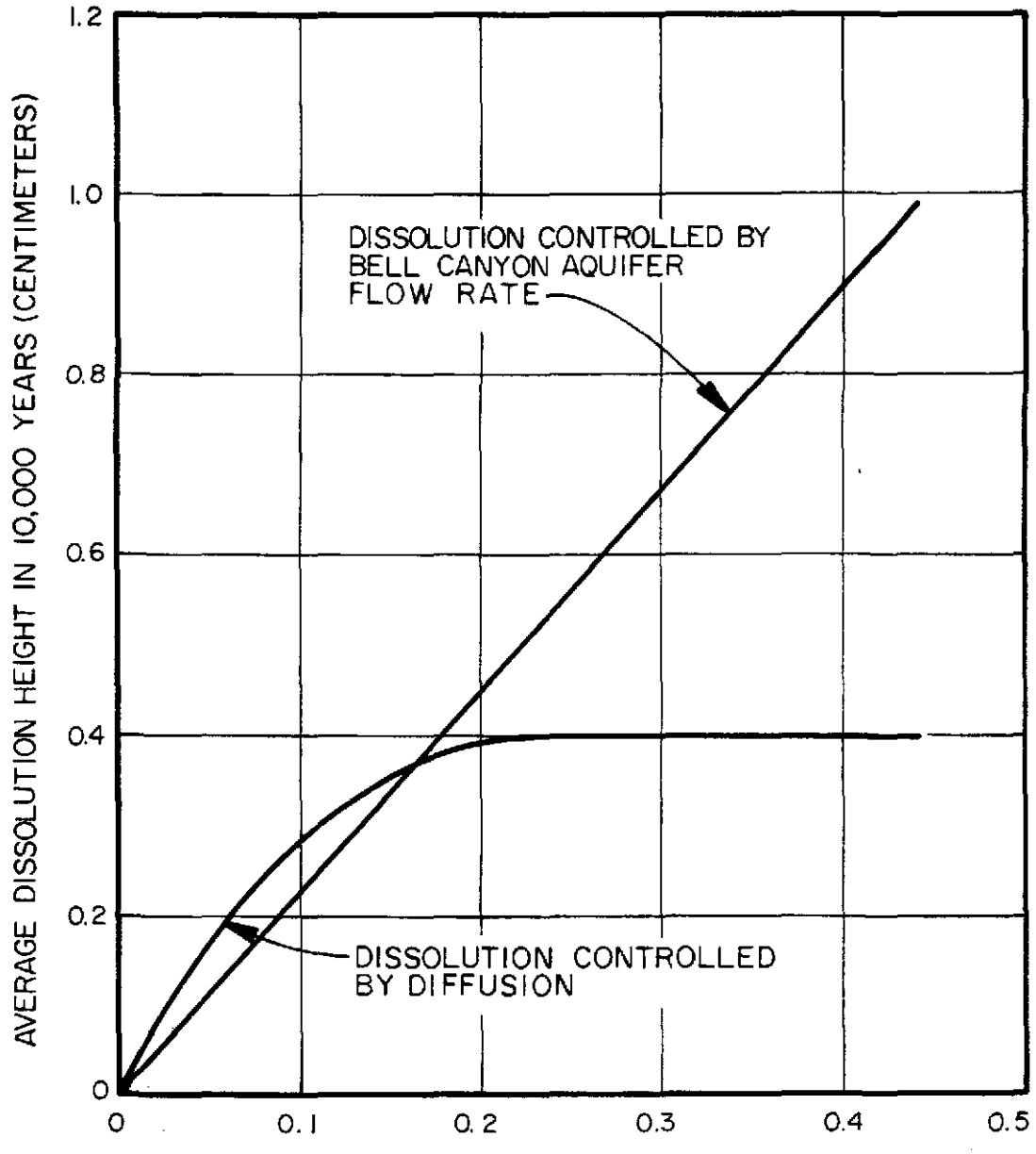

NOTES:

1. THE AVERAGE DISSOLUTION HEIGHT CONTROLLED BY THE BELL CANYON AQUIFER IS BASED ON A CHLORIDE CONCENTRATION INCREASE OF 50 kg/m^3 OVER AN AQUIFER LENGTH OF 16,500m.
2. THE DENSITY OF HALITE IS EQUAL TO 2160 kg/m^3
3. THE AVERAGE DISSOLUTION HEIGHT CONTROLLED BY DIFFUSION WAS DETERMINED BY NUMERICAL MODELING (REFER TO FIGURE 4-3).

FIGURE 5-2

COMPARSION OF DISSOLUTION CONTROLLED BY DIFFUSION AND BELL CANYON AQUIFER

PREPARED FOR

WESTINGHOUSE ELECTRIC CORPORATION
ALBUQUERQUE, NEW MEXICO

D'APPOLONIA

5.2 ANALYSIS OF "WORST CASE" DISSOLUTION POTENTIAL

In Section 5.1, results of computations concerning potential average dissolution beneath the WIPP site were discussed. The previous analysis has indicated that the diffusion mechanism is dominant in controlling the rate of halite dissolution above the Bell Canyon aquifer. However, the possibility of the existence or future formation of isolated fractures which would promote more vigorous dissolution must be addressed. This section presents a methodology for determining a "worst case" estimate of very localized salt dissolution that, although implausible, is imposed over a much smaller plan area than considered in Section 5.1. Two types of mechanisms for removing halite are evaluated:

- Dissolution through a continuous fracture of large vertical extent
- Dissolution through a cylindrically shaped porous zone.

These two mechanisms are illustrated in Figure 5-3 with the results of the salt removal analyses presented in Figures 5-4 and 5-5.

5.2.1 Dissolution Through a Fracture

Figure 5-3(A) shows a diagram of a potential fracture-induced dissolution cavity. Based on discussions in Section 3.2 and the relationship defined by Equations (3-1), (3-5), and (3-6), dissolved salt could be removed from a halite layer and discharged into the Bell Canyon aquifer through convection and diffusion in a single continuous fracture. The rate at which dissolved salt could be removed is a function of the Rayleigh and Nusselt numbers [Equations (3-5) and (3-6)], the fracture width, and the capacity of the aquifer to transport the additional mass away (downgradient) from the fracture. The shape of a dissolution cavity formed by this process will depend on the material characteristics of the halite layer, especially homogeneity and purity. The Halite I is not pure and contains, with varying degree, anhydrite laminae and thin clay partings. These impurities will cause the potential cavity to advance mostly in the horizontal direction rather than in the vertical

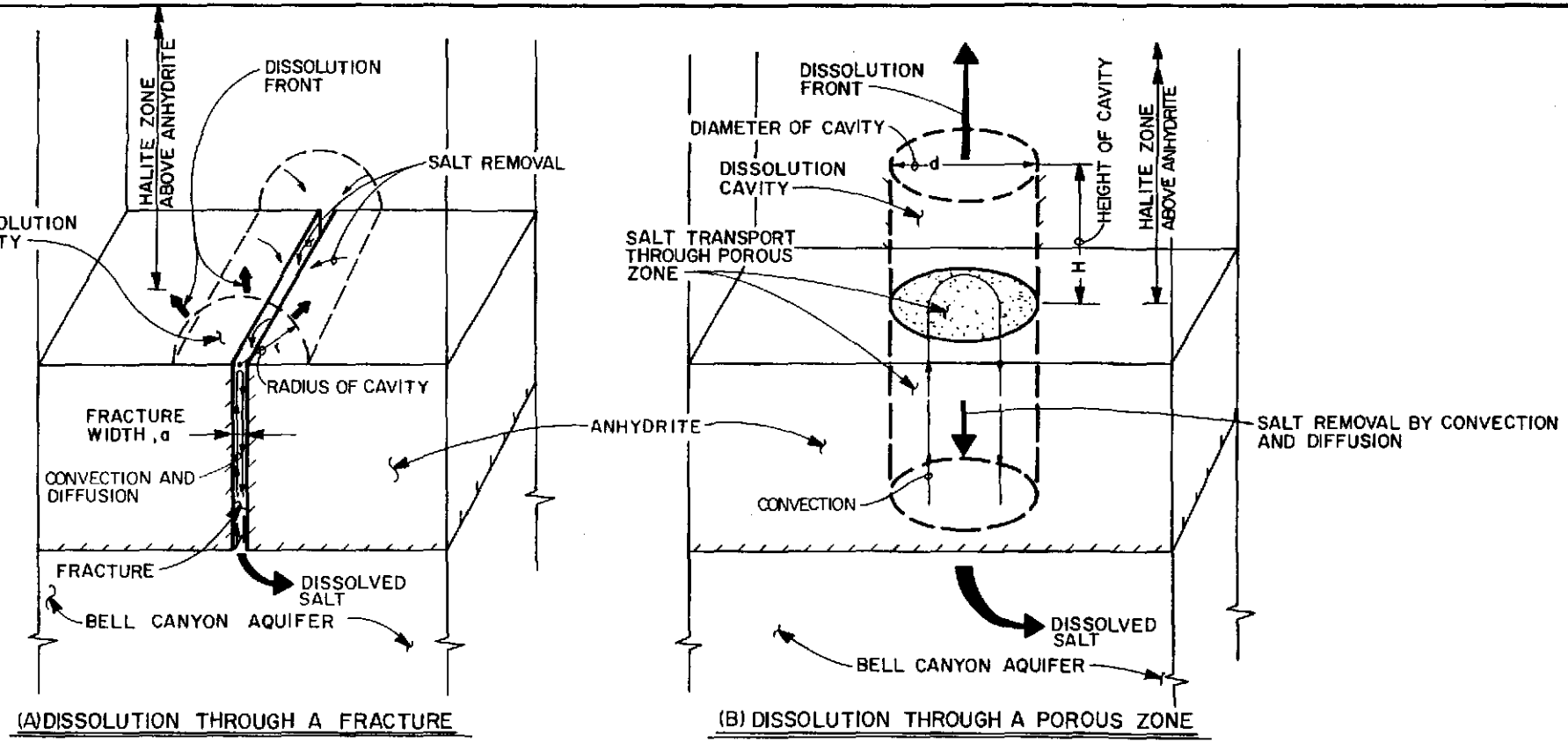

DRAWN BY GAM 11-18-81 | CHECKED BY REI | APPROVED BY LSHO | DRAWING NUMBER NM 78-648-835

FIGURE 5-3

ILLUSTRATION OF IMPLAUSIBLE WORST CASE DISSOLUTION MECHANISMS

PREPARED FOR

WESTINGHOUSE ELECTRIC CORPORATION
ALBUQUERQUE, NEW MEXICO

DAMES & MOORE

DRAWN BY	CHECKED BY	APPROVED BY	DRAWING NUMBER
J.J.L. 1-16-81			NM78-648-B34

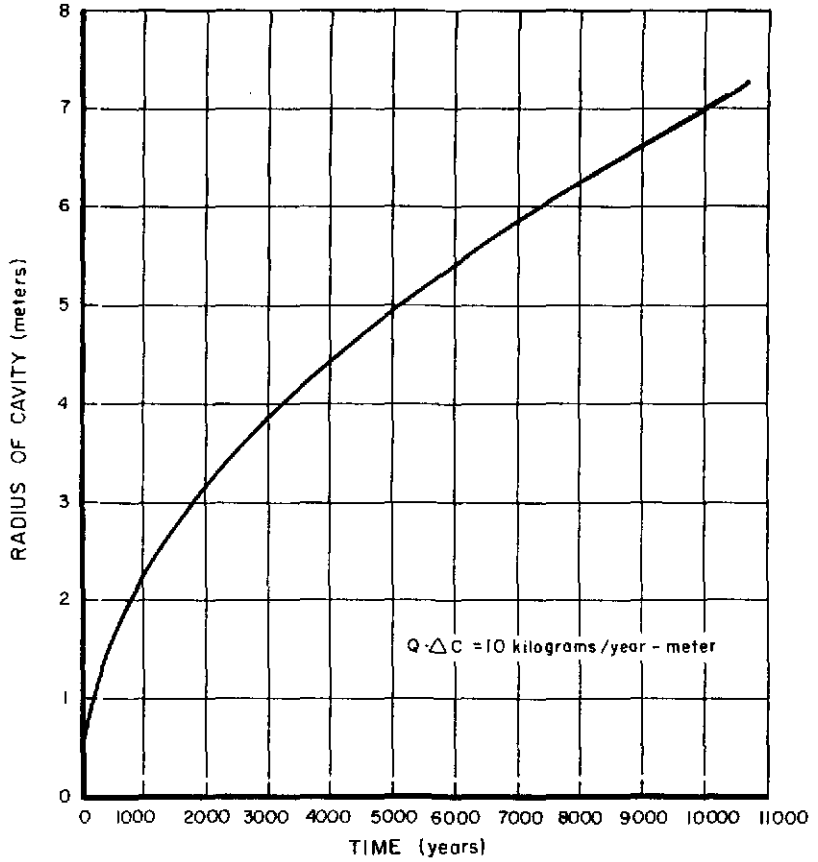

(A) GROWTH OF CAVITY WITH TIME

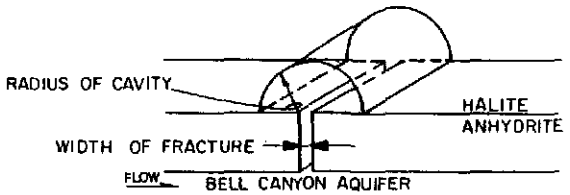

SCHEMATIC OF FRACTURE DISSOLUTION CAVITY

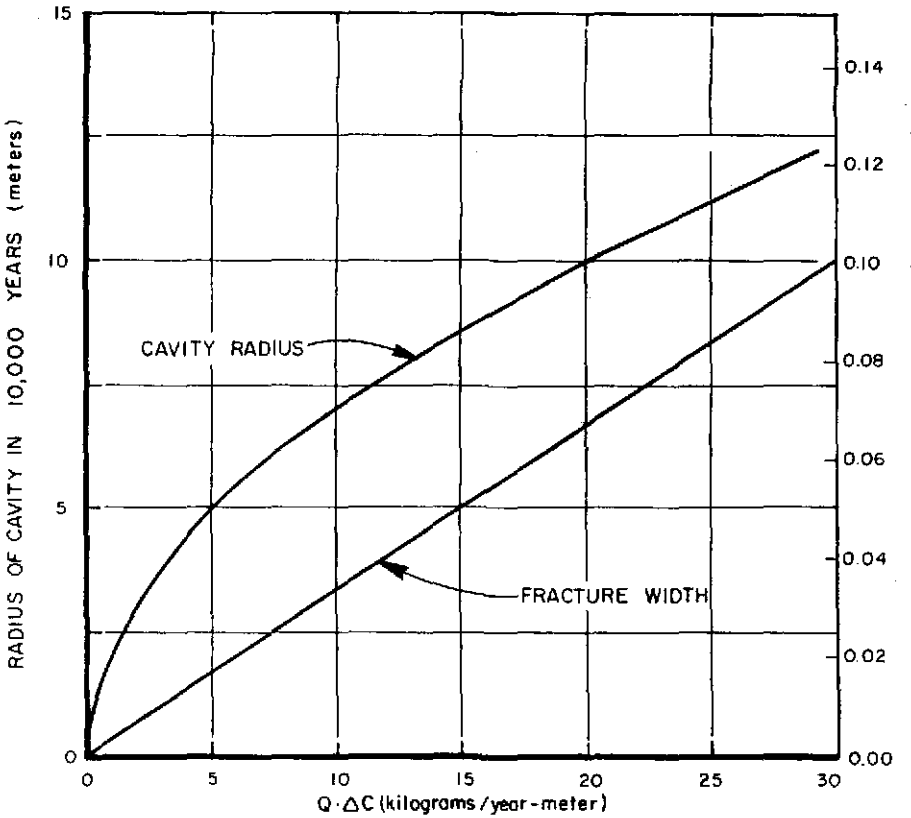

(B) POTENTIAL CAVITY SIZE AS A FUNCTION OF AQUIFER CHLORIDE TRANSPORT CAPACITY

NOTES:

1. THE EFFECTIVE FRACTURE WIDTH REPRESENTS THE TOTAL APERTURE OF A FRACTURE NETWORK OR THE ACTUAL WIDTH OF A SINGLE FRACTURE.
2. SEE FIGURE 5-3 FOR DIAGRAM OF DISSOLUTION MECHANISM AND LOCATION OF POROUS ZONE.
3. QΔC IS THE PRODUCT OF THE FLOW IN THE BELL CANYON AQUIFER, Q (m^3/yr.-m) AND THE ALLOWABLE INCREASE, ΔC(kg/m^3), IN CHLORIDE CONCENTRATION (SATURATION LEVEL) IN THE AQUIFER.
4. RANGE OF Q·ΔC INCLUDES AN AQUIFER THICKNESS FROM 30 meters to 60meters.

FIGURE 5-4

POTENTIAL GEOMETRY OF FRACTURE-INDUCED DISSOLUTION CAVITY

PREPARED FOR

WESTINGHOUSE ELECTRIC CORPORATION
ALBUQUERQUE, NEW MEXICO

DAPTOLONA

DRAWN BY	CHECKED BY	APPROVED BY	DRAWING NUMBER NM78-648-836
J.J.L. 1-19-81			

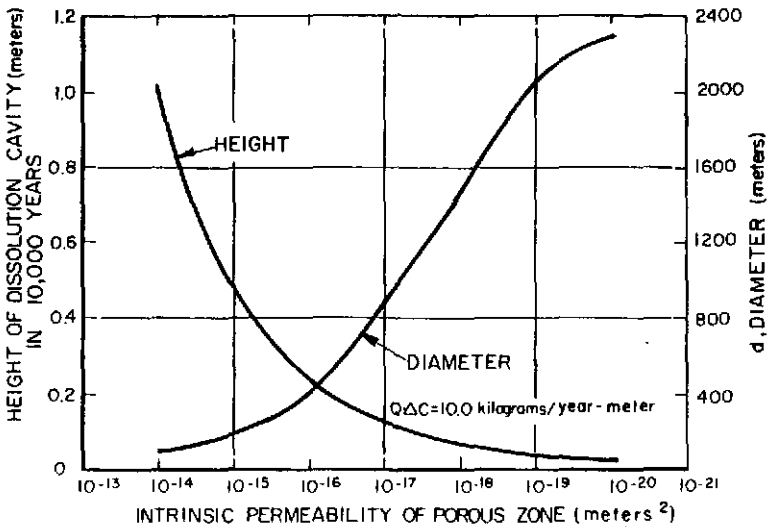

(A) POTENTIAL CAVITY SIZE AS A FUNCTION OF INTRINSIC PERMEABILITY

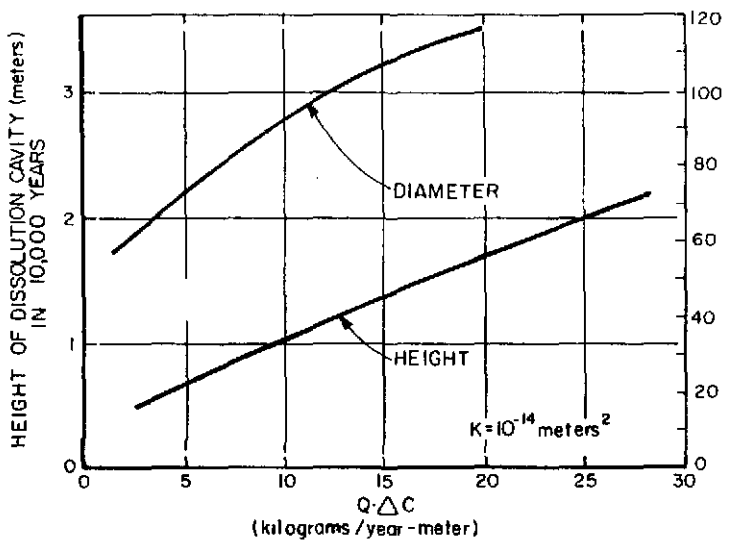

(B) POTENTIAL CAVITY SIZE AS A FUNCTION OF AQUIFER CHLORIDE TRANSPORT CAPACITY

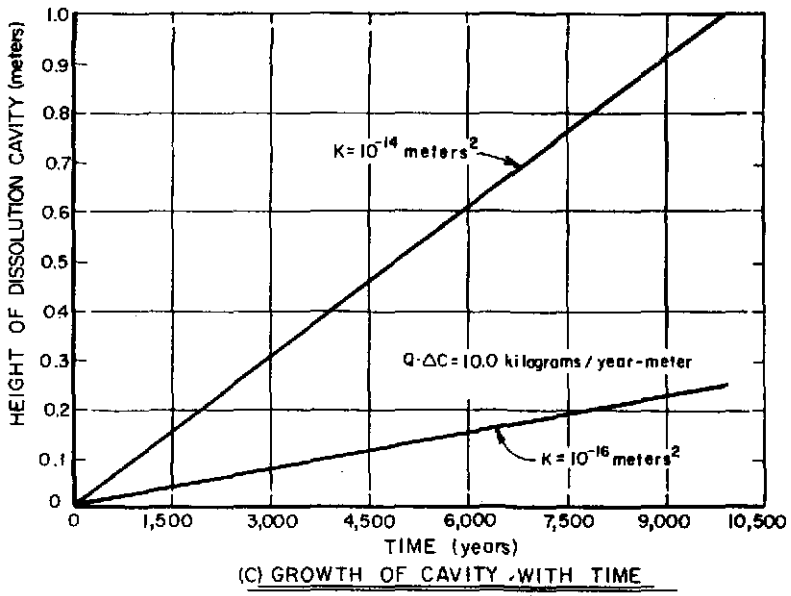

(C) GROWTH OF CAVITY WITH TIME

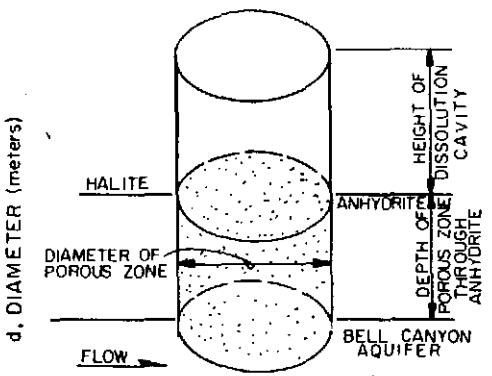

SCHEMATIC OF POROUS ZONE DISSOLUTION CAVITY

NOTES:

1. SEE FIGURE 5-3 FOR DIAGRAM OF *DISSOLUTION MECHANISM* AND LOCATION OF POROUS ZONE
2. Q·ΔC IS THE PRODUCT OF THE FLOW IN THE BELL CANYON AQUIFER, Q (m^3/yr.-m) AND THE ALLOWABLE INCREASE, ΔC (kg/m^3), IN CHLORIDE CONCENTRATION (SATURATION LEVEL) IN THE AQUIFER.
3. RANGE OF Q·ΔC INCLUDES AN AQUIFER THICKNESS FROM 30 meters to 60 meters.

FIGURE 5-5

POTENTIAL GEOMETRY OF POROUS ZONE-INDUCED DISSOLUTION CAVITY

PREPARED FOR

WESTINGHOUSE ELECTRIC CORPORATION
ALBUQUERQUE, NEW MEXICO

D'APPOLONIA

direction. However, to provide a representative geometry, the dissolution is assumed to propagate uniformly in a radial fashion away from the fracture so as to form a cylindrical cavity originating at the bottom of a halite layer. The density gradient which drives the convection mechanism is dependent on the vertical concentration gradient associated with saturated brine in the halite layer and the observed salinity values in the Bell Canyon aquifer. Similar to the procedure used to estimate average salt dissolution, the rate at which salt can be removed from the fracture (i.e., the dissolution rate) is assumed to equal the product of the aquifer flow rate and the downgradient increase in salt concentration above the concentration existing directly below the fracture. For the worst case analysis, the downgradient chloride concentration is the maximum or saturation value, 190 kg/m^3 (315 kg/m^3 salt concentration). As demonstrated in Section 4.4.3, a one-dimensional analysis such as this which does not incorporate the effects of horizontal flow in the Bell Canyon on the vertical concentration gradient is sufficient to evaluate the potential implication of the worst case scenario.

Figure 5-4(A) illustrates the rate of development of a cylindrical cavity for a chloride removal rate of 10 kg/yr-m (16 kg/yr-m salt removal rate). The dissolution rate is based on an aquifer flow rate of 0.135 m^3/yr-m and a chloride concentration increase from 120 kg/m^3 beneath the fracture to 190 kg/m^3 downgradient of the fracture. Figure 5-4(B) illustrates the potential cavity sizes in 10,000 years for a range of chloride removal rates. Also shown are the minimum fracture widths required to transport the indicated chloride removal rates. For a given removal rate, the fracture width is the minimum width that could transport the indicated amount of chloride from the dissolution zone down to the Bell Canyon (100 meters) by a combination of convective and diffusive mechanisms. The magnitudes of convective and diffusive transport that could develop were determined by combining Equations (3-1), (3-5), and (3-6) to give an analytical expression for total salt transport through a fracture as a function of the diffusion coefficient,

fracture height, fluid viscosity, concentration difference between the top and bottom of the fracture, and the fracture width. By holding the chloride concentration difference constant at 70 kg/m^3 (190 to 120 kg/m^3 variation) and equating salt transported through the fracture with salt removed by the aquifer, the fracture width becomes a linear function of the Bell Canyon aquifer salt removal rate. For a particular salt removal rate, a larger fracture than indicated on the curve of Figure 5-4 would produce the same dissolution rate.

A chloride removal rate of 10 kg/yr-m (equivalent to a halite dissolution rate of about 16 kg/yr-m) requires a minimum fracture width on the order of 0.3 millimeter and may result in a dissolution cavity, based on the geometry shown in Figure 5-3, with a radius of approximately 7 meters in 10,000 years for the implausible worst case. Figure 5-6 illustrates the computed hypothetical cavity relative to the stratigraphy beneath the WIPP facility. The computed width of fracture is a minimum value required to sustain the indicated chloride transport rate. If the fracture width were greater than the minimum value, the rate of salt removal would be unchanged. This is because the dissolution rate is limited to 16 kg/yr-m due to the Bell Canyon aquifer salt removal capacity.

As discussed above, the worst case analysis for a fracture-induced cavity beneath the WIPP facility allows the aquifer transport rate to control the rate of dissolution in the Halite I. To assess the most critical conditions, the maximum Bell Canyon transport rate was utilized in the computations. However, because the dissolution and mass inflow from the fracture will raise the aquifer concentration, a reduction in the dissolution rate, which is dependent on the concentration gradient across the anhydrite, will occur. Figure 5-7 illustrates the influence of the mass flow rate into the aquifer and accompanying increase in aquifer concentration on the dissolution rate. Figure 5-7(A) presents the dissolution rate and radius of a hypothetical cavity beneath the WIPP facility. As indicated in the figures, a reduction in

DRAWING NUMBER	NM78-648-A38
CHECKED BY	RFS
APPROVED BY	SHA
R.F.T.	12-21-82
DRAWN BY	
100	6A
OR	6A

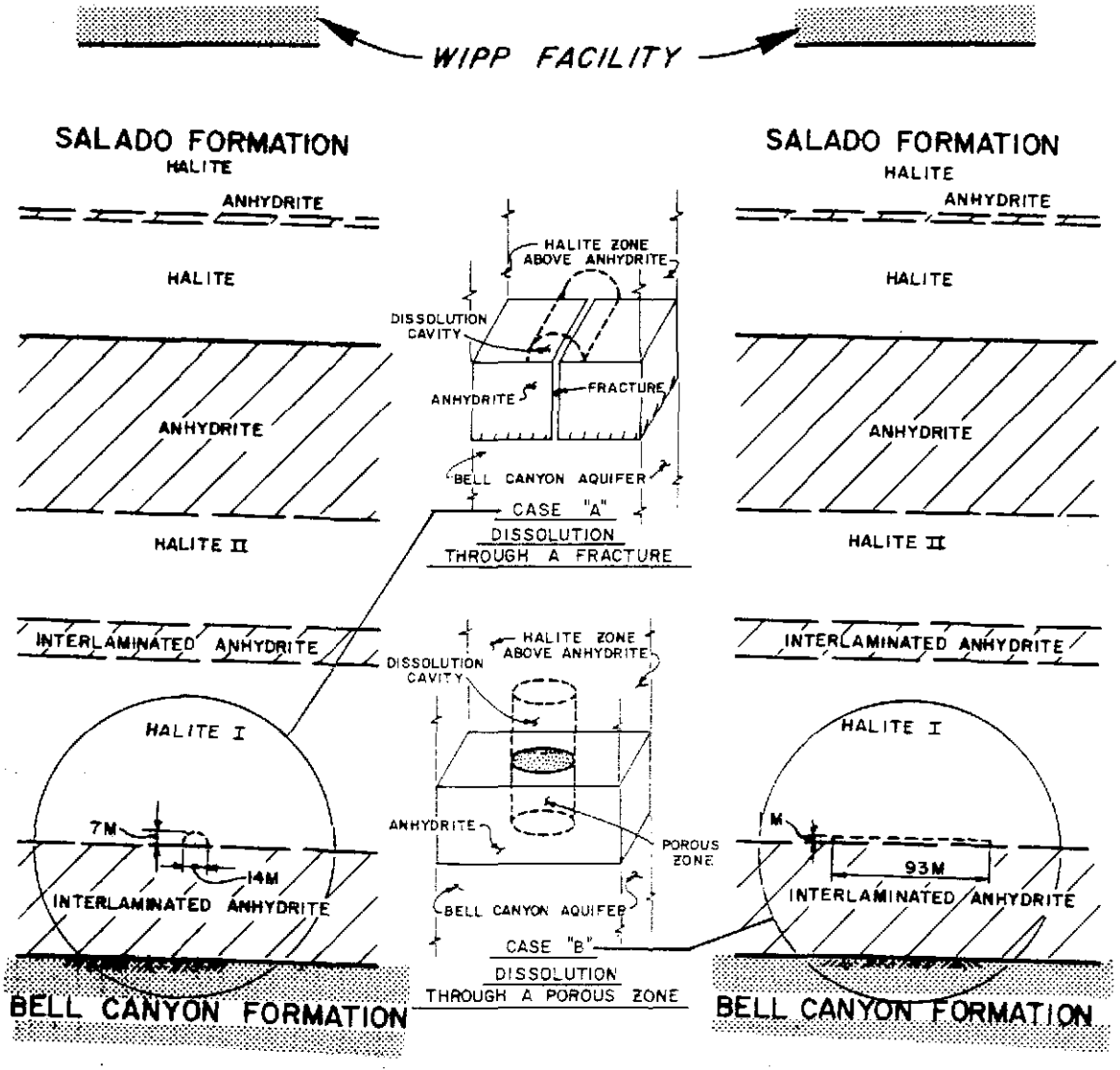

(A) FRACTURE INDUCED DISSOLUTION

(B) POROUS ZONE INDUCED DISSOLUTION

NOTES:

1. SEE FIGURE 5-3 FOR WORST CASE DISSOLUTION SCHEMES.
2. SEE FIGURE 2-1 FOR DETAILED STRATIGRAPHIC COLUMN OF SITE VICINITY.
3. CAVITY SIZES ARE CALCULATED *FOR 10,000 YEAR PERIOD.*

FIGURE 5-6

ILLUSTRATION OF
HYPOTHETICAL SOLUTION CAVITIES
FOR
IMPLAUSIBLE WORST CASE DISSOLUTION

PREPARED FOR

WESTINGHOUSE ELECTRIC CORPORATION
ALBUQUERQUE, NEW MEXICO

SCALE
0 100 200 METERS
0 200 400 600 FEET

D'APPOLONIA

19 1253 HERCULENE. A&B SMITH CO., PGH., PA.

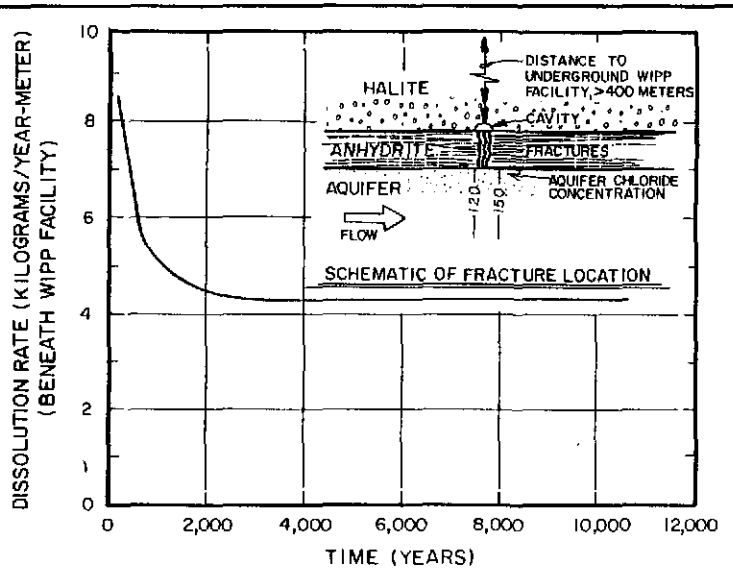

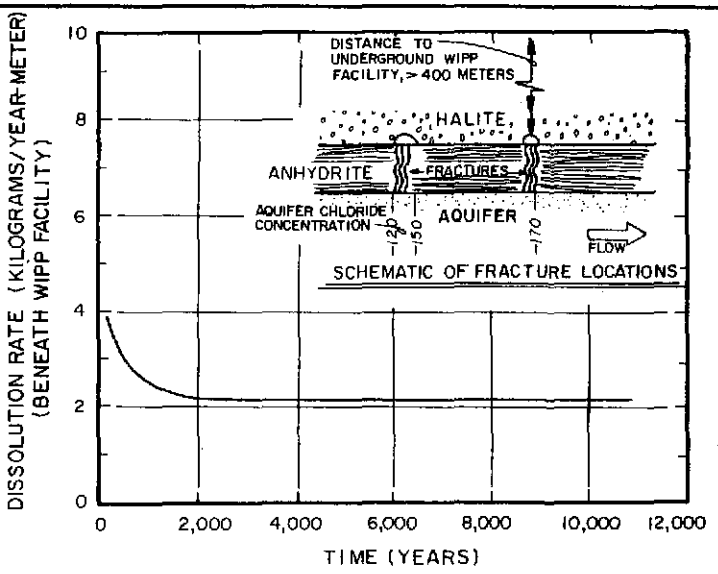

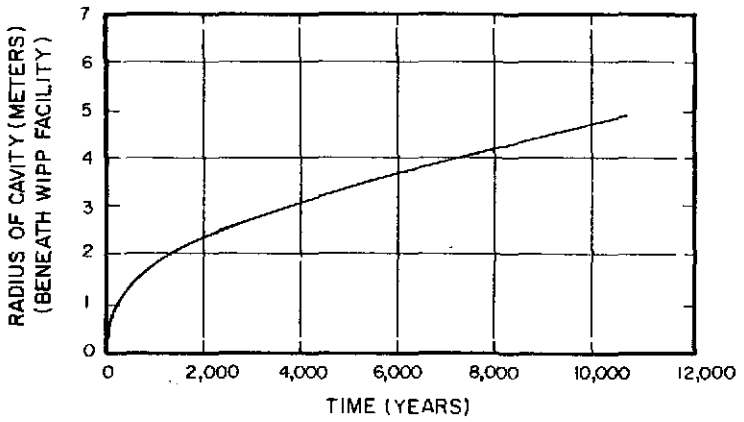

(A) FRACTURES BENEATH WIPP FACILITY

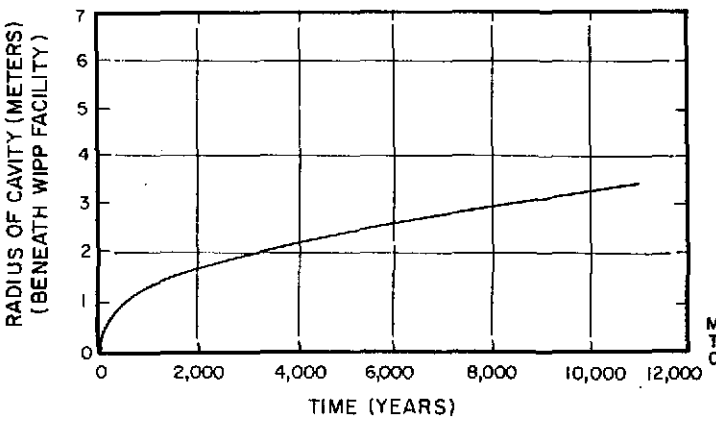

(B) FRACTURES UPGRADIENT AND BENEATH WIPP FACILITY

NOTES:

1. SEE FIGURE 5-6 FOR STRATIGRAPHY UNDERLYING WIPP FACILITY.
2. THE DISSOLUTION RATE AND RADIUS OF CAVITY FOR FRACTURES BENEATH THE WIPP FACILITY ARE BASED ON AN UPGRADIENT AQUIFER CHLORIDE CONCENTRATION OF 120 KG/M^3 AND FLOW RATE OF 0.135 $M^3/YR-M$.
3. THE DISSOLUTION RATE AND RADIUS OF CAVITY FOR FRACTURES UPGRADIENT AND BENEATH THE WIPP FACILITY ARE BASED ON AN UPGRADIENT AQUIFER CHLORIDE CONCENTRATION OF 151.5 KG/M^3 AND FLOW RATE OF 0.135 $M^3/YR-M$.
4. COMPUTATION OF THE DISSOLUTION RATE AND RADIUS OF CAVITY ARE BASED ON INSTANTANEOUS MIXING THROUGHOUT THE 30 METER AQUIFER THICKNESS AND A CONTROL VOLUME 30 METERS IN LENGTH. A SMALLER CONTROL VOLUME WOULD RESULT IN DEVELOPMENT OF THE STEADY STATE DISSOLUTION RATE AT AN EARLIER TIME.

FIGURE 5-7

MITIGATING EFFECT OF BELL CANYON AQUIFER TRANSPORT RATE ON IMPLAUSIBLE WORST CASE DISSOLUTION CAVITY DEVELOPMENT BENEATH THE WIPP FACILITY

PREPARED FOR

WESTINGHOUSE ELECTRIC CORPORATION
ALBUQUERQUE, NEW MEXICO

DAPTOLONIA

DRAWN BY	J.J.	3-1-82	CHECKED BY	
			APPROVED BY	

DRAWING NUMBER NM 78-648-855

the dissolution rate and cavity development occurs during the initial 4,000 years following initiation of mass transport through the assumed fractures due to a rapid increase in aquifer concentration. Beyond this time, the dissolution rate is essentially constant, resulting in a more gradually increasing cavity radius. In comparison with the worst case analysis in which the maximum aquifer chloride transport rate of 10 kg/yr-m is considered constant, Figure 5-7(A) illustrates a decrease in the transport rate to a steady-state value of approximately 4.2 kg/yr-m and the development of a hypothetical cavity radius of about 5 meters in 10,000 years.

An investigation was also conducted in which the dissolution associated with fractures directly beneath and also upgradient of the WIPP facility would be controlled by the maximum aquifer transport rate. The results of this analysis are shown in Figure 5-7(B) which includes the hypothetical time rate of dissolution and cavity development beneath the WIPP facility considering the influence of mass inflow from fractures upgradient of the facility. Should fractures be present upgradient, an increase in concentration in the aquifer would be encountered with the result of decreasing the dissolution rate beneath the WIPP facility due to the reduced concentration gradient across the anhydrite. As indicated in Figure 5-7(B), the dissolution rate is less than 50 percent of the rate presented in Figure 5-7(A) and the radius of a hypothetical cavity would be less than four meters.

An assessment of the impact of a solution cavity, which may be associated with this scenario, on the integrity of the underground WIPP facility is presented in Section 5.3. The following section addresses the second worst case scenario, dissolution through a porous zone.

5.2.2 Dissolution Through a Porous Zone

Figure 5-3(B) presents a diagram of a potential cavity formed by convection and diffusion through a zone of relatively porous material. The

physical meaning of mass transport through such a porous zone may be interpreted as simply movement through a porous medium, such as the anhydrite, or movement through a fractured zone of material with higher permeability. The quantity of salt that could be removed from a region overlying such a zone is a function of the Rayleigh and Nusselt numbers for flow through a cylindrically shaped porous zone [Equations (3-8) and (3-9)], the zone diameter, and the capacity of the Bell Canyon aquifer to transport the additional mass downgradient from the porous zone. As with the fracture, the geometry of a cavity produced by this process is dependent on many complex factors. However, the minimum areal extent (i.e., diameter) of the zone can be determined [Equation (3-4)] so that the maximum total height of a solution cavity can then be calculated by knowing the mass transport capacity of the Bell Canyon aquifer. For the computations that were performed, it was assumed that the dissolution front above the porous zone would propagate in a predominantly vertical direction due to the large horizontal area (as compared to a fracture) over which dissolution takes place.

Similar to the analysis presented in Section 5.2.1, the maximum chloride transport rate based on existing aquifer characteristics is approximately 10 kg/yr-m, corresponding to a halite dissolution rate of about 16 kg/yr-m. As discussed in Section 3.2.4 and presented in Table 3-1, the removal of salt by diffusion is approximately equal to removal by convection for an intrinsic permeability of 4×10^{-17} square meters (approximately equivalent to a hydraulic conductivity of 4×10^{-10} meters per second). At greater permeabilities, convection dominates and, at lesser permeabilities, diffusion is dominant. As may be expected, for large-diameter zones (and small permeabilities), the height of a potential salt cavity approaches the average height calculated with the numerical model (0.34 centimeter in 10,000 years) as presented in Section 5.1 for average dissolution beneath the site.

The results of the calculations are presented in Figure 5-5. Figure 5-5(A) illustrates the dependence of the porous zone diameter and height

on the intrinsic permeability of the porous zone for a Bell Canyon chloride transport rate of 10 kg/yr-m. These curves show the maximum potential size (height and diameter) of a cavity for a wide range of permeability characteristics of the anhydrite unit. Figure 5-5(B) illustrates the hypothetical maximum potential cavity sizes based on the possible range of aquifer chloride removal rates due to parameter variability.

For a chloride transport rate of 10 kg/yr-m, the diameter of a cylindrical cavity as depicted in Figure 5-3 was calculated to be approximately 93 meters and the height was determined to be 1 meter in 10,000 years for an intrinsic permeability of 10^{-14} *square meters* in the Castile anhydrite. Figure 5-6 presents the hypothetical cavity in relation to the overlying stratigraphy in the vicinity of the WIPP facility. Selection of this intrinsic permeability is believed representative of the worst case analysis since this value reflects a high degree of fracturing (approximately equivalent to a hydraulic conductivity of 10^{-7} meters per second). A discussion of the implications for the underground WIPP facility of the generation of dissolution cavities follows in the next section.

5.3 IMPLICATION OF DISSOLUTION ON THE UNDERGROUND WIPP FACILITY

The effects of development of solution cavities in a halite layer, as determined above, have been assessed by considering the physical phenomena associated with development, support, and stabilization of a potential void. The three cases presented above which must be addressed are:

- Average dissolution cavity development over the Delaware Basin area due to diffusion of halite to the underlying aquifer resulting in a potential cavity height of less than 10 centimeters in 10,000 years.

- Implausible worst case dissolution cavity development under the WIPP facility due to convection and diffusion through a fracture of large vertical extent resulting in a cylindrical cavity (Figure 5-6) with a radius of 7 meters in 10,000 years.

- Implausible worst case dissolution cavity development under the WIPP facility due to convection and diffusion through a porous or fractured zone of large horizontal and vertical extent resulting in a cavity (Figure 5-6) with a diameter of 93 meters and a height of 1 meter in 10,000 years.

The purpose of this assessment is to identify the significance of the present diffusion rate and the potential effects of the worst case scenarios. While a more detailed rock mechanics study would be required to analyze and quantify the effects of a void on the overburden stresses, the considerations discussed herein address the physical phenomena which would mitigate the influence of a dissolution cavity on the underground WIPP facility.

Several factors influence the development of a dissolution cavity. The development will be retarded due to the overburden pressures which can initiate creep and flowage of salt into a void. The rate of creep is dependent on the difference in pressure associated with the brine-filled cavity and the lithostatic pressure imposed by the overburden as well as the material properties of the halite. The stress associated with this pressure difference is difficult to predict and consequently an assessment of the effect of creep during development of the cavity has not been quantified at this time. Considering a fracture of large continuous extent, corresponding to the second case identified above, halite at depths associated with the Castile Formation would tend to "heal" such a fracture and limit convective diffusion from the salt unit as well as retard cavity development. Similar mechanisms would influence the ability of a fracture network to sustain a significant dissolution rate.

Should development of a cavity be encountered, the rock overburden may provide support to prevent collapse and influence of overlying halite units. Consideration of support of a possible cavity is more appropriate for the higher dissolution rates associated with the worst case scenarios. It can be anticipated that should a brine-filled solution

cavity develop in the Halite I due to deep-seated dissolution, the overburden would provide some support in mitigating subsidence propagation.

Stabilization of a cavity can occur due to creep and flowage of salt. The extent of influence of this stabilizing mechanism on the overburden is dependent on the stratigraphy and properties of the overlying halite and anhydrite as well as the size of the cavity and rate of creep which is significantly affected by the deviatoric stress. However, the brine pressures in a cavity would decrease the deviatoric stresses around the cavity, hence slowing its closure due to creep.

As indicated above and discussed in detail in Section 5.1, the average dissolution rate may be anticipated to result in a cavity at the Halite I horizon throughout the Delaware Basin of less than 10 centimeters in 10,000 years, provided mechanisms such as creep do not eliminate or retard development. The underground WIPP facility is more than 400 meters above the Halite I horizon. Based on the physical phenomena associated with development, support, and stabilization of a solution cavity, a dissolution zone of 10 centimeters cannot be anticipated to have an effect on the site integrity.

Figure 5-6 presents the potential implausible worst case dissolution cavities (fracture and porous zone induced) relative to the stratigraphy underlying the underground WIPP facility. Dissolution under the implausible worst case conditions analyzed could result in development of a cavity with a 7-meter radius considering a fracture induced mechanism and a cavity 1 meter in height for a porous zone (93 meters in diameter) in 10,000 years. As is evident in Figure 5-6, more than 400 meters of overburden exist between the implausible worst case potential cavities and the floor of the WIPP underground facility. As a result, the propagation of the dissolution front would cause a creep deformation of the overburden salt prompting closure of the cavities. Considering the extremely small volume of salt removed in comparison with the total strata thickness, the vertical propagation of this deformation would

probably be limited to the lower section of the Halite I. As a result, development of a cavity based on the present dissolution rate as applied over the basin area, or associated with the worst case conditions considered here, is not anticipated to influence the performance of the underground WIPP facility.

6.0 CONCLUSIONS

The site geology and specific geologic evidence of dissolution of salt deposits in the Delaware Basin have been reviewed. The origin (near-surface as opposed to deep-seated) and rate of dissolution, as reported by various investigators (Anderson, 1978; Bachman, 1974), together with geochemical data in the Bell Canyon and Capitan Reef aquifers, clearly suggest that some deep-seated dissolution is present in the basin. A study of the potential mechanisms for deep-seated dissolution, molecular diffusion, and convective transport indicates that their solution capabilities are plausible relative to the geochemical and physical evidence of salt removal.

To demonstrate the dissolution capabilities of the salt removal mechanisms, one-dimensional analytical equations describing the mechanisms and their interrelationship have been applied to the Delaware Basin. Two-dimensional numerical modeling of flow and mass transport has provided a more precise study of salt dissolution in the Castile Formation and mass transfer to the Bell Canyon aquifer. The results of the modeling are consistent with observed chloride concentration levels in the Bell Canyon aquifer.

The potential solution zone which may develop based on the present dissolution rate as calculated in this study was determined from the analytical and numerical studies. In addition, two implausible worst case scenarios were also developed and the sizes of associated solution cavities estimated. Based on the calculated solution cavities, the possible implications of development of a dissolution cavity at the Halite I horizon on the integrity of the underground WIPP facility were assessed.

Based on this study, as summarized above, the following conclusions have been developed:

- Observed features which provide evidence for deep-seated dissolution are located at the Capitan Reef margin and consist primarily of breccia pipes. The origin of other dissolution features observed in the basin is open to interpretation although near-surface rather than deep-seated dissolution appears more plausible.

- The residence time of groundwater in the Bell Canyon aquifer is relatively long, with a flow rate which requires more than two million years to travel from recharge near the west reef margin to discharge at the east section of the Capitan Reef.

- The potential dissolution mechanisms include diffusion and convection from halite layers to underlying aquifers. Computation of the present dissolution rate based on observed chloride concentration levels in the Bell Canyon indicates that diffusion and possibly very weak convection result in the removal of halite from the Castile. However, convection may be considerably more significant at locations adjacent to the Capitan Reef aquifer.

- Evaluation of the present DMG hydrogeologic and geochemical conditions and review of their potential range of values indicate that halite dissolution associated with the Bell Canyon aquifer will not impact the underground WIPP facility. A solution zone of less than 10 centimeters in height was calculated based on the maximum dissolution rate in 10,000 years.

- Based on an analysis of potential changes in the hydrologic characteristics (i.e., hydraulic gradient) of the Bell Canyon aquifer, a possible increase in flow rate of one order of magnitude in the future would not impact the WIPP facility over the period of investigation, 10,000 years.

- Based on an analysis of the maximum potential dissolution rate associated with convective and diffusive dissolution mechanisms at the Bell Canyon aquifer-Castile Formation interface (i.e., worst case), no impact should be observed at the underground WIPP facility during the period of investigation, 10,000 years.

As part of this study, the salt dissolution mechanisms consisting of diffusion and convection have been investigated. Chapter 3.0 has addressed hypotheses based on these mechamisms, and the significance of the parameters which influence the diffusion and convection processes was presented. As is evident from this study, brine density flow or convective dissolution is a potential mechanism for removal of halite and its occurrence in the Delaware Basin is possible in areas overlying and at the Capitan Reef aquifer margin. However, the geochemical data from the Bell Canyon aquifer suggest that, if convective dissolution is a phenomenon related to this aquifer, it is not significant and results in dissolution at a rate no greater than that associated with the diffusive dissolution mechanism. Furthermore, the very low flow rate of the Bell Canyon aquifer and the associated salt transport rate indicate that significant convective dissolution of halite in the overlying Castile and Salado Formations would be prevented due to the inability of the aquifer to maintain the density gradient for any significant time period.

BIBLIOGRAPHY

BIBLIOGRAPHY

Adams, J. E., 1965, "Stratigraphic - Tectonic Development of Delaware Basin," Bulletin of the American Association of Petroleum Geologists, Vol. 49, No. 11, pp. 2140-2148.

Anderson, R. Y., W. E. Dean, Jr., D. W. Kirkland, and H. I. Snider, 1972, "Permian Castile Varved Evaporite Sequence, West Texas and New Mexico," Geol. Soc. Am. Bull., Vol. 83, pp. 59-86.

Anderson, R. Y., 1976a, "Correlation and Structural Relationships of the Castile-Salado Evaporite Sequence in ERDA #6, AEC #7 and AEC #8 Boreholes, Eddy and Lea Counties, New Mexico," Report to Sandia Laboratories, Albuquerque, New Mexico, 23 pp.

Anderson, R. Y., 1976b, "Geologic Evaluation of the Los Medanos (ERDA #9) W.I.P.P. Site, Eddy County, New Mexico," Report to Sandia Laboratories, Albuquerque, New Mexico, 28 pp.

Anderson, R. Y., 1978, "Deep Dissolution of Salt, Northern Delaware Basin, New Mexico," Report to Sandia Laboratories, Albuquerque, New Mexico, 106 pp.

Anderson, R. Y., K. K. Kietzke, and D. J. Rhodes, 1978, "Development of Dissolution Breccias, Northern Delaware Basin, New Mexico and Texas," Circular 159, New Mexico Bureau of Mines and Minerals Resources, pp. 47-53.

Anderson, R. Y. and D. W. Powers, 1978, "Salt Anticlines in Castile-Salado Evaporite Sequence, Northern Delaware Basin, New Mexico," Circular 159, New Mexico Bureau Mines and Mineral Resources, pp. 79-84.

Anderson, R. Y., 1979a, "Mechanism and Rates of Development of Regional and Localized Dissolution Features In and Below Evaporites," First Draft of a Preliminary Report to the State of New Mexico, Environmental Evaluation Group, 15 pp.

Anderson, R. Y., 1979b, "Notes on Dissolution and Brine Chambers Related to the W.I.P.P.," Report Submitted to the State of New Mexico, Environmental Evaluation Group, 15 pp.

Anderson, R. Y., 1979c, "Relationship of Deep Seated Dissolution to the W.I.P.P. Site," Report Submitted to the State of New Mexico, Environmental Evaluation Group, 15 pp.

Anderson, R. Y. and D. W. Kirkland, 1980, "Dissolution of Salt Deposits by Brine Density Flow," Geology, Vol. 8, pp. 66-69.

Anderson, R. Y., 1981, "Bacteria Induced Permeability in Delaware Basin Evaporites," Unpublished draft report, 5 pp.

Bachman, G. O., 1974, "Geologic Processes and Cenozoic History Related to Salt Dissolution in Southern New Mexico," Open File Report 74-194, U.S. Department of the Interior, Geological Survey, 81 pp.

Bachman, G. O. 1980a, "Geology of Nash Draw, Eddy County, New Mexico," Open File Report 81-31, U.S. Department of the Interior, Geological Survey, 8 pp.

Bachman, G. O., 1980b, "Regional Geology and Cenzoic History of the Pecos Region, Southeastern New Mexico," Open File Report 80-1099, U.S. Department of the Interior, Geological Survey, 116 pp.

Bachman, G. O. and R. B. Johnson, 1973, "Stability of Salt in the Permian Salt Basin of Kansas," Oklahoma, Texas and New Mexico, with a section on Dissolved Salts in Surface Water by F. A. Swenson, Open File Report USGS-4332-4, U.S. Department of the Interior, Geological Survey, 62 pp.

Basic Data Report for Drillhole WIPP 13 (Waste Isolation Pilot Plant - WIPP), Sandia Lab and U.S. Geol. Surv., SAND 79-0273 (October 1979).

Basic Data Report for Drillhole WIPP 18 (Waste Isolation Pilot Plant - WIPP), Sandia Lab and U.S. Geol. Surv., SAND 79-0275 (March 1980).

Basic Data Report for Drillhole WIPP 19 (Waste Isolation Pilot Plant - WIPP), Sandia Lab and U.S. Geol. Surv., SAND 79-0276 (March 1980).

Basic Data Report for Drillhole WIPP 21 (Waste Isolation Pilot Plant - WIPP), Sandia Lab and U.S. Geol. Surv., SAND 79-0277 (March 1980).

Basic Data Report for Drillhole WIPP 22 (Waste Isolation Pilot Plant - WIPP), Sandia Lab and U.S. Geol. Surv., SAND 79-0278 (March 1980).

Basic Data Report for Drillhole WIPP 25 (Waste Isolation Pilot Plant - WIPP), Sandia Lab and U.S. Geol. Surv., SAND 79-0279 (September 1979).

Basic Data Report for Drillhole WIPP 26 (Waste Isolation Pilot Plant - WIPP), Sandia Lab and U.S. Geol. Surv., SAND 79-0280 (August 1979).

Basic Data Report for Drillhole WIPP 27 (Waste Isolation Pilot Plant - WIPP), Sandia Lab and U.S. Geol. Surv., SAND 79-0281 (October 1979).

Basic Data Report for Drillhole WIPP 28 (Waste Isolation Pilot Plant - WIPP), Sandia Lab and U.S. Geol. Surv., SAND 79-0282 (August 1979).

Basic Data Report for Drillhole WIPP 29 (Waste Isolation Pilot Plant - WIPP), Sandia Lab and U.S. Geol. Surv., SAND 79-0283 (September 1979).

Basic Data Report for Drillhole WIPP 30 (Waste Isolation Pilot Plant - WIPP), Sandia Lab and U.S. Geol. Surv., SAND 79-0284 (April 1980).

Basic Data Report for Drillhole WIPP 32 (Waste Isolation Pilot Plant - WIPP), Sandia Lab and U.S. Geol. Surv., SAND 80-1102 (November 1980).

Basic Data Report for Drillhole WIPP 33 (Waste Isolation Pilot Plant - WIPP), Sandia Lab and U.S. Geol. Surv., SAND 80-2011 (February 1981).

Bear, J., 1972, Dynamics of Fluids in Porous Media, American Elsevier Publishing Company, Inc., New York, 764 pp.

Black, S. R., 1982, D'Appolonia Consulting Engineers, Personal Communication.

Cheesewright, R., 1968, "Turbulent Natural Convection from a Vertical Plane Surface," J. Heat Transfer, ASME, pp. 1-7.

Christensen, C. L. and E. W. Peterson, 1980, "The Bell Canyon Test Summary Report," SAND 80-1375, Sandia Laboratories, Albuquerque, New Mexico, 53 pp.

Collins, M. A. and L. W. Gelhar, 1971, "Seawater Intrusion in Layered Aquifers," Water Res. Research, Vol. 7, No. 4, pp 971-979.

Cooper, J. B., 1962, "Groundwater Investigations of the Project Gnome Areas, Eddy and Lea Counties, New Mexico," U.S. Geological Survey TEI - 802, U.S. Department of the Interior, Geological Survey.

Cooper, J. B. and V. Glanzman, 1971, "Geohydrology of Project Gnome Site, Eddy County, New Mexico," U.S. Geological Survey Prof. Paper 712-A, U.S. Department of the Interior, Geological Survey, 24 pp.

Crank, J., 1975, The Mathematics of Diffusion, 2nd ed., Oxford University Press, 44 pp.

D'Appolonia, 1981, "Modeling Verification Studies Long-Term Waste Isolation Assessment," Report NM78-648-701, D'Appolonia Consulting Engineers, Inc., Pittsburgh, Pennsylvania.

Elder, J. W., 1967, "Steady Free Convection in a Porous Medium Heated From Below," J. Fluid Mech., Vol. 27, pp. 29-48.

Freeze, R. A. and J. A. Cherry, 1979, Groundwater, Prentice-Hall, Inc., New Jersey, 604 pp.

Fried, J. J., 1975, Groundwater Pollution, Elsevier, New York.

Gelhar, L. W., and M. A. Collins, 1971, "General Analysis of Longitudinal Dispersion in Nonuniform Flow," Water Res. Research, Vol. 7 (b), pp. 1151-1521.

Gelhar, L. W., A. L. Gutjahr, and R. L. Naff, 1979, "Stochastic Analysis of Macrodispersion in a Stratified Aquifer," Water Res. Research, Vol. 15 (b), pp. 1387-1397.

Golitsyn, G. S., 1979, "Simple Theoretical and Experimental Study of Convection with Some Geophysical Applications and Analogies," J. Fluid Mech., Vol. 95, Part 3, pp. 567-608.

Gonzalez, D. D., Sandia National Laboratories, Albuquerque, New Mexico, February 1982, Personal Communication.

Gonzalez, D. D., in preparation, "Fracture Flow in the Rustler Formation, Waste Isolation Pilot Plant (WIPP), Southeast New Mexico," SAND 82-1012, Draft, Sandia Laboratories, Albuquerque, New Mexico.

Grabau, A. W., 1920, Geology of Nonmetallic Mineral Deposits Other Than Silicate, Vol. 1, Principals of Salt Deposition, McGraw-Hill Book Company, New York.

Grauten, W. F., 1965, "Fluid Relationship in Delaware Mountain Sandstone," American Association of Petroleum Geologists, Memoir No. 4, Fluids in Subsurface Environment, pp. 294-307.

Griswold, G. B. and V. C. McWhirter, 1980, "Interpretation of Wireline Geophysical Logs ERDA No. 9 Stratigraphic Test Borehole DOE WIPP Site, Eddy County, New Mexico," SAND 80-7119, Sandia Laboratories, Albuquerque, New Mexico.

Haigler, L. B. and R. R. Cunningham, 1972, "Structure Contour Map on Top of the Undifferentiated Silurian and Devonian Rocks in Southeastern New Mexico," Map OM-218 U.S. Geological Survey.

Hale, W. E., L. S. Hughes, and E. R. Cox, 1954, "Possible Improvement of Quality of Water of the Pecos River by Diversion of Brine of Malaga Bend, Eddy County, New Mexico," Report of the Pecos River Commission, New Mexico and Texas with U.S. Geological Survey Water Resources Division.

Hendrickson, G. E. and R. S. Jones, 1952, "Geology and Groundwater Resources of Eddy County, New Mexico," Report 3, New Mexico Bureau of Mines and Mineral Resources Groundwater, Socorro, New Mexico, 167 pp.

Henry, H. R., 1964, "Interface Between Salt Water and Fresh Water in Coastal Aquifers," Water-Supply Paper, 1613-3, Geological Survey.

Hills, J. M., 1968, "Permian Basin Field Area, West Texas and Southeastern New Mexico," Special Paper 88, Geol. Soc. Am. Inc., pp. 17-27.

Hiss, W. L. , 1973, "Capitan Aquifer Observation-Well Network, Carlsbad to Jal, New Mexico," Technical Report 38, New Mexico State Engineer, Santa Fe, New Mexico, 76 pp.

Hiss, W. L., 1975a, "Stratigraphy and Groundwater Hydrology of the Capitan Aquifer, Southeastern New Mexico and Western Texas," Ph.D. Dissertation, University of Colorado, Boulder, Colorado, 374 pp.

Hiss, W. L., 1975b, "Water-Quality Data from Oil and Gas Wells in Part of the Permian Basin, Southeastern New Mexico and Western Texas," Open File Report 75-579, U.S. Department of the Interior, Geological Survey, Albuquerque, New Mexico.

Jessen, F. W., 1973, "Dissolution Processes," SME Mining Engineering Handbook, Vol. 2, A. B. Cummins, ed., SME of AIMMPE, New York, New York, pp. 21-1 to 21-15.

Jones, C. L., M. E. Cooley, and G. O. Bachman, 1973, "Salt Deposits of Los Medanos Area, Eddy and Lea Counties, New Mexico," Open File Report USGS-4339-7, U.S. Department of the Interior, Geological Survey, 67 pp.

Kelly, V. C., 1972, "Geometry and Correlation Along Permian Capitan Escarpment, New Mexico and Texas," The American Association of Petroleum Geologists Bulletin, Vol. 56, No. 11, pp. 2192-2211.

Knapp, R. M. and A. L. Podio, 1979, "Investigation of Salt Transport in Vertical Boreholes and Brine Invasion to Freshwater Aquifers," Technical Report, ONWI-77, Battelle Office Of Nuclear Waste Isolation, 80 pp.

Konikow, L. F. and J. D. Bredehoeft, 1974, "Modeling Flow and Chemical Quality Changes in an Irrigated Stream-Aquifer System," Water Res. Research, Vol. 10, No. 3, pp. 546-562.

Lambert, S. J., 1977, "The Geochemistry of Delaware Basin Groundwaters," SAND 77-0420, Sandia Laboratories, Albuquerque, New Mexico.

Lambert, S. J. and J. W. Mercer, 1977, "Hydrologic Investigations of the Los Medanos Area, Southeastern New Mexico, 1977," SAND 77-1401, Sandia Laboratories, Albuquerque, New Mexico.

Lambert, S. J., in preparation, "Dissolution of Evaporites in and Around the Delaware Basin, Southeastern New Mexico and West Texas," Sand 82-0461, Draft, Sandia Laboratories, Albuquerque, New Mexico.

Lang, W. B., 1937, "The Permian Formations of the Pecos Valley of New Mexico and Texas," Bulletin of the American Association of Petroleum Geologists, Vol. 21, No. 7, pp. 833-898.

Lee, C. H. and T. S. Cheng, 1974, "On Seawater Encroachment in Coastal Aquifers," Water Res. Research, Vol. 10, No. 5, pp. 1039-1043.

Leet, L. D. and S. Judson, 1965, Physical Geology, Third Edition, Prentice Hall, Inc., New Jersey, 406 p.

Lynes, Inc., 1979, Drill Stem Test Results for Boring AEC #7, Houston, Texas.

Maley, V. C. and R. M. Huffington, 1963, "Cenozoic Fill and Evaporate Solution in the Delaware Basin, Texas and New Mexico," Bull. Geol. Soc. Am., Vol. 64, pp. 539-546.

McClure, T. M., 1942-1946, "State Engineer of New Mexico," Sixteenth and Seventeenth Biennial Reports, Santa Fe, New Mexico.

McClure, T. M., 1934-1938, "State Engineer of New Mexico," Twelfth and Thirteenth Biennial Reports, Santa Fe, New Mexico.

McNeal, R. P., 1965, "Hydrodynamics of the Permian Basin," Fluids in Subsurface Environments, Young, Addison, and Galley, eds., American Association Petroleum Geologists Mem. 4, pp. 308-326.

Mercer, J. W. and B. R. Orr, 1977, "Review and Analysis of Hydrogeologic Conditions Near the Site of a Potential Nuclear Waste Repository, Eddy and Lea Counties, New Mexico," Open File Report 77-123, U.S. Department of Interior, Geological Survey, 35 pp.

Mercer, J. W. and B. R. Orr, 1979, "Interim Data Report on the Geohydrology of the Proposed Waste Isolation Pilot Plant Site Southeast New Mexico," U.S. Geol. Surv. Water Resource Investigations, 79-98, U.S. Geological Survey Water Resources, Albuquerque, New Mexico, 178 pp.

Mercer, J. W. and D. D. Gonzalez, 1981, "Geohydrology of the Proposed Waste Isolation Pilot Plant Site in Southeastern New Mexico," Special Publication No. 10, New Mexico Geological Society, pp. 123-131.

Mille, G. De., L. R. Shouldice, and H. W. Nelson, 1964, "Collapse Structures Related to Evaporites of the Prairie Formation, Saskatchewan," Geol. Soc. Am. Bull., Vol. 75, pp. 307-316.

Motts, W. S., 1972, "Geology and Paleoenvironments of the Northern Segment, Captain Shelf, New Mexico and West Texas," Geol. Soc. Am. Bull., Vol. 83, pp. 701-722.

Nicholson, A., Jr. and A. Clebsch, Jr., 1961, "Geology and Groundwater Conditions in Southern Lea County, New Mexico," Groundwater Report 6, New Mexico Bureau of Mine and Mineral Resources, Socorro, New Mexico, 123 pp.

Olive, W. W., 1957, "Solution-Subsidence Troughs, Castile Formation of Gypsum Plain, Texas and New Mexico," Bulletin of the Geological Society of America, Vol. 68, pp. 351-358.

Peterson, E. W., P. L. Lagus, R. D. Broce, and K. Lie, 1981, "In Situ Permeability Testing of Rock Salt," SAND 81-7073, Sandia Laboratories, Albuquerque, New Mexico, 65 pp.

Pickens, J. F. and W. C. Lennox, 1976, "Numerical Simulation of Waste Movement in Steady State Groundwater Flow System," Water Res. Research, Vol. 12, No. 2, pp 171-180.

Pinder, G. F. and H. H. Cooper, Jr., 1970, "A Numerical Technique for Calculating the Transient Position of the Saltwater Front," Water Res. Research, Vol. 6, No. 3, pp. 875-882.

Popielak, R. S., R. L. Beauheim, S. R. Black, W. E. Coons, C. T. Ellingson, R. L. Olsen, in preparation, "Brine Reservoirs in the Castile Formation, Southeastern New Mexico," TME 3153, prepared for the U.S. Department of Energy.

Powers, D. W., S. J. Lambert, S. E. Shaffer, L. R. Hill, W. D. Weart, eds., 1978, "Geological Characterization Report, Waste Isolation Pilot Plant (WIPP) Site, Southeastern New Mexico," SAND 78-1596, Vols. I and II, Sandia Laboratories, Albuquerque, New Mexico.

Powers, D. W., 1982, Sandia National Laboratories, Albuquerque, New Mexico, Personal Communication.

Rau, J. L. and L. F. Dellwig, ed., 1969, "Investigation of Solution Collapse Breccia in Mature Salt Cavities," Third Symposium on Salt, Vol. 1, The Northern Ohio Geological Society, Inc., pp. 422-428.

Reddell, D. L. and D. K. Sunada, 1970, "Numerical Simulation Dispersion in Groundwater Aquifers," Hydrol. Pap. 41, Colorado State University, Fort Collins, Colorado, 79 pp.

Romoser, W. and R. M. Knapp, 1977, "Numerical Simulation of Brine Invasion of Fresh Water Aquifers," Y/OWI/SUB-4082/4, Union Carbide Office of Waste Isolation, Oak Ridge, Tennessee, 122 pp.

Rumer, R. R. and J. C. Shiau, 1968, "Salt Water Interface in a Layered Coastal Aquifer," Water Res. Research, Vol. 4, No. 6, pp. 1235-1247.

Sandia, 1980a, "Summary of Research and Development in Support of a Waste Acceptance Criteria for WIPP," SAND 79-1305, Sandia Laboratories, Albuquerque, New Mexico.

Sandia, 1980b, "Analysis of Bell Canyon Test Results," SAND 80-7044C, Sandia Laboratories, Albuquerque, New Mexico.

Scheidegger, A. E., 1961, "General Theory of Dispersion in Porous Media," J. Geophys. Res., Vol. 66, pp. 3273-3278.

Segol, G., G. F. Pinder, and W. G. Gray, 1975, "A Galerkin-Finite Element Technique for Calculating the Transient Position of the Saltwater Front," Water Res. Research, Vol. 11, No. 2, pp. 343-347.

Segol, G. and G. F. Pinder, 1976, "Transient Simulation of Saltwater Intrusion in Southeastern Florida," Water Res. Research, Vol. 12, No. 1, pp. 65-70.

Spiegler, P., 1980, "Analysis of the Potential Formation of a Breccia Chimney Beneath the WIPP Repository," Environmental Evaluation Group, Environmental Improvement Division, Health and Environment Department, State of New Mexico.

Tang, D. H. and D. K. Baba, 1979, "Analytical Solution of a Velocity Dependent Dispersion Problem," Water Res. Research, Vol. 15 (b), pp. 1471-1478.

Taylor, G., 1954, "Diffusion and Mass Transport in Tubes," Proceedings, Physical Soc. B, 67, pp. 857-869.

U.S. Department of Energy, 1980a, "Final Environmental Impact Statements Waste Isolation Pilot Plant," DOE/E15-0026, U.S. Department of Energy.

U.S. Department of Energy, 1980b, Waste Isolation Pilot Plant Safety Analysis Report (SAR), Vol. 1 and Vol. 2, U.S. Department of Energy, Washington, D.C.

Vine, J. D., 1960, "Recent Domal Structures in Southeastern New Mexico," Bull. Am. Assoc. Petroleum Geol., Vol. 44, No. 12, pp. 1903-1911.

Warner, C. Y. and V. S. Arpaci, 1968, "An Experimental Investigation of Turbulent Natural Convection in Air at Low Pressure Along a Vertical Heated Plate," Int. J. Heat Mass Transfer, Vol. 11, pp. 397-406.

Weast, R. C., ed., 1970, Handbook of Chemistry and Physics, 50th Edition, The Chemical Rubber Co., Cleveland, Ohio.

Wooding, R. A., 1959, "The Stability of a Viscous Liquid in a Vertical Tube Containing Porous Material," Proceedings of the Royal Soc. A., Vol. 252, pp. 120-134.

Wooding, R. A., 1960, "Instability of a Viscous Fluid of Variable Density in a Vertical Hele-Shaw Cell," J. Fluid Mech., Vol. 7, pp. 501-515.

Wooding, R. A., 1963, "Convection in a Saturated Porous Medium at Large Rayleigh Number or Peclet Number," J. Fluid Mech., Vol. 15, pp. 527-544.

Zand, S. M., 1981, "Dissolution of Evaporites and Its Possible Impact on the Integrity of the Waste Isolation Pilot Plant (WIPP) Repository," EEG-14, Environmental Evaluation Group, Environmental Improvement Division, Health and Environmental Department, State of New Mexico, 25 pp.

APPENDIX A

REVIEW OF NUMERICAL SIMULATION TECHNIQUES AND BASIC GOVERNING EQUATIONS OF FLOW AND MASS TRANSPORT

APPENDIX A
TABLE OF CONTENTS

APPENDIX A
REVIEW OF NUMERICAL SIMULATION TECHNIQUES AND BASIC GOVERNING EQUATIONS OF FLOW AND MASS TRANSPORT

In this appendix, theories related to salt transport simulation techniques and the governing equations for flow and mass transport through a porous media in a two-dimensional vertical plane are presented. Numerical techniques are summarized in Section A.1 and the governing equations which include density variations are given in Section A.2. Section A.3 contains the governing equations where density variations are neglected.

A.1 REVIEW OF NUMERICAL SIMULATION TECHNIQUES

Modeling of the effects of salt water (i.e., seawater or brine) merging with relatively fresh water in an aquifer has received considerable attention and has been studied in two different ways. The first approach considers that the salt and fresh waters are two immiscible fluids separated by an abrupt interface. The second approach considers them to be miscible fluids without formation of a distinct interface.

Diffusion is an important process in a zone where salt water mixes with fresh water (Lee and Cheng, 1974). Because the immiscible fluid approach does not take into account the effects of diffusion between the two fluid phases, it should be used only when the influence of diffusion is relatively small. It would, for example, be appropriate for a very short time scale. However, the effect of diffusion should be included (e.g., Rumer and Shiau, 1968) in the evaluation of salt water merging with fresh water over the long time periods (tens of thousands of years) addressed in this study. Therefore, the miscible fluid approach, which incorporates the diffusion mechanism, is used in this study to evaluate the transport of salt into and through the Bell Canyon aquifer.

The Miscible Fluids Approach

The mixing of two miscible fluids is usually referred to as hydrodynamic dispersion. In the context of this investigation, saturated brine from the Castile Formation may be considered to mix with the unsaturated groundwater in the Bell Canyon Formation.

Simulations of hydrodynamic dispersion can be divided into two categories--density-dependent and density-independent cases. In a density-dependent case, groundwater density varies as a function of the salt concentration. In a density-independent case, groundwater density is assumed constant and is independent of the salt concentration. The major difference between these two categories in terms of the governing equations for salt transport is that in the density-independent case the potentiometric head, the sum of water pressure and elevation heads, is a valid physical quantity, but this is not necessarily true in the density-dependent case (Bear, 1972). This difference results in two somewhat different governing equations describing the physical phenomena. However, the basic theories remain the same for both cases. In addition, for relatively shallow and long aquifers where variation of salt concentration with distance is small, the two methods will produce similar results.

In the following paragraphs, important and general features of hydrodynamic dispersion for density-independent cases are reviewed first. Then, density-dependent transport is discussed as a special case of hydrodynamic dispersion.

Density-Independent Hydrodynamic Dispersion

The physical processes that control the salt concentration in an aquifer are convection and hydrodynamic dispersion. Convection is the component of salt movement attributable to transport by flowing groundwater. Hydrodynamic dispersion occurs as a result of mechanical mixing and molecular diffusion (Freeze and Cherry, 1979).

It is usually simulated by using a lumped parameter called the hydrodynamic dispersion coefficient (or simply dispersion coefficient). This dispersion coefficient consists of two parts (Scheidegger, 1961): (1) the mechanical dispersion coefficient, which incorporates the mechanical dispersion mechanism and is dependent on groundwater velocity and dispersivity, and (2) the molecular diffusion coefficient, which represents the molecular diffusion mechanism and is relatively constant for a specific ionic species in a given medium. In a two-dimensional problem, there is a longitudinal and transverse dispersivity. The longitudinal dispersivity is defined as the dispersivity in the direction of flow, and the transverse in the direction normal to flow. Definitions of the dispersion coefficient and the complete density-independent mass transport equations are given in Section A.2. The dispersion coefficients observed in the field can be several orders of magnitude larger than those obtained by laboratory tests with similar materials (Fried, 1975; Konikow and Bredehoeft, 1974). This large difference is attributable to the fact that hydraulic conductivity under field conditions is usually nonhomogeneous. A nonhomogeneous aquifer contains different materials with significantly different hydraulic conductivities. A stochastic analysis was performed by Gelhar, et al. (1979), to study the dispersive process in a nonhomogeneous porous medium. They indicated that the dispersion coefficient for large times is in the form of the product of the mean velocity and a dispersivity. This conclusion agrees in principle with the relationship between the dispersion coefficient and velocity developed by other investigators (e.g., Scheidegger, 1961; Bear, 1972).

Several analytical solutions exist for evaluation of dispersion in groundwater. Most of these treat the flow field as steady state and uniform. A comprehensive review of analytical models is given by Bear (1972). An analytical solution for velocity-dependent dispersion was developed by Tang and Baba (1979).

Numerical techniques have been widely employed to investigate dispersion problems in complex groundwater systems. The finite difference and finite element schemes are the two most popular numerical methods used to simulate field conditions of hydrodynamic dispersion. A large number of articles dealing with numerical simulation of mass transport in groundwater can be located in various technical journals and reports. Only a few of these papers are cited in this report.

Density-Dependent Hydrodynamic Dispersion

In general, variations in salt concentration cause changes in the groundwater density which, in turn, can affect the flow regime (i.e., velocity distribution). However, at relatively low concentrations, groundwater density is often assumed to be constant (Bear, 1972). The other mechanisms, such as hydrodynamic dispersion, that affect the concentration distribution in the density-independent case also apply to the density-dependent problem.

A large amount of work has been performed in studying problems of seawater encroaching fresh water aquifers. Seawater has a density about three percent higher than that of fresh water. For this density contrast, seawater encroachment has been studied by considering groundwater density as a variable (Pinder and Cooper, 1970; Lee and Cheng, 1974; Segol, et al., 1975; and Segol and Pinder, 1976). Pinder and Cooper (1970) and Lee and Cheng (1974) presented results which demonstrated the development of a recirculation process where seawater reverses its direction due to density variations. Lee and Cheng (1974) also indicated that 10 percent or more of the intruded seawater flows back toward the sea through the recirculation. However, investigations of similar problems considering groundwater density as constant fail to depict the recirculation phenomenon (i.e., Romoser and Knapp, 1977).

Segol, et al. (1975), and Segol and Pinder (1976) also solved transient seawater intrusion problems. In their results, they indicated that flow recirculation could be neglected only for small groundwater velocities.

Among these density-dependent simulations, no attempt has been made to examine the significance and influence of ignoring the density variations.

Summary

Density-dependent simulations of salt water intruding a fresh water aquifer have indicated the potential for a recirculation phenomenon in which various flow patterns are established due to vertical and horizontal variations of fluid density. The resulting changes in flow patterns can affect the distribution of salt in the aquifer and the rate of salt influx into the aquifer. In order to understand the implications of ignoring or including density variations for a particular problem, the most direct method is to perform the computations using both assumptions and then compare the results. The implications can also often be determined by analyzing the relevent equations, understanding the assumptions involved in using the equation, and investigating the application of the theories and equations to the problem.

A.2 DENSITY-DEPENDENT FLOW AND MASS TRANSPORT

The governing equation of groundwater flow in a two-dimensional vertical plane is (Pinder and Gray, 1977):

$$\frac{\partial}{\partial x}\left[\frac{\rho k_{xx}}{\mu}\left(\frac{\partial p}{\partial x}\right)\right] + \frac{\partial}{\partial z}\left[\frac{\rho k_{zz}}{\mu}\left(\frac{\partial p}{\partial z} + \rho g\right)\right] - \rho_s \dot{Q} = \frac{\partial}{\partial t}(\rho n) \qquad \text{(A-1)}$$

where

p = the fluid pressure (M/LT^2);

k_{xx} = the principal intrinsic permeability of the medium in the x-direction (L^2);

k_{zz} = the principal intrinsic permeability of the medium in the z-direction (L^2);

μ = the dynamic viscosity of fluid (M/LT);

ρ = the fluid density (M/L^3);

ρ_s = the density of the source (sink) fluid (M/L^3)'

g = the acceleration due to gravity (L/T^2);

x = the horizontal Cartesian coordinate (L);

z = the vertical Cartesian coordinate (L);

n = the porosity (dimensionless);

$\dot{Q}$ = the strength of source or sink (L^2/TL^2); and

t = time.

It is possible to express the term, $\frac{\partial \rho n}{\partial t}$, in Equation (A-1) as a function of pressure and concentration if the density is considered variable (e.g., Reddell and Sunada, 1970). However, in the simulation of density-dependent flow, the movement of solute is so slow relative to the pressure propagation that the pressure response can be considered instantaneous. Also, the concentration change with respect to time can be considered negligible compared to other terms in this equation. Based on these two assumptions, the governing equation of density-dependent flow results in (Segol, et al., 1975):

$$\frac{\partial}{\partial x}\left[\frac{\rho k_{xx}}{\mu}\left(\frac{\partial p}{\partial x}\right)\right] + \frac{\partial}{\partial z}\left[\frac{\rho k_{zz}}{\mu}\left(\frac{\partial p}{\partial z} + \rho g\right)\right] = 0 \qquad \text{(A-2)}$$

Equation (A-2) with pertinent boundary conditions is solved to obtain the fluid pressure in the domain of interest. After fluid pressure is determined, the velocities can be evaluated by Darcy's equation (Bear, 1972):

$$V_x = -\frac{k_{xx}}{n_e \mu}\left(\frac{\partial p}{\partial x}\right) \qquad \text{(A-3a)}$$

and

$$V_z = -\frac{k_{zz}}{n_e \mu}\left(\frac{\partial p}{\partial z} + \rho g\right) \qquad \text{(A-3b)}$$

where

V_x and V_z = the velocities of fluid flowing through pores (L/T), in the x and z directions, respectively, and

n_e = the effective porosity of the medium.

After solving for the pore velocities, mass concentrations can be computed. The equation describing the distribution of mass concentration in a two-dimensional vertical plane is (Segol, et al., 1975):

$$\frac{\partial}{\partial x}\left(D_{xx}\frac{\partial C}{\partial x}\right) + \frac{\partial}{\partial z}\left(D_{zz}\frac{\partial C}{\partial z}\right) - \frac{\partial}{\partial x}\left(V_x C\right) - \frac{\partial}{\partial z}\left(V_z C\right) = \frac{\partial C}{\partial t} \qquad \text{(A-4)}$$

where

C = the mass concentration (M/L^3); and

D_{xx} and D_{zz} = the hydrodynamic dispersion coefficients (L^2/T), in the x and z directions, respectively.

The hydrodynamic dispersion coefficients for an isotropic medium in a two-dimensional vertical plane can be written as (Bear, 1972):

$$D_{xx} = D_L \frac{V_x V_x}{V^2} + D_T \frac{V_z V_z}{V^2} + D_d \overset{*}{T} \qquad \text{(A-5)}$$

and

$$D_{zz} = D_T \frac{V_x V_x}{V^2} + D_L \frac{V_z V_z}{V^2} + D_d \overset{*}{T} \qquad \text{(A-6)}$$

where

V = magnitude of the groundwater velocity (L/T) = $(V_x^2 + V_z^2)^{1/2}$,

D_L = the longitudinal dispersion coefficient (L^2/T),

D_T = the transverse dispersion coefficient (L^2/T),

D_d = the molecular diffusion coefficient (L^2/T), and

$\overset{*}{T}$ = the tortuosity of the medium (dimensionless).

The longitudinal and transverse dispersion coefficients are defined by:

$$D_L = a_I V \qquad \text{(A-7)}$$

$$D_T = a_{II} V \qquad \text{(A-8)}$$

where

a_I = the longitudinal dispersivity in the direction of flow (L), and

a_{II} = the transverse dispersivity normal to the direction of flow (L).

Since the groundwater density changes as a result of salt concentration, an equation of state, which relates the groundwater density to salt concentration, is needed in addition to the governing equations of flow and salt transport. The equation of state in this study is approximated by (Hiss, 1975):

$$s = 6.466 \times 10^{-7} C + 1.002 \qquad \text{(A-9)}$$

where

C = the total dissolved solid concentration (mg/l), and

s = the specific gravity of brine being the ratio of brine density to pure water density (dimensionless).

A.3 DENSITY-INDEPENDENT FLOW AND MASS TRANSPORT

If the fluid density is considered constant, the governing equation for flow (A-1) can be further formulated into a more concise form by introducing the following quantities:

$$\phi = \frac{P}{\rho g} + Z$$

where

ϕ = the potentiometric head (L),

$\frac{P}{\rho g}$ = the pressure head (L), and

Z = the elevation head (L).

$$K_{xx} = \frac{\rho g k_{xx}}{\mu}$$

and (A-10)

$$K_{zz} = \frac{\rho g k_{zz}}{\mu}$$

where

K_{xx} and K_{zz} = the principal hydraulic conductivities (L/T) along the x- and z-directions, respectively.

By introducing ϕ, K_{xx}, and K_{yy} into Equation (A-1), the time derivative term $\frac{\partial \rho n}{\partial t}$ can be presented as a function of storage coefficient, S, potentiometric head, and aquifer thickness, b (Todd, 1959; DeWiest, 1965). As a result, Equation (A-1) can be written in the following form:

$$\frac{\partial}{\partial x}\left(K_{xx}\frac{\partial \phi}{\partial x}\right) + \frac{\partial}{\partial z}\left(K_{zz}\frac{\partial \phi}{\partial z}\right) - \dot{Q} = \frac{S}{b}\frac{\partial \phi}{\partial t} \qquad \text{(A-11)}$$

In Equation (A-11), the density of source fluid is assumed to be equal to the density of fluid in the aquifer. Equation (A-11) is the governing equation of flow in density-independent cases.

The governing equation for mass transport in the density-independent case is identical to Equation (A-4), which is the mass transport equation in the density-dependent condition.

A.4 BIBLIOGRAPHY

Bear, J., 1972, Dynamics of Fluids in Porous Media, American Elsevier Publishing Co., Inc., New York.

DeWiest, R. J. M., 1965, Geohydrology, John Wiley, New York, 366 pp.

Duguid, J. O. and M. Reeves, 1976, "Material Transport Through Porous Media: A Finite Element Galerkin Model," Environmental Sciences Division Publication 733, Oak Ridge National Laboratory, National Technical Information Service, Springfield, Virginia, 201 pp.

Freeze, R. A. and J. A. Cherry, 1979, Groundwater, Prentice-Hall, Inc., New Jersey, 604 pp.

Fried, J. J., 1975, Groundwater Pollution, Elsevier, New York.

Gelhar, L. W., A. L. Gutjahr, and R. L. Naff, 1979, "Stochastic Analysis of Macrodispersion in a Stratified Aquifer," Water Res. Research, Vol. 15 (b), pp. 1387-1397.

Hiss, W. L., 1975, Stratigraphy and Groundwater Hydrology of the Capitan Aquifer, Southeastern New Mexico and Western Texas, Ph.D. Thesis, University of Colorado, Boulder, CO.

Konikow, L. F. and J. D. Bredehoeft, 1974, "Modeling Flow and Chemical Quality Changes in an Irrigated Stream-Aquifer System," Water Res. Research, Vol. 10, No. 3, pp. 546-562.

Lee, C. H. and T. S. Cheng, 1974, "On Seawater Encroachment in Coastal Aquifers," Water Res. Research, Vol. 10, No. 5, pp. 1039-1043.

Pinder, G. F. and H. H. Cooper, Jr., 1970, "A Numerical Technique for Calculating the Transient Position of the Saltwater Front," Water Res. Research, Vol. 6, No. 3, pp. 875-882.

Pinder, G. F. and W. G. Gray, 1977, Finite Element Simulation in Surface and Subsurface Hydrology, Academic Press, New York, 295 pp.

Reddell, D. L. and D. K. Sunada, 1970, Numerical Simulation of Dispersion in Groundwater Aquifers, Hydrology Papers, No. 41, Colorado State University, Fort Collins, Colorado.

Romoser, W. and R. M. Knapp, 1977, "Numerical Simulation of Brine Invasion of Fresh Water Aquifers," Y/OWI/SUB-4082/4, Union Carbide Office of Waste Isolation, Oak Ridge, Tennessee, 122 pp.

Rumer, R. R. and J. C. Shiau, 1968, "Salt Water Interface in a Layered Coastal Aquifer," Water Res. Research, Vol. 4, No. 6, pp. 1235-1247.

Scheidegger, A. E., 1961, "General Theory of Dispersion in Porous Media," J. Geophys. Res., Vol. 66, pp. 3273-3278.

Segol, G., G. F. Pinder, and W. G. Gray, 1975, "A Galerkin-Finite Element Technique for Calculating the Transient Position of Saltwater Front," Water Resources Research, Vol. 11, No. 2.

Segol, G. and G. F. Pinder, 1976, "Transient Simulation of Saltwater Intrusion in Southeastern Florida," Water Res. Research, Vol. 12, No. 1, pp. 65-70.

Tang, D. H. and D. K. Baba, 1979, "Analytical Solution of a Velocity Dependent Dispersion Problem," Water Res. Research, Vol. 15 (b), pp. 1471-1478.

Todd, D. K., 1959, Ground Water Hydrology, John Wiley, New York, 336 pp.

APPENDIX B

SENSITIVITY ANALYSIS OF SALT DISSOLUTION AND TRANSPORT PARAMETERS

APPENDIX B
TABLE OF CONTENTS

APPENDIX B

LIST OF TABLES

LIST OF FIGURES

APPENDIX B
SENSITIVITY ANALYSIS OF SALT DISSOLUTION AND TRANSPORT PARAMETERS

The results of sensitivity analyses performed to determine the significance of various parameters on the salt dissolution rate are presented in this appendix. The appendix is organized in two sections. In Section B.1, the variation of dissolution rate with respect to diffusion controlled mechanisms is discussed. In Section B.2, the significance of the mass transport capacity of the Bell Canyon aquifer on salt removal is discussed.

B.1 SENSITIVITY OF DIFFUSION-CONTROLLED DISSOLUTION PARAMETERS

As discussed in various sections of the text, the Bell Canyon aquifer is separated from the Halite I by an impervious, relatively low solubility anhydrite. Furthermore, among various salt dissolution mechanisms, the diffusion process is the dominant factor in removal of salt from Halite I into the Bell Canyon aquifer. In this section, the significance of various parameters on diffusion-controlled salt dissolution mechanisms is evaluated and their relative importance identified. The types of input parameters required for the modeling of diffusion-controlled dissolution and the ranges of values investigated for the sensitivity analysis are shown in Table B-1. The ranges were established based on the available site data, literature values, and experience with the nature of the input data. The following parameters are used in this analysis:

- Hydraulic conductivity, K, of the Bell Canyon aquifer
- Effective porosity, n_e, of the Bell Canyon aquifer
- Molecular diffusion coefficient, D_m, of chloride in the Castile Formation
- Longitudinal and transverse dispersivity of the Bell Canyon aquifer (D_L and D_T, respectively)

TABLE B-1

NUMERICAL MODEL INPUT PARAMETERS FOR SENSITIVITY ANALYSIS(1)

INPUT PARAMETERS(2)	RANGE OF VALUES	UNITS
Hydraulic Conductivity of Bell Canyon Aquifer, K	0.5 to 18.0	Meters per year (m/yr)
Effective Porosity of Bell Canyon Aquifer, n_e	0.05 to 0.25	Dimensionless
Molecular Diffusion Coefficient, D_m	2.7×10^{-3} to 13.6×10^{-3}	Square meters per year (m^2/yr)
Longitudinal Dispersivity of Bell Canyon Aquifer, D_L	0.3048 to 30.48	Meters (m)
Transverse Dispersivity of Bell Canyon Aquifer, D_T	0.3048 to 30.48	Meters (m)
Ratio of Longitudinal to Transverse Dispersivity, D_L/D_T(3)	0.1 to 10.0	Dimensionless
Effect Thickness of Aquifer, b	30 to 300	Meters (m)
Thickness of Diffusion Zone(4) in Castile Formation	100 to 600	Meters (m)
Hydraulic Gradient, i	0.0013 to 0.0039	Meters per meter (m/m)
Upgradient Chloride Concentration Boundary Condition in Bell Canyon Aquifer, C_u	0 to 150	Kilograms per cubic meter (kg/m^3)

(1) Refer to Appendix A for parameter definitions.

(2) Range of the parameter values selected for sensitivity analysis are for identifying the significance of key parameters on the dissolution rate. These ranges do not represent the variation of these parameters either in the Bell Canyon aquifer or the Castile Formation.

(3) For $D_L/D_T = 0.1$, $D_L = 3.048$m and $D_T = 30.48$m.
For $D_L/D_T = 1.0$, $D_L = 3.048$m and $D_T = 3.048$m, also $D_L = D_T = 0.3048$m and $D_L = D_T = 30.48$m.
For $D_L/D_T = 10.0$, $D_L = 30.48$m and $D_T = 3.048$m.

(4) Refer to Figure 4-3 for location of diffusion zone.

- Ratio of longitudinal to transverse dispersivity, D_L/D_T
- Thickness of the Bell Canyon aquifer, b
- Thickness of the diffusion zone between the halite and the Bell Canyon Formation
- Upgradient concentration boundary condition for chloride, C_u

The results of the analyses are graphically presented in Figure B-1 and are summarized in Table B-2. This table relates the percentage change (in relation to the values in Table 4-1) in an input parameter to the resulting percentage change in average salt dissolution rate. The graphs in Figure B-1 show the relationship between the changes in the salt dissolution rate and the individual parameters shown in Table 4-1. The vertical axes of the graphs are nondimensionalized with the average salt dissolution height (0.34 centimeter per 10,000 years) obtained from the modeling described in Section 4.4.3. This average salt dissolution height is based on parameters which are considered most representative of conditions at the WIPP site. The graphs can be used to determine what effect the change in a parameter such as hydraulic conductivity, effective porosity, or molecular diffusion coefficient will have on the salt dissolution height. As shown in Figure B-1(A), an increase in Bell Canyon aquifer hydraulic conductivity from 1.8 to 18.0 meters per year would result in a 17 percent increase in dissolution height (H/H_{ref}, dimensionless dissolution rate, increases from 1.0 to 1.17). Similar effects due to other parameter variations can be seen from the additional curves in Figure B-1.

Based on the results presented in Figure B-1 and Table B-2, the following conclusions related to diffusion-controlled dissolution of salt in the Castile Formation can be made:

- The dissolution rate is sensitive to the hydraulic conductivity of the Bell Canyon aquifer. Since flow is also directly proportional to the hydraulic gradient, the effects of relative

TABLE B-2

SUMMARY OF THE RESULTS OF SENSITIVITY ANALYSIS OF SALT DISSOLUTION PARAMETERS(1)

INPUT PARAMETER(2)	VALUE	UNITS	PERCENTAGE CHANGE OF INPUT PARAMETER FROM BASE VALUE	SALT DISSOLUTION HEIGHT (centimeters per 10,000 years)	PERCENTAGE CHANGE OF SALT DISSOLUTION RATE FROM BASE VALUE
Hydraulic conductivity of Bell Canyon aquifer, K	0.5	Meters per year (m/yr)	-72	0.14	-57
	1.8*		-	0.34*	-
	18.0		+900	0.40	+17
Molecular diffusion coefficient, D_m	2.7×10^{-3}	Square meters per year (m^2/yr)	-68	0.13	-61
	8.7×10^{-3}*		-	0.34*	-
	13.6×10^{-3}		+56	0.42	+24
Effective porosity of Bell Canyon aquifer, n_e	0.05	Dimensionless	-69	0.12	-63
	0.16*		-	0.34*	-
	0.25		+56	0.42	+26
Dispersivity coefficient of Bell Canyon aquifer(3)	.3048	Meters (m)	-90	0.34	+0
	3.048*		-	0.34*	-
	30.48		+900	0.34	+0
Ratio of longitudinal to transverse dispersivity, D_L/D_T	0.1	Dimensionless	-90	0.34	+0
	1.0*		-	0.34*	-
	10.0		+900	0.34	+0
Thickness of diffusion zone in Castile Formation(4)	100*	Meters (m)	-	0.34*	-
	300		+200	0.13	-61
	600		+500	0.05	-86
Effective thickness of Aquifer, b	30*	Meters (m)	-	0.34*	-
	100		+233	0.52	+55
	300		+900	0.62	+86
Upgradient chloride concentration boundary condition in Bell Canyon aquifer, C_u	0	Kilograms per cubic meter (kg/m^3)	-100	0.77	+129
	100*		-	0.34*	-
	150		+50	0.12	-64
Hydraulic gradient, i	0.0013	Meters per meter (m/m)	-48	0.25	-25
	0.0025*		-	0.34*	-
	0.0039		+56	0.37	+10

*Indicates base value from Table 4-1.

(1) Refer to Appendix A for parameter definitions.

(2) Range of parameter values selected for sensitivity analysis are for identifying the significance of key parameters on the dissolution rate. These ranges do not represent the variation of these parameters either in the Bell Canyon aquifer or the Castile Formation.

(3) Equal longitudinal and transverse dispersivities are used.

(4) Refer to Figure 4-3 for location of diffusion zone.

DRAWN BY	CHECKED BY	APPROVED BY	DRAWING NUMBER
R.W. 11-18-81			NWTB-648-E3

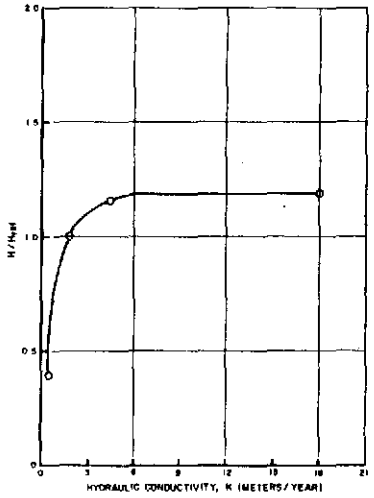

(A) SENSITIVITY TO AQUIFER HYDRAULIC CONDUCTIVITY

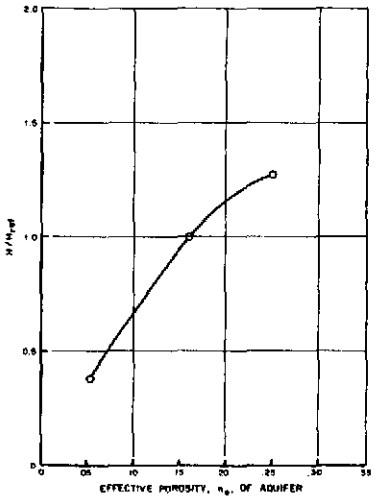

(B) SENSITIVITY TO EFFECTIVE POROSITY OF AQUIFER

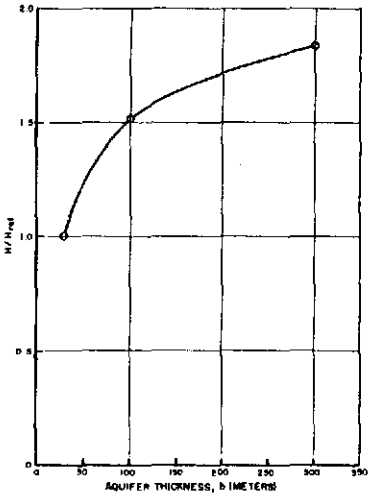

(C) SENSITIVITY TO AQUIFER THICKNESS

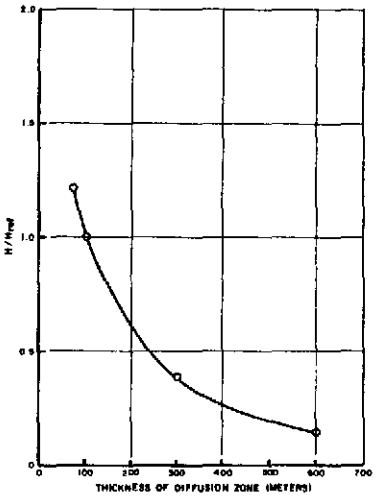

(D) SENSITIVITY TO DIFFUSION ZONE THICKNESS

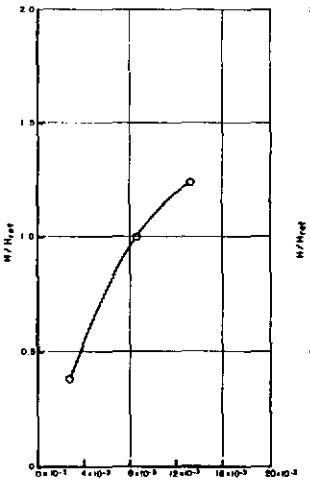

(E) SENSITIVITY TO MOLECULAR DIFFUSION COEFFICIENT

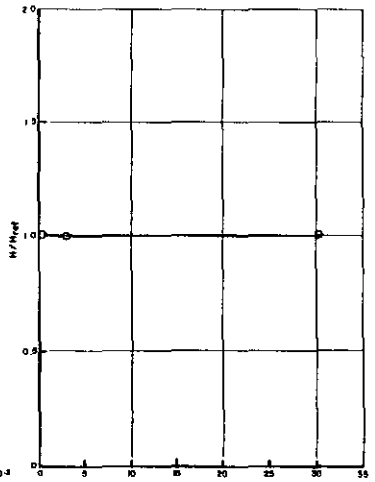

(F) SENSITIVITY TO DISPERSIVITY OF AQUIFER

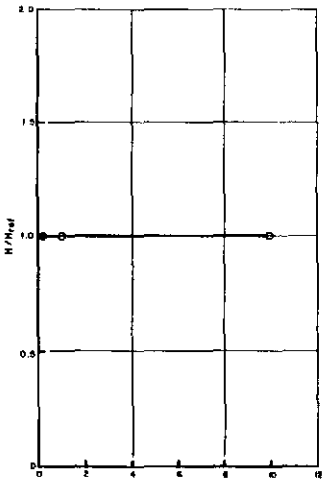

(G) SENSITIVITY TO RATIO OF LONGITUDINAL TO TRANSVERSE DISPERSIVITY

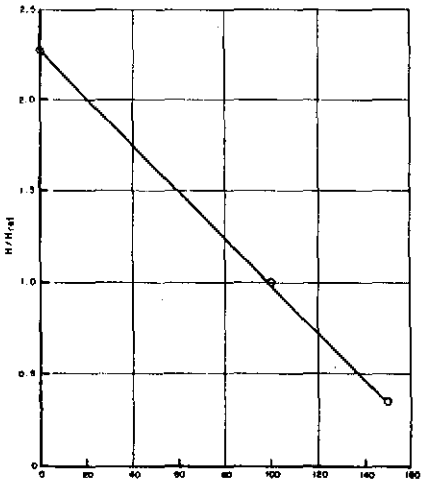

(H) SENSITIVITY TO UPGRADIENT CHLORIDE CONCENTRATION

NOTES:

1. H/H_ref IS THE AVERAGE NONDIMENSIONAL DISSOLUTION HEIGHT IN THE CASTILE FORMATION OVER THE LENGTH OF THE SECTION IN FIGURES 4-3 AND 4-4.
2. AVERAGE HEIGHT OF DISSOLUTION CAVITY H_{ref} = 0.34 CENTIMETERS PER 10,000 YEARS.
3. RANGE OF THE PARAMETER VALUES SELECTED FOR SENSITIVITY-ANALYSIS ARE FOR IDENTIFYING THE SIGNIFICANCE OF KEY PARAMETERS ON THE DISSOLUTION RATE. THESE RANGES DO NOT REPRESENT THE VARIATION OF THESE PARAMETERS EITHER IN THE BELL CANYON AQUIFER OR THE CASTILE FORMATION.

FIGURE B-1

NUMERICAL MODEL SENSITIVITY

PREPARED FOR

WESTINGHOUSE ELECTRIC CORPORATION
ALBUQUERQUE, NEW MEXICO

D'APPOLONIA

changes in flow rate can be inferred using Figure B-1(A).

- The variability in effective porosity [Figure B-1(B)] of the Bell Canyon aquifer is also an important factor in the salt dissolution rate, but its variation is not expected to produce more than a 65 percent change.

- The effective aquifer thickness of the Bell Canyon Formation is also a significant parameter in the dissolution rate. Most of the available data suggest that this thickness is about 30 meters. An increase in thickness to 300 meters would result in a 80 to 90 percent increase in dissolution rate [Figure B-1(C)].

- The dissolution rate decreases as the thickness of the diffusion zone increases. However, as the thickness exceeds 400 meters, the effect becomes less pronounced [Figure B-1(D)].

- The dissolution rate increases with the increase of the molecular diffusion coefficient. For example, a 56 percent increase in molecular diffusion will result in a 25 percent increase in dissolution rate [Figure B-1(E)].

- The dispersivity of the Bell Canyon aquifer does not significantly influence the dissolution rate [Figures B-1(F) and (G)].

- The dissolution rate is directly proportional to the chloride (salt) concentration of the Bell Canyon aquifer [Figure B-1(H)]. Lower chloride levels will result in more dissolution from the Castile Formation. The greatest rate of salt removal would occur if fresh water exists in the aquifer beneath the WIPP site. This could potentially double the dissolution rate presented in Section 4.4.3.

The significance of the sensitivity analysis with respect to the integrity of the WIPP site is discussed in Section 5.1.

B.2 SENSITIVITY OF DISSOLUTION CONTROLLED BY THE BELL CANYON AQUIFER

The salt dissolution rate is also affected by the Bell Canyon aquifer salt transport rate. In this case, the rate of removal can conservatively be correlated with the mass transport capacity of the Bell Canyon aquifer because the amount of dissolved salt is restricted by the amount that can be transported away from the dissolution zone. As a result, an important factor in evaluating and interpreting existing data is the Bell Canyon aquifer flow rate, Q. It is defined by:

$$Q = Kib \qquad (B-1)$$

where

Q = the flow rate per unit width (m^3/m-yr),
K = the hydraulic conductivity (m/yr),
i = the hydraulic gradient (m/m), and
b = the aquifer thickness (m).

The salt transport rate within any segment of the aquifer, ΔM, is equal to the salt dissolution rate from the Castile at that specific section. It can be stated as:

$$\Delta M = Q\Delta C = Kib\Delta C \qquad (B-2)$$

where ΔC is the concentration difference (kg/m^3) between the two ends of the segment. Therefore, given the concentration variation shown in Figures 2-5 and 4-1 based on observed data for the WIPP site, the actual salt dissolution rate can be calculated. However, it is linearly dependent on flow rate which is a function of hydraulic conductivity, hydraulic gradient, and aquifer thickness. Figure B-2 illustrates the relationship between the potential average dissolution rate with flow rate for aquifer thicknesses between 30 and 300 meters and for ranges of K and i outlined in Table B-1. For a 300-meter effective aquifer thickness, the current dissolution rate could be as large as 6 centimeters per 10,000 years compared to 0.34 centimeter as presented in Section 4.3.3.

DRAWN BY	RW 11-19-81	CHECKED BY	RCS	DRAWING NUMBER NM78-648-A26
		APPROVED BY	SHS	

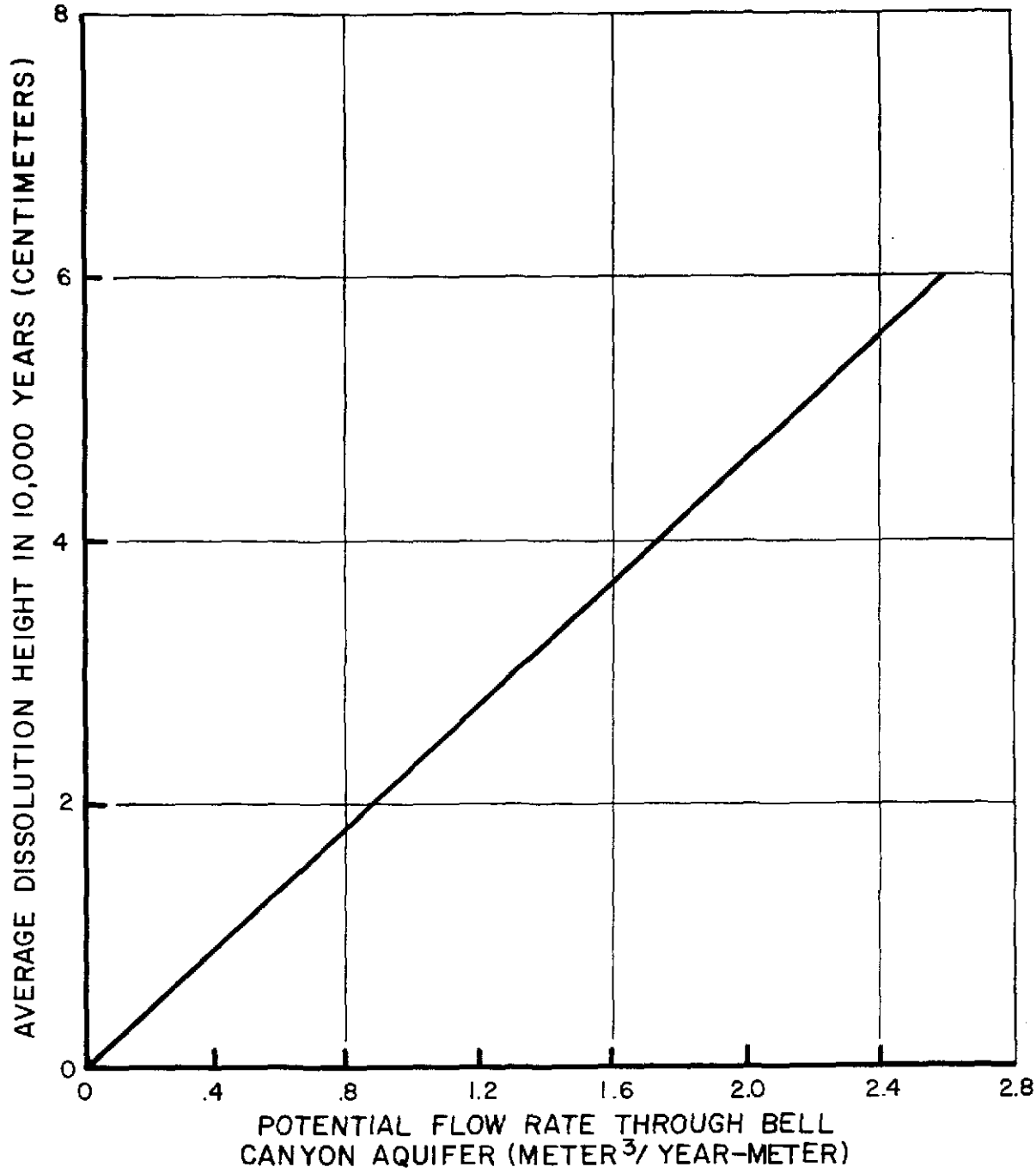

NOTES:

1. THE AVERAGE DISSOLUTION HEIGHT IS BASED ON A CHLORIDE CONCENTRATION INCREASE OF 50 Kg/m^3 OVER AN AQUIFER LENGTH OF 16,500m. THE DENSITY OF HALITE IS EQUAL TO 2160 Kg/m^3.
2. REFER TO NOTE 3 OF FIGURE B-1, FOR REASONS IN SELECTING THE RANGE OF THE PARAMETER VALUES.

FIGURE B-2

AVERAGE DISSOLUTION HEIGHT VARIATION WITH BELL CANYON FLOW RATE

PREPARED FOR

WESTINGHOUSE ELECTRIC CORPORATION
ALBUQUERQUE, NEW MEXICO

D'APPOLONIA